Chemical Sensors Based on Amplifying Fluorescent Conjugated Polymers

Samuel W. Thomas III, Guy D. Joly, and Timothy M. Swager*

Department of Chemistry, Massachusetts Institute of Technology, Cambridge, Massachusetts 02139

Received August 22, 2006

Contents

1. Introduction 1339
1.1. Amplification 1339
1.2. Role of Dimensionality, Dynamic Range, and Sensory Mechanism 1341
2. Small Ion Sensing with AFPs 1342
2.1. Crown Ether-Based Materials for Metal Ion Sensing 1342
2.2. AFPs with Nitrogen-Based Ligands for Metal Ion Sensing 1347
2.3. The Detection of Fluoride and Other Anions 1351
3. Detection of Explosives 1352
4. Conjugated Polyelectrolytes as Biosensors 1356
4.1. Early AFP Biosensing Reports 1356
4.2. Conjugated Polyelectrolytes and Viologen Quenchers 1357
4.3. Detection of Small Biomolecules 1362
4.4. Detection of Proteins 1363
4.5. Nonspecific Interactions of CPEs 1367
4.6. Nonionic AFPs for Biosensing 1371
4.7. AFPs for Biosensing on Unique Substrates 1375
5. Detection of DNA 1376
5.1. Regioregular Cationic Poly(thiophene)s for DNA Detection 1376
5.2. DNA Detection Based on Fluorescence Resonance Energy Transfer from Cationic Poly(fluorene-*co*-phenylene)s 1379
6. Concluding Remarks 1383
7. Note Added after ASAP Publication 1383
8. References 1383

1. Introduction

The field of chemical sensing is becoming ever more dependent upon novel materials. Polymers, crystals, glasses, particles, and nanostructures have made a profound impact and have endowed modern sensory systems with superior performance. Electronic polymers have emerged as one of the most important classes of transduction materials; they readily transform a chemical signal into an easily measured electrical or optical event. Although our group reviewed this field in 2000,[1] the high levels of activity and the impact of these methods now justify a subsequent review as part of this special issue. In this review we restrict our discussions to purely fluorescence-based methods using conjugated polymers (CPs). We further confine our detailed coverage to articles published since our previous review and will only detail earlier research in this Introduction to illustrate fundamental concepts and terminology that underpin the recent literature.

* To whom correspondence should be addressed. E-mail: tswager@mit.edu.

1.1. Amplification

The dominant attribute that has driven interest in fluorescent CP sensory materials is their ability to produce signal gain in response to interactions with analytes. This has led to them being referred to as amplifying fluorescent polymers (AFPs), while some researchers have referred to this gain in terms of superquenching. In analogy to microelectronic devices, the increased sensitivity (amplification) is derived from the ability of a conjugated polymer to serve as a highly efficient transport medium. However, unlike a silicon circuit, which transports electrons or holes, AFPs transport electronic excited states. The geometric relaxation of molecular structure around an excited state gives it a finite size. As a result, it is typical to refer to these excited states as quasiparticles called excitons. Excitons in AFPs are highly mobile and can diffuse throughout an isolated polymer chain or within an AFP solid by mechanisms that involve both through space dipolar couplings and strong mixing of electronic states.

The conceptual underpinnings of this field began with a model study published by our group in 1995.[2] Although others have more recently used exciton mobility within conjugated polymers to develop other mechanisms for amplified fluorescent detection, this study serves as a general introduction to the prototypical mechanism of chemical sensing by amplified fluorescence quenching with conjugated polymers. We demonstrated amplification in a poly(phenylene ethynylene) (PPE) possessing well-defined cyclophane receptors integrated directly into the polymer backbone, effectively connecting the receptors in series. Cyclophane receptors were chosen because they form complexes with paraquat, a powerful electron acceptor and well-known electron-transfer quenching agent. To determine the ability of exciton transport to amplify binding events, a model compound containing a single receptor with the same local environment was synthesized. The large binding constant of the receptors resulted in paraquat quenching processes that were static in nature. In other words, the quencher is bound to the receptor and, once generated, the excited state is immediately and quantitatively quenched. Quenching due to diffusion of the quencher to an excited state was insignificant in this case. The quenching processes in AFPs can be analyzed by Stern−Volmer relationships (eqs 1 and 2), where

$$F_0/F = (1 + K_{SV}[Q]) \quad (1)$$

$$\tau_0/\tau = (1 + k_q\tau_0[Q]) \quad (2)$$

F_0 is the fluorescence intensity in the absence of added

10.1021/cr0501339 CCC: $65.00
Published on Web 03/27/2007

Samuel Thomas was born in southeastern Massachusetts in 1978 and received his B.S. in Chemistry from the University of Rochester in 2000. He spent 1 year as a research chemist at Eastman Kodak, after which he began graduate studies at MIT. He earned his Ph.D. in organic chemistry in 2006, under the supervision of Professor Timothy M. Swager, for studies on luminescent chemosensors. He is currently a postdoctoral fellow in the laboratory of Professor George M. Whitesides at Harvard University.

Guy D. Joly obtained his B.A. degree in Chemistry from Hamline University in 1999. He earned his Ph.D. (2004) under the supervision of Professor Eric N. Jacobsen at Harvard University. His Ph.D. research focused on the discovery and development of useful asymmetric catalytic methodologies. After completing his graduate work, he moved to MIT to perform postdoctoral research with Professor Swager in the area of conjugated polymer-based sensors. His research interests broadly encompass organic chemistry, catalysis, sensing, and materials science.

quencher, F is the fluorescence intensity as a function of quencher concentration [Q], τ_0 is the lifetime without added quencher, and τ is the lifetime at [Q]. The slope of the plots gives the Stern−Volmer quenching constant (K_{SV}) or the diffusional quenching constant (k_q).

A linear relationship of [Q] with F_0/F implies a purely static (bound to the polymer) or dynamic (diffusion limited) quenching. Moderate to large binding constants give rise to Stern−Volmer quenching constants (K_{SV}) that exceed the rate achievable at the diffusion limit, and hence, static quenching can be inferred. Another method to determine if quenching in an AFP is static or dynamic is to determine the dependence of the lifetime on the quencher concentration (eq 2). When the quencher is not bound to the fluorophore, the additional deactivation pathway (diffusional quenching) shortens the observed lifetime of the fluorophore according to eq 3,

$$\tau = (k_r + k_{nr} + k_q[Q])^{-1} \quad (3)$$

wherein k_r is the radiative (fluorescence) rate of decay, k_{nr} is the intrinsic nonradiative rate of decay, and k_q is the bimolecular rate constant of fluorescence quenching. In the case of static quenching, a fluorophore bound to a quencher is in a dark nonemissive state. The unbound fluorophores exhibit their natural lifetimes, and the slope of F_0/F vs [Q] yields a binding constant.

Timothy M. Swager is the John D. MacArthur Professor of Chemistry and the Head of the Department of Chemistry at the Massachusetts Institute of Technology. A native of Montana, he received a B.S. from Montana State University in 1983 and a Ph.D. from the California Institute of Technology in 1988. His research interests are in design, synthesis, and study of organic-based electronic, sensory, and liquid crystalline materials.

The apparent binding constant of the receptor-containing AFP measured by the Stern−Volmer method is the individual repeating unit binding constant multiplied by the amplification factor. Comparison of the apparent binding constant (K_{SV}) of receptor PPEs revealed a linear increase with molecular weight up to a critical molecular weight of $\approx 1.3 \times 10^2$ phenylene ethynylene repeating units (Figure 1). Higher chain lengths did not increase the apparent binding constant. These results reveal that the exciton was not able to visit the entire length of the higher molecular weight polymers because of its limited mobility and its finite lifetime (there is always competitive relaxation to the ground state). The amplification is due to exciton mobility and should be properly separated from the binding constant. However, this analysis is seldom performed because of the need for nontrivial synthesis and other complexities inherent to

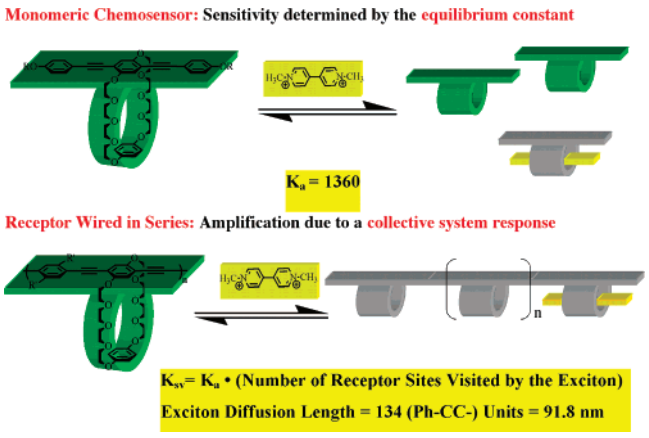

Figure 1. Demonstration of amplified quenching in a CP. The determination of the Stern−Volmer quenching reveals the constant for binding of paraquat to a single cyclophane receptor (top). In the polymer the larger (amplified) quenching constant reflects the fact that the quencher can be bound to any of the repeating units visited by the exciton (bottom).

polymer aggregates and thin films (*vide infra*). This method also can be used to determine the exciton diffusion length of a CP in solution (Figure 1).

The subsequent discussion emphasizes that quantifying amplification requires knowledge of the actual binding constant of an analyte to a polymer and is intended to guide the reader to scrutinize claims encountered in this field. Indeed, if one simply looks at the K_{SV} with no knowledge of the binding constants, then the amplification due to exciton mobility cannot be quantified. As a result, researchers (especially those new to the field) should be wary of claims of extraordinary amplification that lack proper control experiments. To make this point explicitly and hopefully prevent future misconceptions, we draw attention to one of the most highly cited papers that was detailed in our 2000 review that reported biosensing with an AFP,[3,4] in which the authors reported amplification factors of 10^6. As will be discussed in the section of the review concerning biosensors, the AFPs were polyanions and the quenchers were cationic whereas the reference fluorescent compound (stilbene) was neutral. It is not likely that the cationic quencher would have strong interactions with the neutral reference fluorophore in water, whereas polyanion AFPs exhibit very high binding constants with the cationic quenchers. Considering that the binding constant of the oppositely charged species is likely more than 10^4, the intrinsic amplification due to exciton transport is 10^2, in accord with earlier reports.

1.2. Role of Dimensionality, Dynamic Range, and Sensory Mechanism

The physical state of an AFP has profound effects on its ability to amplify. In the case of rigid AFPs, which often exhibit large persistent lengths in solution,[5] we can approximate them as presenting the exciton with a one-dimensional diffusional conduit. The excitons therefore undergo a one-dimensional random walk when the polymers are in solution, which is inefficient for amplification: the exciton visits the same receptor many times. If the exciton can be made to undergo vectorial transport in a given direction, then much higher amplification factors can be achieved. Vectorial transport is not easily achieved in most systems; however, greatly enhanced amplification can be achieved by simply increasing the diffusional pathways available to the exciton. In other words, the greater the number of possible exciton migration pathways, the higher the probability that an exciton will visit a new receptor and detect an analyte. The situation is more complicated in polymer films, however, wherein receptors may only be able to bind some analytes when located at a surface. Hence, for the detection of large biomolecules, either polymer aggregates or very thin films are optimal. Analyte vapors that can diffuse rapidly into a polymer are best detected by an AFP film that has more three-dimensional character.[6] Enhancements of the performance of AFPs in aggregates or films are also possible due to greater rates of energy transfer. Close proximity of the neighboring polymer chains facilitates interchain energy migration, and AFPs often exhibit more planar conformations in thin films and aggregates, which appears to promote exciton diffusion.[7] As a result of these issues, new methods for assembly of AFPs into optimal organizations for energy transfer remain an important area for future investigations.

The range over which a sensory response is well behaved (ideally linear) with analyte concentration is important. In the case where the AFP sensory signal is fluorescence attenuation (quenching), the sensitivity of the polymers decreases at higher analyte concentrations, because the distance between quenchers bound to the AFP can be less than the exciton diffusion length. This can be easily understood by considering the polymer in Figure 1. The binding of a second quencher to a quenched segment of the polymer will have no effect. Indeed, the K_{SV} is only linear at low [Q] and becomes sublinear at higher quencher concentrations. As a result, in the absence of analyte-induced changes in binding constants or degrees of aggregation, AFPs are most sensitive at very low quencher concentrations and are thereby appropriate for application in ultratrace chemical sensors.

An alternative method to utilize AFPs is to remove quenching sites by interactions with an analyte and create an increase in fluorescence. The virtues of such a "turn-on" response relative to the "turn-off" quenching response are often espoused in the literature. "Unquenching" schemes with a completely dark or highly quenched AFP, however, require that the interquencher spacing is less than the exciton diffusion length. In this case, the sensitivity of the turn-on response will be decreased relative to the case of the turn-off method. Specifically, removing a quenching site may not give the fully desired response because another quencher's influence could overlap much of the same quenching volume. Also, contrary to many claims in the literature, a "turn-on" signal (increase in fluorescence) is not always easier to detect than a quenching signal. As long as the background noise of the fluorescence detection electronics does not fluctuate strongly with the intensity of the signal, a "turn-on" signal is only easier to observe if the new signal is detected on a completely dark background so that the detection is not simply based on a ratio of signals. However, when there is background fluorescence, as is often the case, there is no sensitivity advantage of a turn-on over a turn-off response. For trace detection in complicated environments, however, turn-on detection schemes do have an advantage in selectivity, as there are many more environmental interferants that would cause a "false-positive" by adventitious quenching as opposed to adventitious fluorescence enhancement.

In Figure 2 we illustrate the features of dimensionality and quenching mechanism as they relate to the sensitivity of an AFP-based sensor. The horizontal direction illustrates that the quenching (or unquenching) of polymer chains in

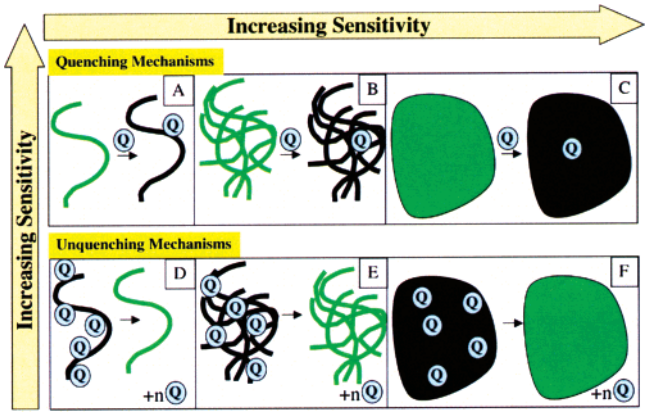

Figure 2. Role of mechanism and dimensionality in determining the relative sensitivities of AFP sensors. Unquenching generally results in overlapping quenching domains and is less sensitive than quenching. Sensitivity increases as polymer chains are assembled into structures that provide the exciton with additional energy migration pathways that exhibit greater efficiency.

solution is generally much less sensitive than that in thin films, because the dimensionality of the exciton transport is reduced. In addition, the vertical axis shows that unquenching (turn-on) is generally less sensitive than quenching, because many quenchers may have to be removed in order to observe a signal enhancement. We further note that the quencher can also be emissive and thereby function as a turn-on sensor. We point out that the specific application can dictate the best mechanism and form of the AFP. In the case of sensors for ultratrace detection, quenching mechanisms with the highest level of dimensionality for exciton diffusion are most appropriate. For less sensitive detection wherein the analyte concentration of interest may be higher, an unquenching scheme may be most appropriate.

The assembly of polymer chains into aggregates and films is not without difficulties. A general phenomena is the tendency of polymer chains to assemble parallel to neighboring chains, which leads to strong self-quenching. These strong electronic interactions generally give rise to new, broad emission peaks at longer wavelengths that are often described as having excimer-like behavior. The characterization of the emissive species as excimers (excited-state dimers) is often tenuous: it is not clear that the ground state necessarily has a repulsive interchromophore potential. Nevertheless, structure−property studies of polymer chains aligned face-to-face at the air−water interface reveal that cofacial spacing of polymer chains less than about 4.3−4.5 Å gives rise to dominant excimer-like emissions with dramatically reduced quantum yields.[8] The excimer-like states of these materials generally provide traps that restrict the mobility of the excitons and reduce the sensory performance of the AFPs. These issues have been particularly problematic in the formation of AFPs that function optimally in aqueous environments. As a result, strong interchain interactions are often purposely avoided and rigid scaffolds appended to polymers have been developed to provide robust excimer-free films.[9] On the other hand, the general tendency of AFPs to exhibit self-quenching also has presented opportunities for transduction mechanisms wherein interactions with target analytes either promote aggregation of polymers to give a quenching response or reduce self-quenching to give a turn-on response. Indeed, examples of both mechanisms will be covered in this review.

In this Introduction, we have endeavored to bring the reader up to speed on general issues regarding AFP sensory materials. The physics of these systems and a comprehensive understanding of the dynamics of energy migration is an active area of study and is complicated by the fact that polymers have inherent disorder. Nevertheless, general guiding principles have been established that allow for the rational design of sensory materials for specific applications. In the following sections, there are many examples with innovative transduction mechanisms and an expanding diversity of polymer structures.

2. Small Ion Sensing with AFPs

2.1. Crown Ether-Based Materials for Metal Ion Sensing

Although great lengths have often been taken to prevent polymer aggregation in solution and in thin films, analyte-induced aggregation and the subsequent optical response can be used as a sensitive transduction mechanism for analyte detection. In 2000, Swager and co-workers reported a conjugated-polymer-based sensor for potassium ion that operates via ion-induced aggregation.[10] The sensor relies on 15-crown-5-functionalized poly(*p*-phenylene ethynylene) **1** (Figure 3). This system takes advantage of the ability of 15-crown-5 to form a 2:1 complex with K^+ ions. Exposure of the functionalized polymer to K^+ generated potassium-bridged polymer aggregates containing nonemissive traps. The potassium-aggregated polymer displayed a red-shifted absorption spectrum in which λ_{max} had shifted from 434 to 459 nm, consistent with the formation of π-stacked aggregates in which polymer chains are brought together through intermolecular complexation of K^+ ions. The K^+ ion-induced aggregation resulted in fluorescence quenching as well; emission intensity decreased 82% at the fluorescence λ_{max} (452 nm) at a 2:1 crown ether to K^+ mole ratio. The weak emission of the potassium-aggregated polymer was broad, and the emission maximum had shifted from 452 to 540 nm, further evidence of the formation of π-stacked aggregates. In fact, the potassium-aggregated polymer displayed almost identical absorption and emission spectra to those obtained from a Langmuir−Blodgett film of polymer **1** in which the polymer chains were co-facially π-stacked. The authors explored the effect of polymer structure on this sensing scheme. As the steric demand of the side chains increased, the ability of K^+ ions to bring about polymer aggregation decreased. Consistent with K^+ ion-induced aggregation producing the observed spectral changes, a 1500-fold excess of either Li^+ or Na^+ did not significantly change polymer absorption or emission, as these cations form 1:1 complexes with 15-crown-5.

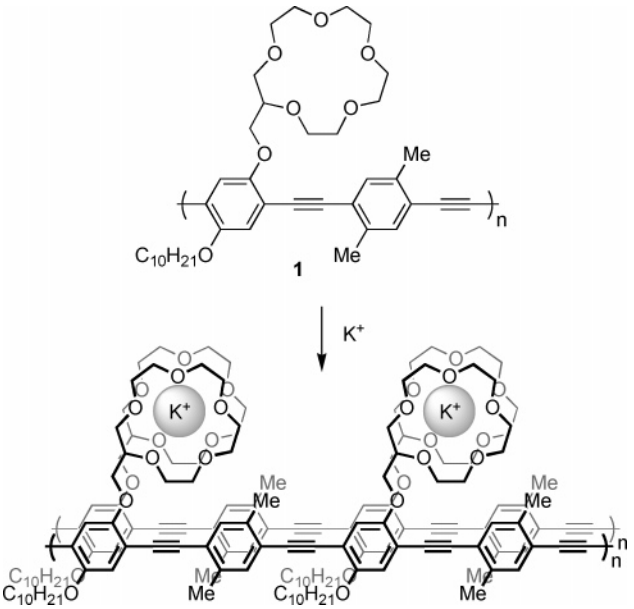

Figure 3. K^+-induced aggregation of crown ether-functionalized polymer **1**.

Leclerc et al. synthesized a 15-crown-5-functionalized poly(thiophene) as a fluorescent probe for K^+.[11] This material exhibited selectivity for K^+ over Li^+ and Na^+, although all three cations did quench polymer emission at millimolar concentrations. The authors postulated that the quenching response was due to potassium ion-induced aggregation.

Xi et al. developed a similar assay for K^+ using a crown ether-functionalized poly(*p*-phenylene vinylene) **2**.[12] In this case, the crown ether was based upon the larger benzo-18-crown-6. These authors also observed red-shifted and diminished emission in the presence of potassium ion.

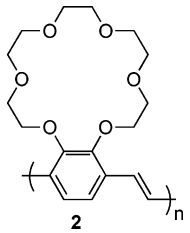

2

However, polymer **2** did not display selectivity for K^+ over Na^+ or Li^+, as all three cations quenched polymer emission. While the emission was responsive to metal ions, the absorption spectra remained unchanged. Films of the polymer obtained by spin casting from solutions containing 6 equiv of K^+ revealed the formation of wormlike aggregated structures (as determined by AFM) whereas films generated from solutions containing Li^+ or Na^+ were made up of largely isolated individual particles.

In 2004, Liu and co-workers reported a poly(*p*-phenylene ethynylene) functionalized with triethylene glycol monomethyl ether groups (**3**) that responded to Li^+ and Na^+ but not K^+.[13] While the absorption spectrum of the polymer was largely unresponsive to the addition of Li^+ or Na^+ ions, its fluorescence was significantly quenched by these cations.

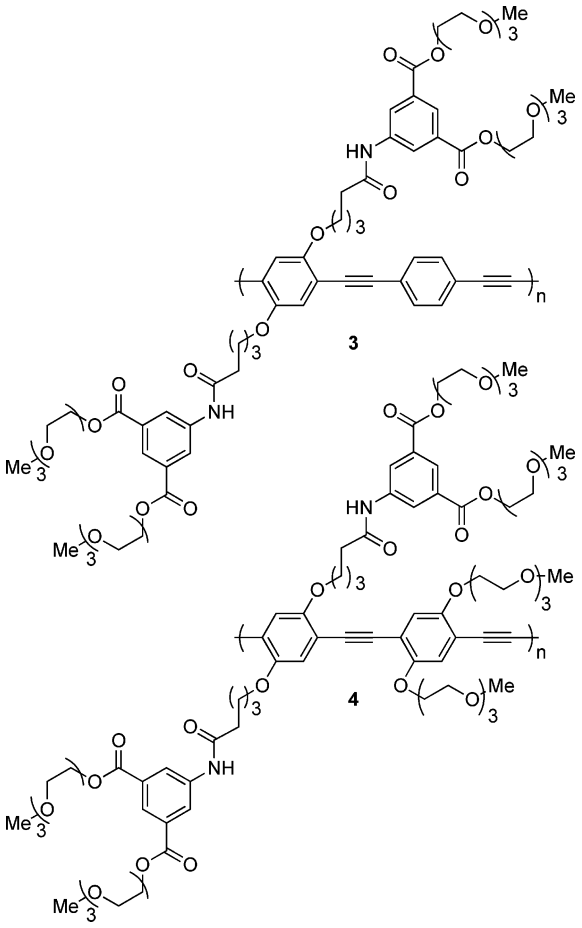

3

4

By tuning the steric demand of the comonomer, the authors were able to produce a polymer (**4**) with selectivity for Li^+ over Na^+. This polymer responded selectively to Li^+ at a concentration of 4×10^{-5} M even in the presence of 5×10^{-4} M Na^+. The authors proposed that **4** was selective for Li^+ because the tri(ethylene glycol) monomethyl ether groups on the comonomer limited the ability of the podand binding sites to expand and accommodate larger cations.

Smith and co-workers synthesized a benzo-15-crown-5-containing poly(*p*-phenylene vinylene) that responded to Eu^{3+}.[14] The polymer fluorescence intensity increased more than 8-fold upon exposure to Eu^{3+} in 99:1 methanol/chloroform solution. The absorbance spectrum was unchanged upon addition of Eu^{3+}, demonstrating the greater sensitivity of the fluorescence response relative to changes in absorption. A static event was responsible for the emission response, as time-resolved experiments revealed that the added Eu^{3+} did not affect fluorescence lifetime. The authors proposed that the increase in emission was due to inhibition of an internal change-transfer process upon cation binding. Solvent effects supported this mechanism; in acetonitrile, Eu^{3+} *quenched* polymer emission, in contrast to the emission enhancement observed in 99:1 methanol/chloroform.

Valiyaveettil et al. investigated the optical responses of phenol-containing poly(*p*-phenylene)s to metal cations.[15] The metal-free polymer had an emission maximum at 403 nm. The authors obtained red-shifted fluorescence spectra in the presence of Na^+ (474 nm), Cu^{2+} (436 nm), Co^{2+} (436 nm), and Fe^{3+} (509 nm). They observed similar effects in the absorption spectra, but they did not report any quantitative quenching studies.

Recently, Wang and co-workers developed a mercury-sensing strategy based on Hg^{2+}-induced aggregation of a conjugated polymer and subsequent fluorescence self-quenching.[16] Their system also relied on K^+-induced aggregation of crown ether-functionalized conjugated polymers.[10] Exposure of thymine-functionalized polymer **5** to

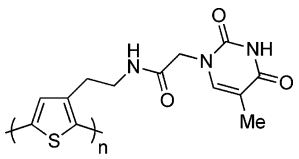

5

Hg^{2+} resulted in a 5 nm red shift in the absorption maximum and substantial fluorescence quenching. These changes were attributed to Hg^{2+}-induced polymer aggregation via coordination of thymine residues to Hg^{2+}. Thymine$-Hg^{2+}$ coordination formed cross-links between conjugated polymer chains and led to the generation of π-stacked polymer aggregates. The assay allowed for the determination of Hg^{2+} over a concentration range from 3.0×10^{-5} to 30×10^{-5} M. In addition, the fluorescence quenching response of thymine-functionalized **5** was selective for Hg^{2+} over Mg^{2+}, Ca^{2+}, Mn^{2+}, Co^{2+}, Ni^{2+}, Cu^{2+}, and Zn^{2+}. Cu^{2+} provided the most interference but was still 2.5-fold less effective at quenching polymer emission than Hg^{2+}. The authors demonstrated that the fluorescence quenching response to Hg^{2+} could be reversed by the addition of Cl^-.

Bunz and co-workers have explored the use of sugar-functionalized poly(*p*-phenylene ethynylene)s **6** and **7** as fluorescent sensors for Hg^{2+} and Pb^{2+} in dimethyl formamide (DMF) solution.[17] Polymer **6** exhibited the highest sensitivity toward Hg^{2+}, as its emission was efficiently quenched by $HgCl_2$ ($K_{SV} = 1.1 \times 10^4$), $Hg(OAc)_2$ ($K_{SV} = 1.6 \times 10^4$), $Hg(NO_3)_2$ ($K_{SV} = 3.8 \times 10^4$), and $Hg(tfa)_2$ ($K_{SV} = 4.8 \times 10^4$). The sugar residues of **6** were critical for achieving high sensitivity toward Hg^{2+} salts; polymer **8**, which lacked sugar functionalization, was unresponsive to $HgCl_2$ and $Hg(OAc)_2$. Hg^{2+} salts containing more easily dissociated counterions, $Hg(NO_3)_2$ and $Hg(tfa)_2$, did quench the emission of polymer **8**, but this polymer was still more than 10-fold less sensitive

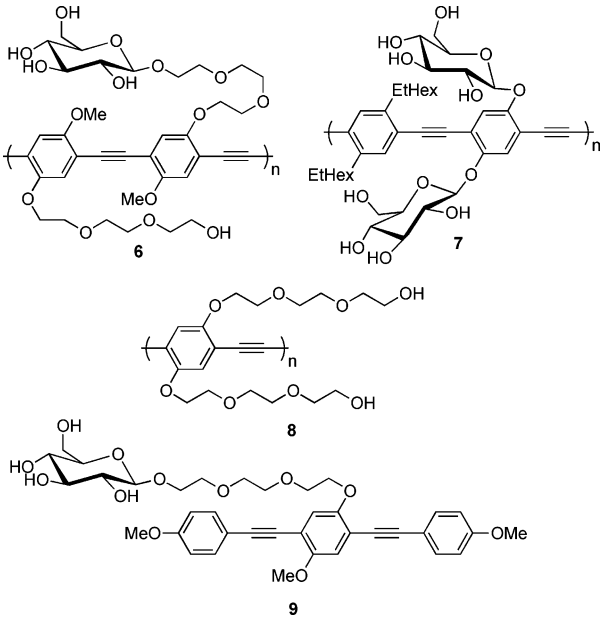

to these salts than the sugar-functionalized polymer **6**. Polymer **7**, which contained two sugar moieties per repeat unit, was most sensitive to Pb^{2+} ($K_{SV} = 7.2 \times 10^4$ for $Pb(OAc)_2$) but was almost unresponsive to Hg^{2+} salts. Polymer **7** was almost 5-times more sensitive toward $Pb(OAc)_2$ than polymer **8**, a further demonstration that the sugar residues were necessary to achieve high sensitivity.

The authors also examined a small molecule model **9**.[17] The sugar-functionalized small molecule **9** did not respond to $HgCl_2$ or $Hg(OAc)_2$ and was more than 30-fold less sensitive to $Hg(NO_3)_2$ and $Hg(tfa)_2$ than polymer **6**. In addition, sugar-functionalized polymer **7** was more than 1000-fold more sensitive toward $Pb(OAc)_2$ than **9**. The increases in sensitivity observed upon moving from a small molecule, **9**, to the conjugated polymers **6** and **7** were too large to be completely accounted for by the transport properties of the conjugated polymers alone. The authors reasonably suggested the enhanced quenching responses of the conjugated polymers could be attributed to a combination of the polymer transport properties as well as to a cooperative binding event (multivalency) in which the sugar-containing conjugated polymers **6** and **7** bound Hg^{2+} and Pb^{2+} metal ions with more than one sugar residue simultaneously.

Bunz and co-workers, in the development of a more sensitive second-generation lead sensor, further exploited the benefits of multivalent interactions between a functionalized conjugated polymer and a metal cation.[18] The fluorescence of the carboxylated, water-soluble poly(*p*-phenylene ethynylene) **10** was quenched by metal ions in aqueous solution.

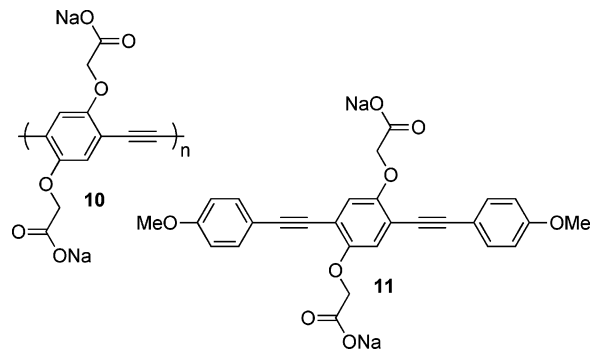

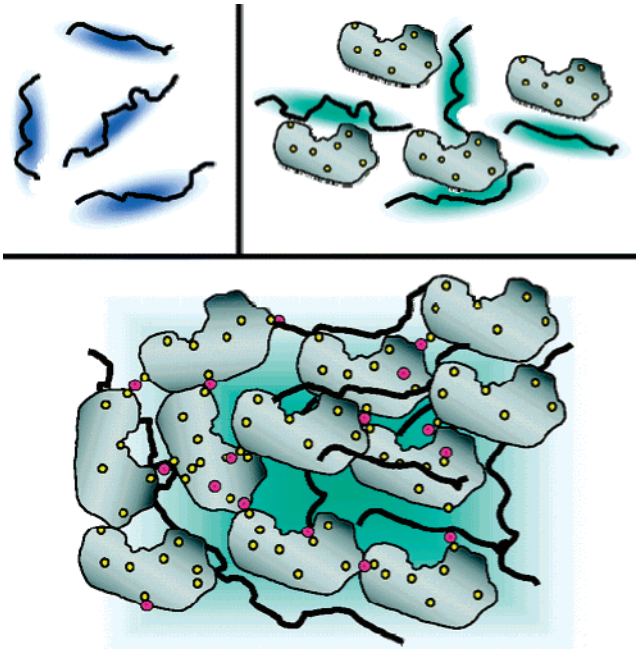

Figure 4. Illustration of Hg^{2+}-induced agglutination of the **10**−papain complex. Top left: **10** alone. Top right: Electrostatic complex between **10** and papain. Bottom: Agglutination of the **10**−papain complex in the presence of Hg^{2+} (pink) through Hg^{2+}-based cross-links. (Reprinted with permission from ref 19. Copyright 2006 American Chemical Society.)

The authors examined a variety of divalent cations including Pb^{2+}, Ca^{2+}, Zn^{2+}, Hg^{2+}, Mg^{2+}, Cu^{2+}, Mn^{2+}, and dimethyl viologen. Polymer **10** was most sensitive to Pb^{2+} salts; **10** exhibited more than 10-fold higher sensitivity toward $Pb(NO_3)_2$ ($K_{SV} = 8.8 \times 10^5$) and $Pb(OAc)_2$ ($K_{SV} = 6.9 \times 10^5$) than any of the other cations investigated. The sensitivity was more than 100-times lower for the detection of Pb^{2+} in phosphate buffer than in PIPES (piperazine-1,4-bis-2-ethanesulfonic acid) buffer. The lower sensitivity in phosphate buffer was likely due to the ability of phosphate anions to interact with metal cations such as Pb^{2+}. Polymer **10** was more than 1500-fold more sensitive to Pb^{2+} than the small molecule model **11**. The superior sensitivity of the conjugated polymer was ascribed to a combination of the transport properties of the conjugated polymer and a multivalency effect through which the Pb^{2+} cation could be simultaneously bound by more than one carboxylate from the same polymer chain. Consistent with the involvement of a cooperative binding contributing to the high sensitivity of **10**, the addition of polymer **10** to a concentrated solution of $Pb(OAc)_2$ resulted in the formation of a weakly emissive yellow precipitate.

Bunz et al. have also applied carboxylated polymer **10** to a creative fluorescence-based sensory scheme for Hg^{2+}.[19] The assay relied upon the formation of an electrostatic complex between the anionic conjugated polymer **10** and papain, a cationic cysteine protease (Figure 4). In addition to the **10**−papain complex, the authors examined complexes between **10** and poly(dimethyldiallylammonium chloride) (Pdac), histone, and bovine serum albumin (BSA) for their ability to detect cations in water. In each case, the **10**−cofactor complexes had unique response profiles to the variety of metal cations assayed. For instance, the **10**−Pdac complex was unresponsive to metal cations with the exception of Fe^{3+}, which weakly quenched **10**−Pdac emission. Polymer **10** alone was relatively insensitive to Hg^{2+}; 0.1 mM Hg^{2+} was

required to achieve readily observable fluorescence quenching. The **10**−papain complex, however, was most sensitive to Hg^{2+}. The high sensitivity of **10**−papain toward Hg^{2+} was due to agglutination of **10**−papain in the presence of as little as 20 μM Hg^{2+}. Papain contains free thiol groups and is known to bind Hg^{2+}. The authors proposed that the **10**−papain complex is a mixture of oligomers in which protein chains are effectively cross-linked by the anionic conjugated polymer. Due to the cross-linking, the supramolecular assemblies were more prone to agglutinate in the presence of Hg^{2+} than either **10** or papain alone. The agglutinated complex precipitated at sufficiently high concentrations of Hg^{2+}. Mercury-induced precipitation provided a very weakly emissive precipitate and a fluorescence-free solution. To demonstrate selectivity, the authors showed that an aqueous solution containing Hg^{2+} and nine other metal cations at a concentration of 0.4 mM each was easily distinguished from a mixture of the nine metal cations in the absence of Hg^{2+}. In the solution containing Hg^{2+}, **10**−papain agglutinated and formed a weakly emissive precipitate, leaving the solution nonfluorescent. The Hg^{2+}-free mixture, on the other hand, retained the bulk fluorescence from solution.

In 2004, Leclerc and co-workers reported a conjugated polymer/DNA-based aptamer complex that was optically responsive to K^+.[20] The combination of a cationic poly(thiophene) **12** and ssDNA produced an electrostatically bound complex. Such complexes between DNA and conjugated polyelectrolytes[21] have found excellent use in biosensing applications (see section **5**). Upon forming a complex with ssDNA, the poly(thiophene) absorption was red-shifted due to an increase in the effective conjugation length upon going from a random-coil conformation in solution (yellow in color) to a more planar, potentially aggregated, structure in the polymer-ssDNA adduct (red-violet in color). They examined an ssDNA sequence that formed a quadruplex in the presence of K^+. The formation of the ssDNA quadruplex-conjugated polymer adduct produced an absorbance spectrum that was in between (in terms of energy) that of the free conjugated polymer and that of the unfolded ssDNA-conjugated polymer complex. The change to a quadruplex structure in the presence of K^+ could be detected visually by a change in color from red-violet (unfolded ssDNA) to orange (K^+-bound quadruplex). The poly(thiophene) absorption change upon going from a complex with unfolded ssDNA to a complex with the ssDNA quadruplex was likely due to the greater degree of twisting required of the conjugated polymer backbone in order to wrap itself around the quadruplex as compared to unfolded ssDNA. Application of ssDNA aptamer−poly(thiophene) complexes to protein

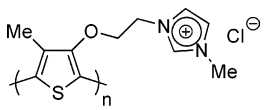

12

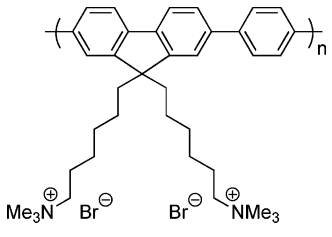

13

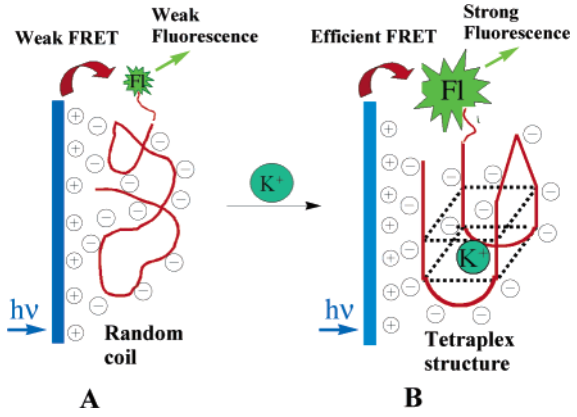

Figure 5. K^+ detection using polymer **13** in conjunction with ssDNA. The ssDNA folds into a quadruplex in the presence of K^+. (Reprinted with permission from ref 22. Copyright 2005 American Chemical Society.)

detection was also reported and is described in greater detail in section 4.4.

Building on the work of Leclerc et al., in 2005 Wang and co-workers reported a K^+ sensor based upon energy transfer from the water-soluble cationic polyfluorene **13** to a dye-labeled DNA G-quadruplex (Figure 5).[22] Cationic polyfluorene **13** formed a complex with a G-rich DNA sequence through electrostatic attraction between the cationic polymer backbone and the anionic phosphate groups of the ssDNA. The ssDNA used in this study was labeled at its terminus with a fluorescein dye. The authors asserted that the conjugated polymer−ssDNA complex was weakly bound and that fluorescence resonance energy transfer (FRET) from **13** to the fluorescein dye was inefficient in this loose complex due to a large average distance between the conjugated polymer donor and the dye acceptor. The addition of KCl produced a change in the ssDNA conformation from an unfolded state to a more compact K^+-bound G-quadruplex. It was proposed that the space-charge density of the ssDNA increased upon adopting the G-quadruplex structure, which in turn created a stronger electrostatic attraction between polyfluorene **13** and the G-quadruplex. The distance between the polyflouorene donor **13** and the fluorescein acceptor decreased as a result and led to more efficient FRET in the presence of K^+. The FRET ratio of the emission intensity at 527 nm (fluorescein−ssDNA emission maximum) to the intensity at 422 nm (polymer **13** emission maximum) was 16-fold higher in a solution containing 50 mM K^+ in comparison to a K^+-free solution. In the K^+-bound quadruplex state, emission from fluorescein−ssDNA was more than 10-fold more intense when polymer **13** was excited at 380 nm followed by energy transfer to fluorescein than when fluorescein was directly excited at 480 nm, a testament to the light-harvesting capability of the conjugated polymer employed in this system. This sensory methodology was selective for K^+ over Na^+, NH_4^+, Li^+, Mg^{2+}, and Ca^{2+}.

Swager and co-workers reported rotaxanated conjugated polymers that were sensors for alcohols.[23] The syntheses of phenanthroline-containing polymers **14** and **15** were aided by microwave irradiation during the polymerization step. The vapor of acidic alcohols, including various phenols (phenol, 4-nitrophenol, and 4-*tert*-butylphenol) and 2,2,2-trifluoroethanol, quenched the emission of thin films of **14** and **15**. The most efficient quenching response was between phenol vapor and a thin film of **15**; emission from **15** decreased more than 40% upon exposure to phenol vapor for 5 min.

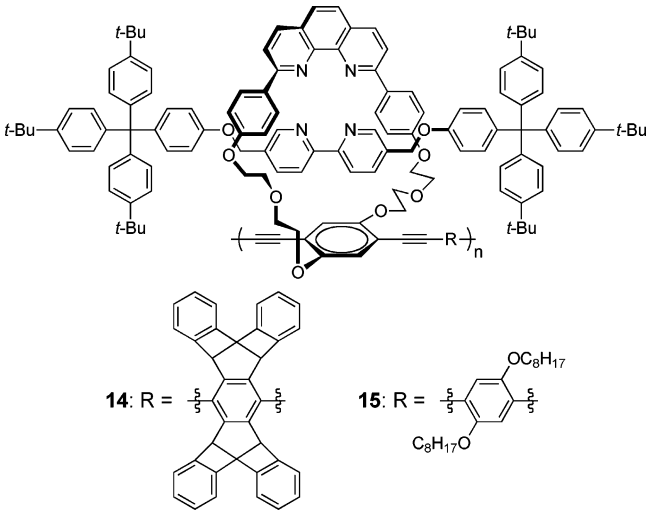

Two control polymers, one that lacked the rotaxinated thread present in **14** and one that replaced the entire phenanthroline-containing macrocycle with diethylene glycol monomethyl ether groups, did not respond to phenol vapors. These control experiments support the authors' hypothesis that the three-dimensional binding pockets provided by the rotaxane groups were necessary recognition sites required for efficient alcohol binding. NMR experiments suggested that hydrogen bonding, not complete proton transfer, was responsible for alcohol recognition. The rotaxane unit also provided a preorganized pocket for metal ion binding. Thin films of polymers **14** and **15** cast in the presence of Zn^{2+} were sensitive to alcohol vapor. Exposure of the Zn-containing thin films to methanol, ethanol, 2-ethylhexanol, or cyclohexanol produced an unquenching response. The response was largest for methanol, which brought about a 25% increase in emission intensity.

Although conjugated polyelectrolytes[21] have been used extensively in biosensing applications (see sections 4 and 5), they have also been effectively employed as metal ion sensors. Selectivity, however, is difficult to achieve using these materials to detect metal ions, as the association between the conjugated polyelectrolyte and the complementarily charged quencher is driven by nonspecific electrostatic interactions. In 2000, Schanze and co-workers reported a fluorescence quenching study of conjugated polyelectrolyte **16**, which was first prepared by Reynolds in 1999 as part of

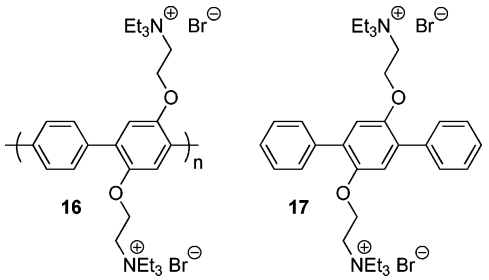

an effort to develop materials that could function as blue emitters in light emitting devices (LEDs).[24,25] The fluorescence of polymer **16** was efficiently quenched by $Ru(phen')_3^{4-}$ (phen′ = 4,7-bis(4-sulfophenyl)-1,10-phenanthroline) ($K_{SV} = 1.4 \times 10^8$) and $Fe(CN)_6^{4-}$ ($K_{SV} = 9.3 \times 10^7$) in aqueous solution. Fluorescence quenching by $Ru(phen')_3^{4-}$ was shown to occur via energy transfer from the cationic conjugated polymer to the metal-to-ligand charge-transfer state of $Ru(phen')_3^{4-}$. The authors attributed the exceptionally high Stern−Volmer quenching constants to the combination of a very large association constant between the cationic polyelectrolyte and the anionic quencher, driven primarily by electrostatic interactions, and to facile exciton transport within the conjugated polymer. The quenching response was highly dependent upon the polymer concentration; the Stern−Volmer quenching constant decreased by a factor of 175 upon increasing the concentration of **16** from 1.0 μM to 10 μM. The large decrease in sensitivity was ascribed to increased polymer aggregation at higher polymer concentration. The combination of large Stern−Volmer constants and the short fluorescence lifetime of **16** is most consistent with a dominant static quenching event involving an ion-paired fluorophore−quencher complex. Small molecule model **17** (at 10 μM) was also quenched by $Ru(phen')_3^{4-}$ and $Fe(CN)_6^{4-}$, but to a much lesser extent. When compared to polymer **16** at the same concentration, **17** was more than 30-fold less sensitive to fluorescence quenching by $Ru(phen')_3^{4-}$. The greater sensitivity of polymer **16** was likely due both to the transport properties of the conjugated polymer (rapid migration of excitons to quenching sites) and to stronger association of the anionic quenchers to polycationic **16** than to dicationic small molecule **17**. The Stern−Volmer plots for fluorescence quenching of polymer **16** by $Ru(phen')_3^{4-}$ and $Fe(CN)_6^{4-}$ displayed upward curvature as quencher concentration was increased. This effect is inconsistent with simple quenching responses, that should display downward curvature. The upward curvature was attributed to quencher-mediated aggregation of **16**.[26] More efficient fluorescence quenching occurred in the aggregate due to increased exciton migration facilitated by interpolymer interactions. Thin films of polymer **16** could detect $Ru(phen')_3^{4-}$ and $Fe(CN)_6^{4-}$ down to 20 nM.

Huang and co-workers have also examined cationic conjugated polyelectrolytes as fluorescent sensors of anionic metal complexes. The fluorescence of water-soluble poly(*p*-phenylene ethynylene) **18** was quenched by $Fe(CN)_6^{4-}$ in aqueous solution.[27] A Stern−Volmer analysis of the

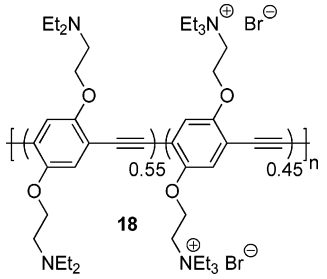

quenching response revealed upward curvature as the quencher concentration increased. The authors attributed the nonlinearity to a sphere-of-action mechanism.[28] The sphere-of-action mechanism has also been put forth to explain the upward curvature in Stern−Volmer plots (also referred to as "superquenching" or a "superlinear" response) for the fluorescence quenching of anionic polyelectrolytes by cationic viologen quenchers.[29] Considering the large enhancements in quenching resulting from increased energy migration pathways, quencher-induced aggregation most likely accounts for the large nonlinear fluorescence quenching response often observed with conjugated polyelectrolytes and oppositely charged quenchers. It should be noted that aggregation of polyelectrolytes also enhances the binding of oppositely charged quenchers. As the reader will see

throughout this review, aggregation instead of a sphere of action mechanism, has been confirmed to be the dominant cause of the upward curvature in Stern−Volmer plots.

Huang and co-workers also investigated polycationic poly(*p*-phenylene vinylene)s.[30] In methanol, the fluorescence of a number of poly(*p*-phenylene vinylene)-based cationic polyelectrolytes was quenched by $Fe(CN)_6^{4-}$. Downward-curving Stern−Volmer plots were obtained from polymers that contained a large number of *cis*-vinyl groups. The presence of two populations of fluorophores was postulated to account for the unusual Stern−Volmer response. Potentially due to a high degree of twisting and coiling of the poly(*p*-phenylene vinylene) chain in materials that contained a high proportion of *cis*-linkages, one of the fluorophore populations may not have been readily accessible to quenchers.

Smith et al. synthesized the disulfonated poly(*p*-phenylene vinylene) **19** and found that its fluorescence was quenched by Eu^{3+} and Cu^{2+}.[31] The Stern−Volmer response to Eu^{3+} was linear over a large concentration range. Fluorescence

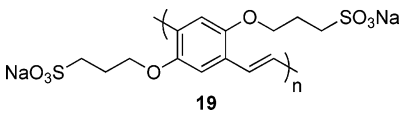

19

quenching by Cu^{2+}, however, produced a nonlinear Stern−Volmer plot that exhibited upward curvature. The authors attributed the response to Cu^{2+} to a sphere-of-action mechanism that became more prominent as the quencher concentration increased. However, we believe that polymer aggregation is likely the proper interpretation.

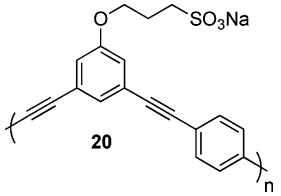

20

The polyanionic *meta*-linked poly(*m*-phenylene ethynylene) **20** has been synthesized by Schanze and co-workers and was shown to undergo solvent-dependent conformational transitions that affected the quenching response (Figure 6).[32] In methanol, a good solvent, polymer **20** appeared to assume a random coil conformation. In water, however, the authors proposed the polymer adopted a helical conformation. The polymer was studied in mixtures of methanol/water that ranged from pure water to pure methanol. As the percentage of water was increased, the polymer's absorption decreased and, consistent with a transition to a helical structure, a larger fraction of the polymer backbone adopted a cisoid conformation, as evidenced by a more significant reduction of the long wavelength absorption attributed to the transoid conformation. The exchange of water for methanol as solvent produced large fluorescence changes as well; as the solvent composition was shifted to larger percentages of water, the fluorescence was reduced and became red-shifted and broad. The broad emission was attributed to the helical conformation of **20** in which the aryl rings were π-stacked, allowing for the formation of an "excimer-like" excited state.

The helical and random-coil conformations of polymer **20** displayed unique responses to $Ru(bpy)_2(dppz)^{2+}$ (bpy = 2,2′-bypyridine; dppz = dipyrido[2,2-*a*:2′3′-*c*]phenazine), a metal complex that is almost nonemissive in aqueous solution but

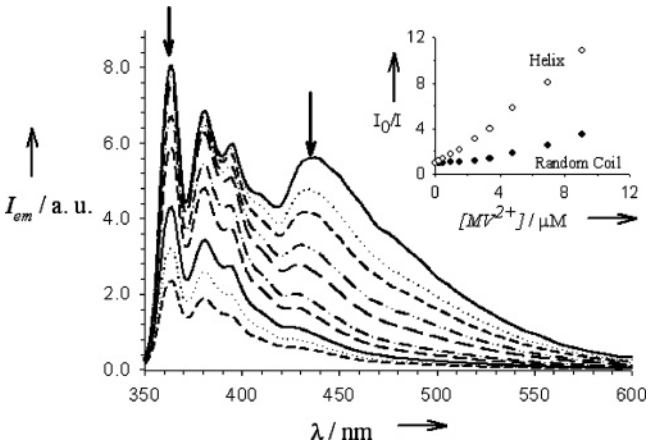

Figure 6. Emission quenching of **20** (2.0×10^{-5} M) by dimethyl viologen in a 7:3 methanol/water mixture. Arrows in the main figure show how the intensity changes with increasing $[MV^{2+}]$. The inset shows the Stern−Volmer plots of the random-coil state (●) and the helix (○), using the emission intensities at 363 and 445 nm, respectively. Linear fits of the quenching plots afforded Stern−Volmer constants of 2.6×10^5 M^{-1} and 1.1×10^6 M^{-1} for the random-coil and helical conformations, respectively. (Reprinted with permission from ref 32. Copyright 2004 Wiley-VCH Publishers.)

becomes emissive upon intercalation into the major groove of DNA. The addition of polymer **20** to an aqueous solution of $Ru(bpy)_2(dppz)^{2+}$ resulted in a large increase in emission from the ruthenium complex. In analogy to the interaction of $Ru(bpy)_2(dppz)^{2+}$ with DNA, the authors proposed the emission increase was due to intercalation of the metal complex into helical **20**. While $Ru(bpy)_2(dppz)^{2+}$ did bind to polymer **20** in methanol, as indicated by fluorescence quenching of **20**, the ruthenium complex did not become more emissive. In methanol, polymer **20** assumed a random coil conformation, thus precluding intercalation of the ruthenium complex and preventing the turn-on response observed in water. The quenching response of **20** to dimethyl viologen (MV^{2+}) in 7:3 methanol/water, a solvent system in which both random coil and helical conformations were present, was investigated. The broad red-shifted emission of the helical conformation was quenched more strongly than the emission emanating from the random-coil conformation. The authors postulated the increased sensitivity of helical **20** was due either to greater delocalization as a result of π-stacking in the helical structure or to the possibility that a bound quencher could interact with a greater portion of the polymer backbone in the helix than in a random coil.

2.2. AFPs with Nitrogen-Based Ligands for Metal Ion Sensing

Pyridine-based moieties such as 2,2′-bipyridine (bipy) and other multidentate amine-containing ligands effectively coordinate a variety of metal ions. They are typically stronger ligands for transition metals than for alkali or alkaline earth metal ions, making them somewhat complementary to crown ethers. This family of ligands has been used as luminescent chemosensors for transition metal ions.[33] Since the first report of 2,2′-bipyridine incorporation into a poly(phenylene vinylene) backbone for metal ion sensing by Wang and Wasielewski,[34] there have been increasing efforts to develop new conjugated polymers for sensitive and selective metal ion sensing and also to fundamentally understand the mechanisms by which this sensing takes place.

In 2001, Huang and co-workers published a study concerning the metal ion sensing properties of three structurally related conjugated polymers, the main chains of which incorporated 2,2′-bipyridine moieties.[35] The purpose of this study was to understand the effect that the structure of the polymer backbone has on metal ion sensitivity. They synthesized conjugated polymers **21**−**23** via Suzuki, Wittig−Horner, and Sonogashira polymerizations, respectively, with number-average molecular weights ranging between 35 and 59 kDa.

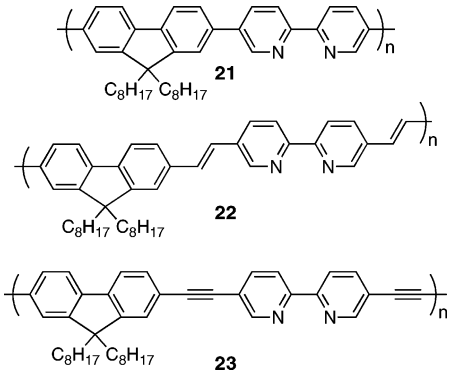

Addition of various transition metals to THF solutions of these polymers caused changes in both their absorption and fluorescence spectra. The fluorescence quenching of **21** by Mn^{2+} is displayed in Figure 7. The authors found that Zn^{2+}, Ni^{2+}, and Co^{2+} caused a large red shift in the absorbance spectra of all three polymers. Ni^{2+} and Co^{2+} also strongly quenched all the polymers at low concentrations (<0.1 ppm) with no observable difference in the sensitivities of the three materials. The similar responses were attributed to very strong coordination of these metals to the bipyridyl groups. Amplification was confirmed by the observation that complete quenching occurred at a 50:1 ratio of receptors to metal ions. Other transition metal ions, such as Mn^{2+}, Pd^{2+}, Ag^{+}, Al^{3+}, Cu^{2+}, Cd^{2+}, and Fe^{2+}, provided much smaller absorbance shifts and much less sensitive fluorescence quenching.

The authors attributed the absorbance spectral red shifts to enhanced planarity of the bipy ligands and changes in the polymer electron density upon metal complexation. In these experiments, **21** always gave the strongest response of the three polymers, whereas **23** consistently gave the weakest response. The authors attributed the higher sensitivity of **21** to weaker resistance (highest backbone flexibility) to coplanarity of the bipy unit when joined by a single bond, as opposed to a double or triple bond.

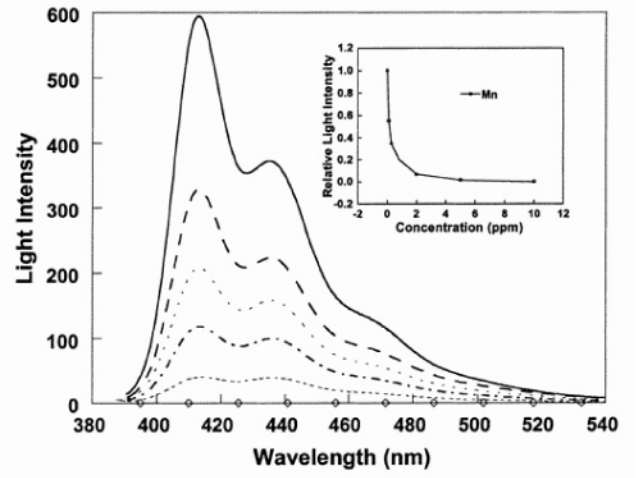

Figure 7. Quenching of the fluorescence of **21** upon addition of different amounts of $MnCl_2$. The inset shows a titration curve for Mn^{2+}/**21** in THF. (Reprinted with permission from ref 35. Copyright 2001 American Chemical Society.)

Extending these studies of the effect of backbone structure on bipy-containing conjugated polymers, Ding and coworkers studied polymer **24**, which showed mostly similar spectral responses and sensitivities to transition metals as observed with **21**−**23**.[36] This polymer, however, showed good sensitivity for Mg^{2+} relative to the other alkaline earth ions. They also investigated other bipy-containing thiophene-based PPVs that showed similar responses to Mg^{2+}.[37] Although the reasons for these specific effects are not completely clear, these combined studies emphasize the importance of backbone structure in developing bipy-based conjugated polymer sensors for metal ions.

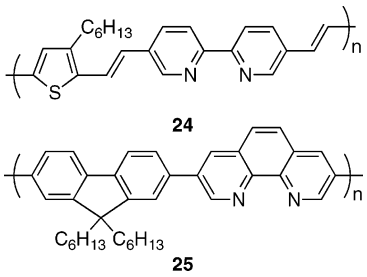

Ma and co-workers have challenged the interpretation that the spectral red shifts that occur upon metal complexation in these materials is primarily due to enhanced conjugation along the polymer backbone.[38] They compared a bipy-containing polymer very similar to **21** to the structurally related polymer **25**, which has a planar 1,10-phenanthroline (phen) unit. They observed similar results to Huang's **21** with their bipy-based polymer, but they found that the binding constants of the metal ions did not correlate with the magnitude of the absorbance red shifts. In addition, although the rigid phen ligand could not provide substantially more conjugation upon metal ion complexation, **25** also showed strong ion-induced red-shifted absorbance spectra. From this, the authors concluded that electron density variations of the polymer chain upon metal complexation, and not conformational changes along the polymer backbone, were the primary causes of metal-induced ionochromic effects. Also, most metal ions quenched **25** more efficiently than **21**, which the authors attributed in part to stronger binding of metal ions to the rigidified phen ligand. Phen-based conjugated polymers have shown ionochromic responses in both absorbance and fluorescence not only to transition metals but also to Li^{+}, Ca^{2+}, and Mg^{2+}.[39]

Wang, Xu, and Lai have also investigated cyclophane-containing conjugated polymers **26** and **27** as metal ion sensors.[40] The fluorescence and absorbance of polymers **26** and **27** were red-shifted relative to those of reference polymers that lack the bipy-containing cyclophane. The red shifts were attributed to electronic perturbation of the conjugated polymer backbone via aromatic CH−π interactions between the conjugated polymer aryl system and bipy-based hydrogen atoms (Figure 8). The authors proposed that the steric influence of the cyclophane moiety may also contribute to the red-shifted absorbance and fluorescence. The fluorescence of polymer **26** was quenched by Cu^{2+}, Co^{2+}, Ni^{2+}, Zn^{2+}, Mn^{2+}, and Ag^{+}. Polymer **27**, however, was only quenched by Cu^{2+}, Co^{2+}, and Ni^{2+}, and it was

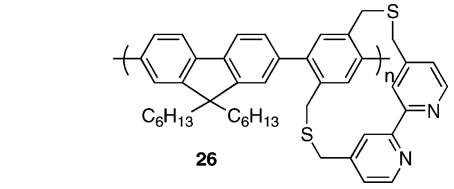

26

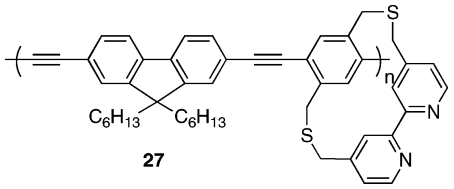

27

quenched less efficiently by these cations than polymer **26**. The authors attributed the different quenching responses to differences in polymer flexibility. The fluorescence quenching by metal ions was not accompanied by shifts in polymer absorbance or fluorescence. The absence of spectral shifts in the presence of metal cations was attributed to the fact that the binding sites in **26** and **27** are not in conjugation with the conjugated polymer backbone.

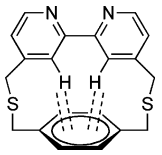

Figure 8. CH$-\pi$ interactions in cyclophane-containing polymers **26** and **27**.

There have been several other studies recently published concerning the metal ion-sensing properties of fluorescent conjugated polymers that incorporate pyridine rings into the backbone. Lee and co-workers reported a poly(pyridyl phenylene)[41] as well as a poly(cyanostyryl) derivative,[42] the fluorescence intensities of which were quenched in the presence of Fe^{3+}. In addition, a series of poly(pyridyl phenylene)s capable of inter- and intramolecular hydrogen bonding have shown strong ionochromic and fluorescence quenching responses to Cu^{2+} and Fe^{3+} in THF.[43]

Fluorescence changes caused by binding-induced aggregation of pyridine-containing conjugated polymer chains have also been explored as a potential signal for more specific metal ion detection. In 2004, Wang and co-workers reported the use of such a design (**28**) to selectively detect Pd^{2+} ions in THF.[44] Monopyridyl groups, which can selectively bind

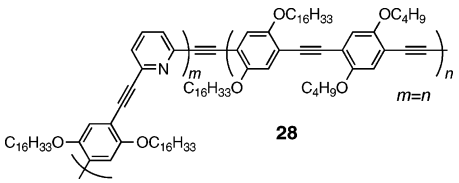

28

Pd^{2+} by self-assembly, were polymerized through a *meta* linkage to encourage backbone flexibility, whereas a more traditional poly(*p*-phenylene ethynylene) segment was included to enhance signal amplification. The fluorescence quenching response of polymer **28** was compared to those of two control polymers, each consisting of one of the two segments of **28**, as well as to that of the small molecule model 2,6-di(phenylethynyl)pyridine (DPP). The Stern−Volmer quenching constant of **28** (4.34×10^5 L mol^{-1}) was 56 times greater than that of DPP, indicating that the

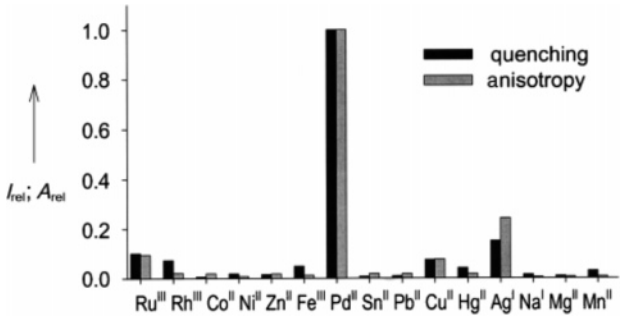

Figure 9. Relative fluorescence quenching and anisotropy values of **28** in the presence of different metal ions. (Reprinted with permission from ref 44. Copyright 2004 Wiley-VCH publishers)

conjugated polymer chain significantly amplified the quenching. In addition, polymer **28** was 144 times more sensitive than a similar polymer that contained no pyridine ligand. As illustrated in Figure 9, **28** showed very good selectivity for Pd^{2+} over many other transition metal ions.

The authors also determined that Pd-induced aggregation of the polymer chains was critical to the high sensitivity of **28** to Pd^{2+}. The evidence for this was a red shifting of the absorbance of **28** that correlated with increasing Pd^{2+} concentration, in addition to fluorescence anisotropy values that correlated with fluorescence quenching as a function of transition metal concentration. These enhanced anisotropy values indicated that the polymer chains were aggregated to give a larger molecular weight adduct. Addition of cyanide to Pd^{2+}-quenched polymer solution restored original anisotropy values and fluorescence intensities.

Conjugated polymer aggregation has also been implicated in the sensing of Ag^+ by polyquinoline **29** via fluorescence quenching, although changes in the electron density along the backbone were also considered as a possible origin of the high Stern−Volmer quenching constant (1.4×10^5 M^{-1}).[45] This value was found to be 15 times higher than

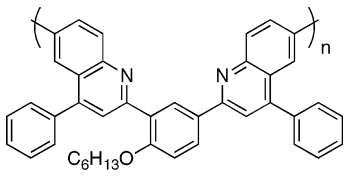

29

that for the monomeric model compound, highlighting the amplification supplied by the conjugated backbone. The authors found the quenching to be reversible upon addition of aqueous ammonia to a THF solution of the quenched polymer. The same group also reported in a related publication that the selectivity of **29** for Ag^+ or Fe^{2+} could be tuned as a function of solvent, which the authors attributed to a combination of metal ion solvation and a solvent-dependent chain conformation.[46]

In addition to **29**, other groups have used non-pyridine nitrogen-based heterocycles in the backbone of conjugated polymers for metal ion and acid sensory purposes. These polymers have included quinoline- and quinoxaline-containing poly(arylene ethynylene)s,[47,48] poly(phenylene vinylene)s containing phenothiazylene and pyridylene groups,[49] an internally hydrogen-bound poly(benzoxazole),[50] and a variety of poly(oxadiazoles).[51]

An alternative strategy to directly incorporating heterocyclic ligands into the conjugated polymer main chain is to

covalently attach them as pendent groups. This more modular approach could allow for the use of a wider variety of ligands with more finely tuned selectivities while still preserving the amplification inherent to conjugated polymers. In 2002, Jones and co-workers described a series of poly[*para*-(phenylene ethynylene)-*alt*-(thienylene ethynylene)s] (compounds **30**−**32**) with pendent oligopyridine groups for metal ion binding.[52] These polymers had identical main chains, but they differed in either the identity of the oligopyridine ligand [bipy (**30**) or terpyridine (ttp, **31** and **32**)] or the nature of the connectivity of the ligand to the backbone [insulated (**32**) or cross-conjugated (**30** and **31**)]. The receptors had only small effects on the intrinsic emission spectra of the materials. Addition of small concentrations (as low as 4×10^{-9} M) of Ni^{2+} to **31** gave easily observed fluorescence quenching in THF, but it had no effect on a model polymer that lacked receptors. Other transition metal ions, such as Cr^{6+}, Co^{2+}, Cu^{2+}, and Mn^{2+}, showed fluorescence quenching responses in THF solution of varying intensities. The polymer that included tridentate ligands (**31**) was more sensitive than **30**. Although the mechanism of quenching for these systems is still indefinite, more recent work suggests that it is highly dependent on the identity of the metal ion.[53]

The authors also determined that although the polymer with cross-conjugated ttp (**31**) receptors was 2.6 times more sensitive to Ni^{2+} than the polymer that employed an insulating ether linkage (**32**), conjugation of the receptors to the polymer backbone was not required for an effective fluorescence response. The insensitivity to how the receptor is attached to the polymer backbone allows for the more flexible design of receptor/backbone combinations to potentially enhance selectivity. Jones used this principle in the 2005 report of fluorescence "turn-on" chemosensors that showed some selectivity toward Hg^{2+} at concentrations above 100 μM, although the "unquenching" mechanism of operation precluded amplification.[54] Lowering the concentration of receptor sites did not give increased sensitivity, which the authors attributed to slow energy transfer along the polymer backbone.[55] Most recently, in 2006, Jones reported the selective fluorescent "turn-on" detection of Fe^{2+} in THF by displacement of prebound Cu^{2+} quenchers from pendent ligands.[56]

Others have also taken advantage of ligands appended on the conjugated polymer for the detection of transition metal ions. In 2004, Pei and co-workers reported the metal-sensing properties of imidazole-substituted poly(fluorene) **33**, which was synthesized by Suzuki coupling with a number-average molecular weight of about 15,000 Da.[57] This polymer, which showed no absorption or fluorescence response to alkali or alkaline earth metal ions, could be completely quenched by Cu^{2+} in THF with a K_{sv} of 1.2×10^7. The polymer-quenching response was ten times greater than that of an oligofluorene model compound, which indicated the amplified nature of the conjugated polymer-based fluorescence quenching response. Solid-state **33** could reversibly detect aqueous Cu^{2+}, as demonstrated by alternately dipping a thin film into $CuCl_2$ and ammonium hydroxide solution. Other metal ions, such as Al^{3+}, Zn^{2+}, Pb^{2+}, Ag^{+}, Co^{2+}, Sn^{2+}, and Cr^{3+}, also partially quenched the fluorescence of **33**. Interestingly, Ni^{2+} only quenched **33** very slightly even at 100 ppm, illustrating the differences in coordination selectivities between oligopyridine and imidazole receptors and further highlighting the potential utility of pendent ligands.

Although it does not involve nitrogen-based heterocyclic ligands, included here is a study Wang and co-workers published in 2005 that involved phosphonate-substituted poly(fluorene)s (**34** and **35**).[58] These materials showed strongly amplified and reversible fluorescence quenching by Fe^{3+} in dichloromethane (Figure 10). The authors also reported strong selectivity for Fe^{3+} over a wide variety of other metal ions. Increasing the number of carbon atoms that constituted the alkyl spacers between the polymer backbone and phosphonate groups from three (**34**) to six (**35**) reduced the K_{sv} for Fe^{2+} by almost a factor of 2, highlighting the strong distance dependence of the fluorescence quenching response. Sensing in ethanol reduced the sensitivity by 1 order of magnitude because of competitive binding of solvent to the phosphonate groups.

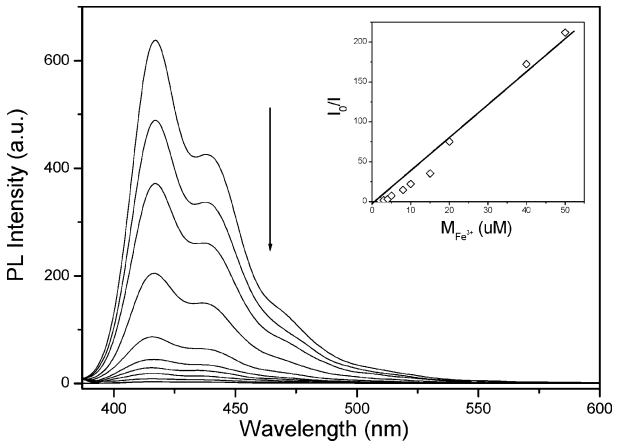

Figure 10. Fluorescence spectra of **34** upon addition of Fe^{3+} in CH_2Cl_2. The inset shows the corresponding Stern−Volmer plot. (Reprinted with permission from ref 58. Copyright 2005 American Chemical Society.)

2.3. The Detection of Fluoride and Other Anions

There has been a substantial effort to develop conjugated polymers that detect cations with high sensitivity and selectivity. Reports of fluorescent polymer sensors for anions, however, have been comparatively scarce. The preponderance of such efforts has focused on fluoride ion detection. The detection of fluoride is of growing interest because of its association with nerve gases as well as the manufacture of nuclear weapons.

Several systems have relied upon the binding properties of fluoride for sensing. In 2002, Miyata and Chujo reported a σ-conjugated organoboron polymer (**36**) that was optically sensitive to fluoride in chloroform due to fluoride coordination to boron.[59] This coordination changed the hybridization

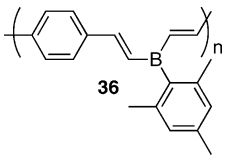

36

of the boron atom from sp^2 to sp^3, which interrupted the conjugation and quenched the emission of the polymer. A significant blue shift in the absorbance spectrum of **36** accompanied the fluorescence quenching, supporting the proposed mechanism. The other halide anions did not affect the fluorescence of the polymer. The reported amplification, however, was disappointing, as even 0.1 equiv of F^- did not produce a response.

Fujiki et al. have used the latent affinity of fluorine and silicon to detect F^- with very high sensitivity (nanomolar range) by fluorescence quenching of **37**, a σ-conjugated poly(silane).[60] The authors observed a high Stern−Volmer

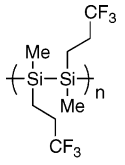

37

quenching constant ($K_{SV} = 1.35 \times 10^7$) upon addition of tetrabutylammonium fluoride (TBAF) to a THF solution of **37**. The response was attributed to a combination of a large number of silicon binding sites on each polymer and the amplification inherent to conjugated polymers. The emission spectrum was not changed by the addition of other halide ions. The terminal trifluoromethyl groups were essential to sensitivity; the fluorescence spectrum of poly(propylmethylsilane) did not exhibit any significant changes upon addition of micromolar concentrations of F^-. The authors attributed the trifluoromethyl-dependent sensitivity to activation of backbone Si atoms to attack by F^-. Also, the interchanging of methyl for a longer alkyl chain such as hexyl gave a material insensitive to TBAF, presumably because of steric effects.

Research groups have also used the basicity and hydrogen-bonding characteristics of fluoride to develop other conjugated polymer sensory materials for fluoride. The group of Wang employed this tactic in 2003, reporting that the phenolic derivative of polyquinoline **29** could sense a 100-fold excess of F^- in DMSO via an amplified red-shifted fluorescence "turn-on" signal.[61] ^1H NMR experiments supported a deprotonation mechanism, whereby the phenolate anion participated in an intramolecular charge-transfer transition with the adjacent quinoline moiety. The less basic Cl^- and Br^- anions showed no response, while ^-OH was a strong interferent. Wang also reported a series of poly(phenylene)s containing phenol-substituted oxadiazole ring systems for the detection of F^- by fluorescence quenching.[62] The authors varied the feed ratio of oxadiazole and fluorene monomers to synthesize random copolymers (one of which was **38**) via Suzuki coupling. Polymer **38** was the most sensitive polymer

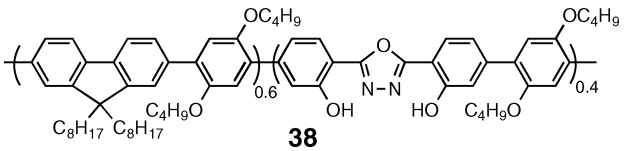

38

of the series to fluoride ($K_{sv} = 7.1 \times 10^5$), due to an optimized combination of high molecular weight and an increased number of binding sites. Polymer **38** also showed approximately 100-fold amplification over a monomeric model compound. All the polymers synthesized were about 1 order of magnitude more sensitive to F^- relative to $H_2PO_4^-$. They were insensitive to Cl^-, Br^-, I^-, BF_4^-, and PF_6^-. On the basis of solvent-dependent quenching and absorbance spectroscopy studies, the authors concluded that the mechanism for this quenching was the formation of an intramolecular charge-transfer interaction in a hydrogen-bonded complex.

In 2006, Sun and co-workers reported **39**, a poly(phenylene ethynylene) based on dipyrrolylquinoxaline (DPQ) units.[63] The authors observed both a red-shifted colorimetric response and fluorescence quenching ($K_{sv} = 5.2 \times 10^4$) upon the

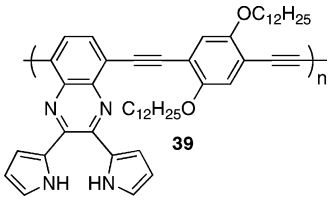

39

addition of TBAF in CH_2Cl_2. NMR experiments and mass spectroscopic analysis indicated that the photophysical perturbations upon fluoride addition were due to deprotonation of the DPQ unit. Although **39** showed 34-fold amplification over a small molecule model compound, it did not show significant selectivity for F^- over phosphate.

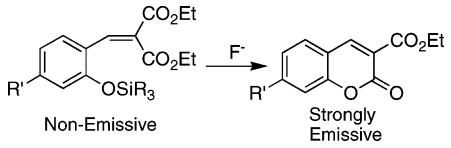

Figure 11. Fluoride-triggered coumarin dye formation used by Kim and Swager for turn-on wavelength-responsive F^- detection.

In 2003, Kim and Swager reported a fluoride-sensing system triggered by the unique chemical reactivity of F^- with silicon.[64] The authors developed a fluoride ion-triggered formation of coumarins, a family of strongly emissive laser dyes, as illustrated in Figure 11. Bulky silyl protecting groups provided selectivity for fluoride, and the diethyl malonate group avoided potential problems associated with double-bond isomerization. In order to achieve amplification, the authors electronically coupled the indicator to the band structure of a poly(phenylene ethynylene) (**40**) through a

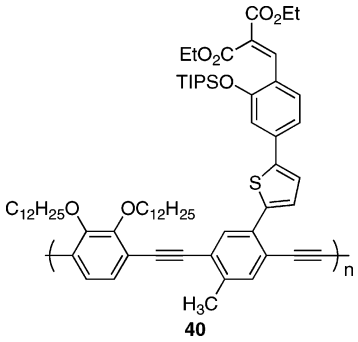

40

thiophene ring. Polymer **40**, with a molecular weight of 10 kDa, was synthesized by Sonogashira polymerization. The formation of a small number of local band gap traps upon reaction with fluoride resulted in facile electron-exchange (Dexter) energy transfer from the polymer to the dye to provide an amplified fluorescence "turn-on" sensory methodology (Figure 12). The authors found that the polymer was 100-fold more sensitive to F^- than a corresponding small molecule.

Although most anion-sensitive, fluorescent, conjugated polymer sensors have focused on fluoride, there have been several reports of related materials designed for the detection of other anions. For example, Lee and co-workers described a hydroxide-sensing bipyridine-based polymer linked with cyanostyryl groups.[65] Also, Ho and Leclerc reported in 2003 the colorimetric and fluorometric detection of iodide in deionized water using a cationic poly(3-alkoxy-4-methylthiophene).[66] The mechanism for this fluorescence modulation, which will be discussed in the DNA sensing section, is analyte-promoted aggregation and planarization of the polymer backbone. In this study, hydrophobic anions such as PF_6^-, BF_4^-, SCN^-, and ClO_4^- were interferents.

3. Detection of Explosives

The detection of trace explosives is a problem of increasing importance and one that researchers from many scientific fields have been addressing for years. Nevertheless, undetected explosives remain a major security concern in airports and other security checkpoints important for homeland security, as well as in less-controlled environments, such as battlefield locations, where the detection of land mines and other explosive devices is vitally important. Summaries of many of the various technologies designed for trace explosives detection have recently appeared in the literature and are beyond the scope of this review.[67,68]

Many explosives are highly nitrated organic compounds such as nitroaromatics, nitramines, or nitrates. This property renders them electron-deficient. This electron deficiency has been important in explosives detection using methods such as gas chromatography coupled with electron capture detection (GC/ECD) and the widely used negative polarity ion mobility spectrometry (IMS).

Good electron acceptors can efficiently quench fluorescence by photoinduced electron transfer. In 1998, Yang and Swager used a fluorescence quenching transduction mechanism together with the amplifying nature of conjugated polymers to design **41**, a material highly sensitive to TNT vapor.[6,9] TNT is the major explosive component of most land mines. An important design feature of **41** is the rigid pentiptycene group, which prevents the polymer chains from strongly aggregating and self-quenching in the solid state. These effects are important because a solid-state thin film allows for multidimensional exciton transport and higher

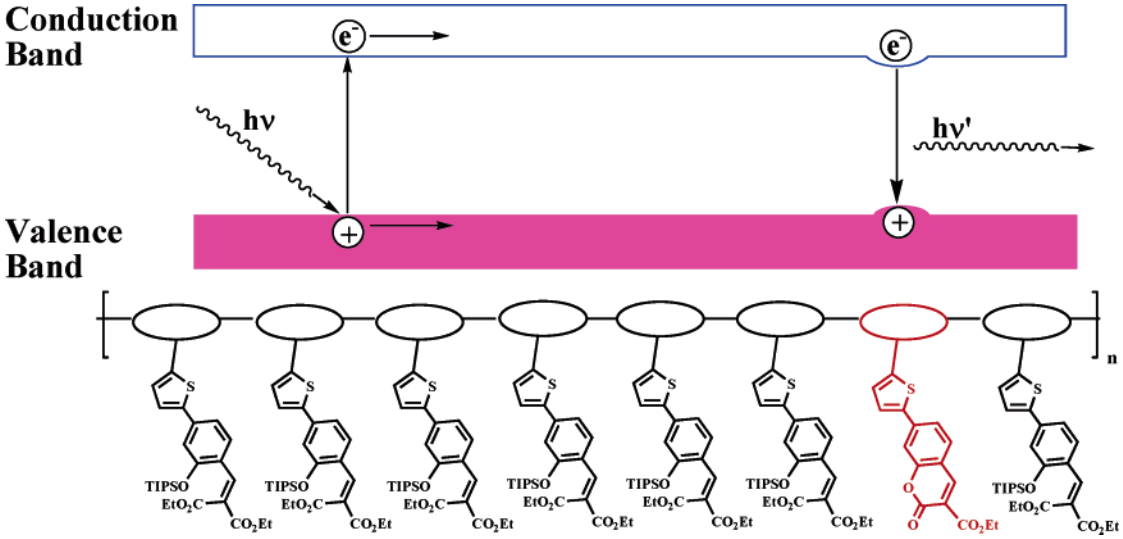

Figure 12. Mobile excitons created by photoexcitation migrate along the backbone of **40**. Fluoride-induced lactonization of side chains produced trapping sites with a smaller band gap that gave a new amplified emission. (Reprinted with permission from ref 64. Copyright 2003 Wiley-VCH publishers.)

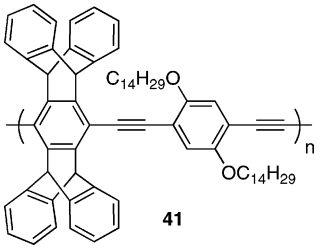

41

amplification, which are critical for successful ultratrace detection.[69]

ICx Nomadics, Inc., has developed several versions of a sensory device built around the high sensitivity of **41** for the detection of TNT vapor, as well as a common contaminant in land mines, 2,4-dinitrotoluene (DNT), which has a higher vapor pressure than TNT. This commercially available device, called "Fido", allows for the real-time monitoring of conjugated polymer thin-film fluorescence intensity while simultaneously exposing the film to vapors. Femtogram sensitivity to TNT was demonstrated during Fido device testing in 2001. In field tests with buried land mines, Fido exhibited sensitivity and selectivity comparable to those of trained canines.[70] This is the only known technology to achieve such strong performance in the field.

The Swager group has reported several sensitivity-enhancing improvements to the TNT-sensing material. Amplification depends strongly on how many binding sites each exciton can visit. One potential way to improve this quantity is to increase the fluorescence lifetime of the sensing material. If each exciton has a longer time before it decays intrinsically to the ground state, excitons may be able to sample more locations within the polymer film. Fused polycyclic aromatics often have forbidden or weakly allowed transitions that can result in longer excited-state lifetimes. In 2001, Rose, Lugmair, and Swager reported a series of PPEs that incorporated triphenylene moieties into the backbone of a conjugated polymer, such as **42**.[71]

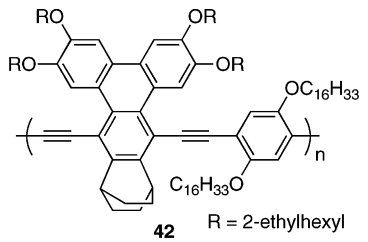

42 R = 2-ethylhexyl

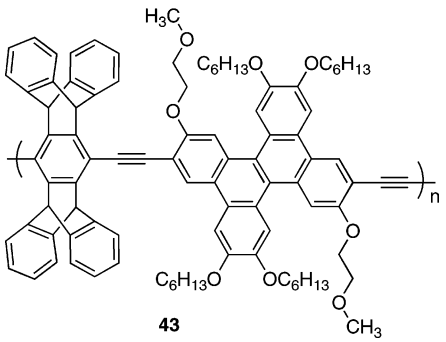

43

Relative to the more traditional phenylene-based PPEs, the authors found that the triphenylene-containing PPEs had longer excited-state lifetimes. In addition, fluorescence depolarization measurements of high molecular weight triphenylene-based PPEs showed larger fluorescence depolarization than the analogous phenylene polymers. The materials studied were of high enough molecular weight to be considered rotationally static over the emission lifetime of the polymer. Therefore, the increased depolarization was due to greater diffusion along each disordered polymer chain. Also in 2001, Yamaguchi and Swager reported dibenzochrysene-based PPEs such as **43** that have excited-state lifetimes between 1 and 3 ns (corresponding phenylene-based materials have sub-nanosecond lifetimes).[72] Sensing experiments with these polymers showed that they had higher sensitivity to TNT than polymers such as **41** and **42**.

In 2002, Zahn and Swager demonstrated that three-dimensional electronic interactions enhance exciton transport and TNT sensitivity.[73] On the basis of solvent-dependent circular dichroism and absorbance spectroscopy, the authors found that enantiomerically pure **44** formed restricted chiral

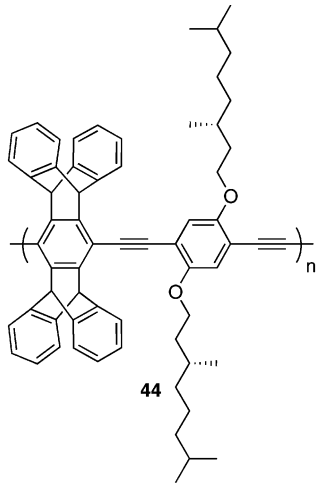

44

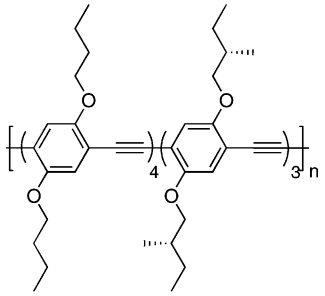

45

aggregates in a poor solvent (methanol) yet still retained the majority of its fluorescence intensity ($\Phi = 0.61$). A similar polymer lacking iptycene groups, **45**, formed chiral aggregates with strongly decreased fluorescence intensity in 40% methanol/chloroform but ultimately favored a stronger aggregate with coincident alignment of polymer chains at methanol concentrations higher than 50%. The unique photophysical properties of **44** in the aggregated state were attributed to an interlocked structure that required the presence of the pentiptycene groups, which hinder $\pi-\pi$ stacking in an edge-on conformation.

This unique aggregated state of **44** also showed sensitivity enhancements toward nitroaromatics. In solution, fully aggregated **44** was 15-fold more sensitive to fluorescence quenching by TNT and DNT compared to the fully solvated polymer. In addition, spun-cast films of aggregated **44** had a 4-fold increase in sensitivity toward TNT vapor (75% fluorescence quenching within 10 s) over optimized thin films of **41**. This data is summarized in Figure 13. The

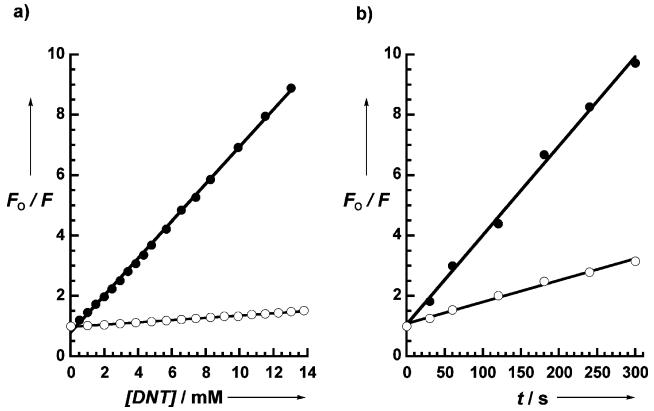

Figure 13. (a) Stern−Volmer plots of **44** in nonaggregated (○) and aggregated forms (●). (b) Stern−Volmer plots for thin films of **41** (C_{16} chains, ○) and **44** (●) upon exposure to TNT vapor. (Reprinted with permission from ref 73. Copyright 2002 Wiley-VCH publishers.)

increased sensitivity of the fluorescent, chiral aggregate was proposed to derive from an improved exciton diffusion length in the 3D-coupled chiral grids and extension of the polymer conjugation length in the highly organized aggregate structure.[74]

Bulovic, Swager, and co-workers have also demonstrated how lasing action in organic polymers can provide higher sensitivities to nitroaromatic analytes.[75] In principle, any organic conjugated polymer can lase. For practical applications, however, the material must be able to survive the punishing optical pumping conditions required to induce the necessary population inversion. This is a challenging goal, especially under ambient conditions and with extended operation times, both of which are necessary for many sensing applications. Swager and co-workers designed and prepared **46**, which is emissive in the solid state ($\Phi = 0.80$)

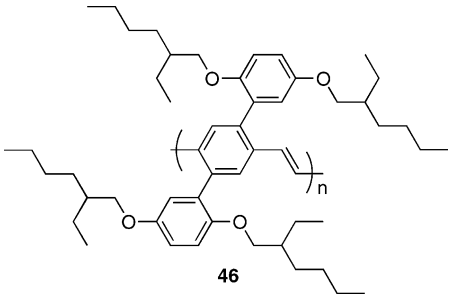

46

and exceptionally stable to photobleaching. These favorable properties were attributed to the pendent aromatic rings encapsulating the polymer backbone in a protective sheath that prevents self-quenching and photobleaching. Optical pumping of this material with a nitrogen laser gave amplified spontaneous emission (ASE) at 535 nm. The ASE performance of **46** compared favorably with other demonstrations of stimulated emission of organic materials and can be attributed to an improved molecular design that maximizes thin-film absorption and luminescence efficiency.

It was found that the ASE signal was up to 30 times more sensitive to quenching than the spontaneous emission upon exposure of the film to saturated DNT vapor for 1 s. By using a ring-mode lasing structure, the higher sensitivity of the ASE signal to saturated TNT vapor is obvious, as illustrated in Figure 14. The mechanism for increased ASE sensitivity can be understood in terms of excited-state

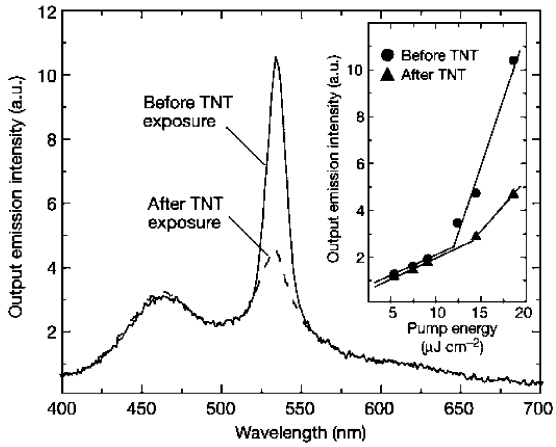

Figure 14. Spectral response of a ring-mode structure of **46**. ASE attenuation in the absence of spontaneous emission attenuation (solid line) and after a 1.5 min exposure to saturated TNT vapor pressure (dashed line). Inset: plots of ASE peak emission intensity (λ = 535 nm) as a function of excitation power. TNT exposure increases the pump energy threshold.

kinetics. The lasing threshold for a material (the minimum pump energy at which ASE can be observed) depends strongly on the material's emission lifetime; shorter lifetimes result in higher lasing thresholds, while longer lifetimes give lower lasing thresholds by allowing more emissive excitons to build up in the system. Introduction of a quencher decreases the lifetime of the average exciton within the material, thereby resulting in an increased lasing threshold. Therefore, pumping the material close to the intrinsic lasing threshold maximized trace sensitivity with ASE.

In 2005, Zhou and Swager reported a nitroaromatic quenching study of poly(iptycenebutadiynylene)s (**47**−**49**) that contained elaborated iptycene structures with electron-donating alkoxy groups.[76] TNT, DNT, *p*-mononitrotoluene, and even benzophenone efficiently quenched these polymers in chloroform solution. Unlike **41**, these materials showed significant static quenching constants (up to 185 M^{-1} for **48** and TNT), indicating ground-state associations between these polymers and the nitroaromatic quenchers. The association was attributed to a strong tendency of the electron-rich dialkoxyphenyl rings on the "wings" of the iptycene groups to associate with the electron-deficient analytes via electrostatic and $\pi-\pi$ interactions. These polymers, however, showed a slower quenching response to DNT and TNT in the thin film relative to **41**. In addition, compared to the case of **41**, the fluorescence of these polymers recovered much more slowly after removal of TNT or DNT vapor. These observations were attributed to the unique quencher-sequestering property of these polymers. This example illustrates that solid-state sensitivity can be governed by different factors than those that determine solution-state quenching efficiency.

Trogler and Sailor have published several papers detailing how poly(silole)s can be used for the detection of nitroaromatics by amplified photoinduced electron-transfer quenching.[77] Poly(silole)s, such as poly(tetraphenyl-1,1-silole) **50**, have a Si−Si backbone. Like poly(silane)s, poly(silole)s demonstrate delocalization of σ electrons along the main chain. In addition, the unsaturated five-membered ring of **50** shifts the band gap into the visible region of the electromagnetic spectrum.These polymers feature a helical structure and fluoresce efficiently in the solid state. An initial communication on this subject focused on using **50** to detect

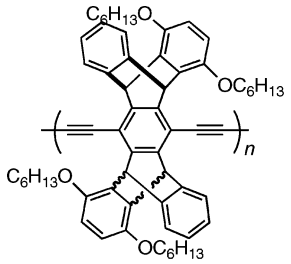

47

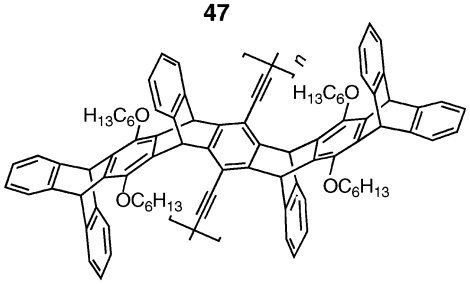

48

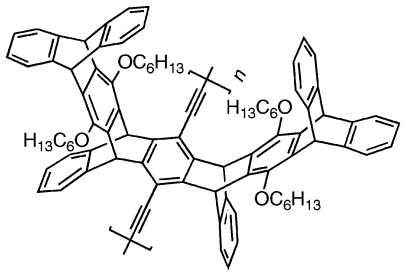

49

TNT in seawater and on surfaces.[78] The authors observed efficient fluorescence quenching of thin films immersed in seawater only when it was spiked with 50 ppb TNT. They also observed a 38% increase in fluorescence quenching of **50** relative to an oligomeric model compound, attributed to a shorter diffusion length of the exciton in the oligomer. The films also showed sensitivity to TNT vapor in oxygenated air, with an 8.2% decrease in emission intensity over a 10-min exposure to 4 ppb TNT. Aqueous acids such as H_2SO_4 or HF did not interfere with the response. Nevertheless, the response to TNT vapor was significantly smaller than the 50% quenching of **41** achieved in 1 s.[76]

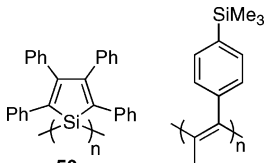

50

51

A later publication by Trogler, Sailor, and co-workers compared the nitroaromatic-induced quenching efficiencies of a series of 12 different poly(metallole)s (including Si- and Ge-based materials).[79] The authors observed large quenching constants for these materials toward nitroaromatics in toluene solution, with K_{sv} as high as 4340 M^{-1} for TNT and 11,000 M^{-1} for picric acid. They observed no change in polymer lifetime upon addition of TNT, which indicated a static quenching process. This difference between the stronger solution-state performance of **50** in organic solvent and the

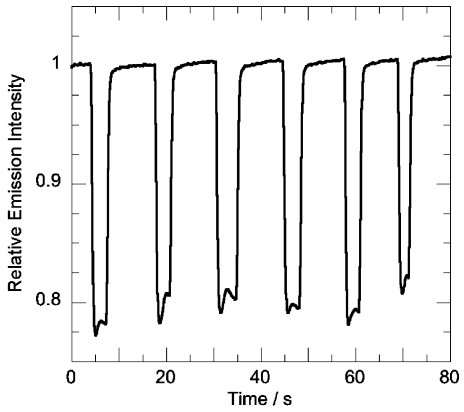

Figure 15. Emission intensity response of a film of **52** to repeated exposures to equilibrium DMNB vapor. (Reprinted with permission from ref 87. Copyright 2005 Royal Society of Chemistry.)

superior vapor sensing capabilities of **41** highlights the profound differences that can occur between solution and solid-state behavior with fluorescent conjugated polymer sensors. The authors suggested that because each of the 12 polymers they studied exhibited a different ratio of fluorescence quenching for the nitroaromatic analytes investigated (TNT, DNT, nitrobenzene, picric acid), a sensor array of these materials combined with pattern recognition methods could be useful for analyte detection and identification.[80] More recently, Trogler and co-workers have reported the use of luminescent silole nanoparticles for the sensing of aqueous TNT[81] and Cr(VI).[82]

In addition to the Swager and Trogler groups, other research groups have reported fluorescent conjugated polymers that have shown sensitivity to nitroaromatic molecules by amplified fluorescence quenching. Schanze and co-workers showed that thin films of the fluorescent diaryl poly(acetylene) **51** are readily quenched by DNT vapor, as well as the vapors of other nitroaromatic molecules.[83] Hsieh compared the nitroaromatic vapor-quenching efficiencies of a series of PPV thin films.[84] Wang detailed the development of a PPE-based optode for the selective sensing of *o*-mononitrophenol.[85] Earlier this year, Lee and co-workers reported on the solution-state static quenching of oxadiazole-based conjugated polymers by picric acid, DNT, and *m*-dinitrobenzene.[86]

In addition to nitroaromatic molecules, there are other explosives that pose challenges for detection by fluorescent conjugated polymers, particularly plastic explosives. The Swager group targeted 2,3-dimethyl-2,3-dinitrobutane (DMNB) as a target analyte because it is a taggant that is added to nearly all legally manufactured plastic explosives.[87] DMNB has a reduction potential of −1.7 V vs SCE (reduction potential of TNT is −0.7 V). This unfavorable reduction potential makes photoinduced electron-transfer quenching with **41** endergonic, and therefore, no quenching was observed when DMNB was added to **41** in solution or when thin films of **41** were exposed to DMNB vapor. To increase the driving force for fluorescence quenching, the class of blue-shifted poly(phenylene-*co*-fluorene)s was investigated for this application. Polymer **52** has a band gap 0.3 eV larger than that of **41**, and this extra excitation energy allowed for efficient fluorescence quenching via a diffusion-controlled dynamic biomolecular quenching mechanism. **52** was the most efficient of the polymers screened for solid-state

quenching by DMNB vapor (equilibrium vapor pressure ~ 3 ppm), giving ~20% fluorescence quenching that was reproducible and reversible (Figure 15).

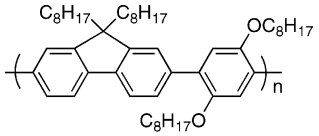

52

Because many potential analytes contain hydrogen-bond acceptors, Amara and Swager reported derivatives of **41** that incorporated strong hydrogen-bond donors, hexafluoroisopropanol (HFIP) groups.[88] Polymers **53** and **54** showed strong

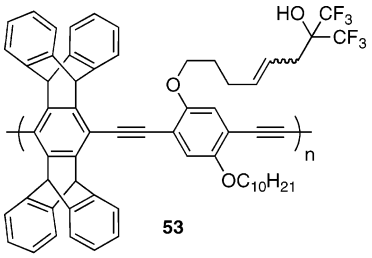

53

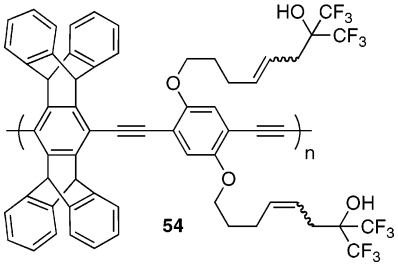

54

decreased fluorescence intensity upon exposure to pyridine vapor, while **41** did not. The authors concluded that the HFIP groups not only increased analyte−polymer interactions but also activated the analytes for photoinduced charge-transfer quenching by modulation of their electronic properties.

In 2006, Thomas and Swager reported that fluorescent conjugated polymers could be used to detect trace hydrazine (a component of liquid rocket fuel) vapor via a fluorescence turn-on mechanism.[89] It was found that the highly electron-rich **55** was the most sensitive to hydrazine vapor of the

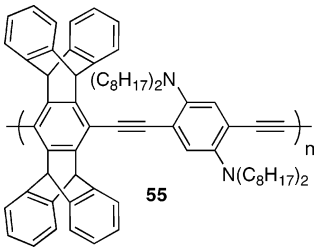

55

materials screened, giving a 2-fold increase in emission intensity with no change in the spectral shape or position of the emission. The proposed mechanism is hydrazine reduction of oxidized defect quenchers in the polymer film to give an amplified turn-on response. The sensitivity of this method was below 1 ppm, the permissible exposure limit of hydrazine.

4. Conjugated Polyelectrolytes as Biosensors

4.1. Early AFP Biosensing Reports

The use of fluorescent conjugated polymers in biosensing applications has undergone enormous growth in recent years. For the most part, this growth has been driven by the use of conjugated polyelectrolytes (CPEs), conjugated polymers that are functionalized with ionic side chains.[90] These water-soluble materials have come to dominate the application of conjugated polymers to biosensing. Much of the activity in this area was spurred by a publication by Whitten and co-workers in 1999 that was pointed out in our Introduction.[3] These authors reported fluorescence quenching of poly(2-methoxy-5-propyloxy sulfonate phenylene vinylene) (**56**), a

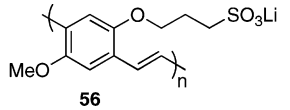

56

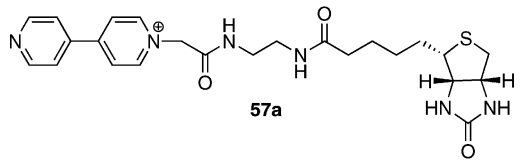

57a

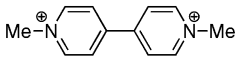

57b

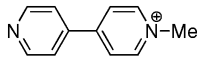

57c

conjugated polyelectrolyte first reported by Shi and Wudl in 1990,[91] with dimethyl viologen (**57b**) ($K_{SV} = 1.7 \times 10^7$) in water. As we pointed out in the Introduction, the high sensitivity is properly credited both to strong association between the cationic quencher and the polyanionic conjugated polymer and to efficient exciton transport to quencher sites. The quenching response was attributed to a dominant electron-transfer mechanism involving the viologen quencher. Analyte-induced polymer aggregation may also contribute to the quenching response. Polymer fluorescence was quenched by divalent metal cations including Ca^{2+} and Mg^{2+}, consistent with polymer **56** fluorescence quenching due to cation-induced aggregation. The fluorescence-quenching response of **56** to dimethyl viologen was asserted to be amplified by more than a factor of a million relative to that of a "similar" small molecule. However, the small molecule model (*trans*-stilbene) used to provide a reference point was a poor choice. Unlike **56**, stilbene lacks anionic residues. Therefore, in comparison to polymer **56**, stilbene was unable to participate in the same attractive electrostatic interactions with dimethyl viologen. The strikingly high quenching "amplification" reported for polymer **56** relative to stilbene can reasonably be attributed both to a significantly higher association constant between **56** and the viologen quencher and to conjugated polymer-based exciton transport. Although exciton delocalization likely played a role, the electrostatic advantage of conjugated polyelectrolyte **56** may well have been the dominant factor contributing to the greater sensitivity of the polymer versus *trans*-stilbene.

The biotin-functionalized viologen quencher **57a** also quenched **56** fluorescence in aqueous solution.[3] Addition of avidin to a solution of polymer **56** and the biotin-functionalized viologen **57a** resulted in an unquenching, or fluorescence turn-on, response. The authors attributed the fluorescence increase upon exposure to avidin to binding of the biotin-functionalized viologen by avidin. The avidin-bound quencher was proposed to be sterically encumbered, thus preventing close association of quencher with conjugated polymer and producing the fluorescence recovery. Relevant control experiments demonstrated that the response was due to specific biotin−avidin interaction; addition of avidin to a

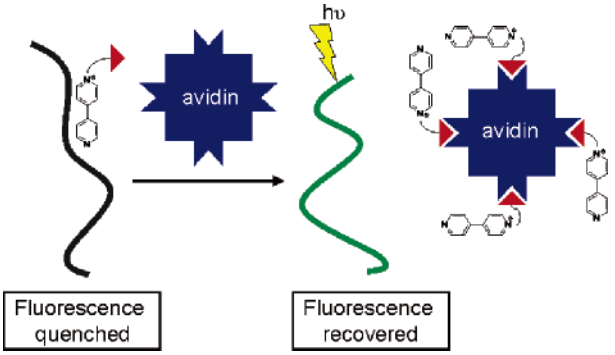

Figure 16. Whitten's quencher−tether−ligand-based strategy to biosensing. Addition of avidin to a solution of conjugated polyelectrolyte **56** and biotin-functionalized quencher **57a** resulted in a turn-on (fluorescence recovery) response.

solution of conjugated polyelectrolyte quenched by *N*-methyl-4,4′-pyridylpyridinium (**57c**, a quencher lacking biotin functionality) resulted in no fluorescence recovery, and avidin alone did not modulate the fluorescence intensity of **56**. The authors speculated that their fluorescence recovery strategy might be generally applicable to conjugated polymer-based biosensing. Indeed, the strategy has found further use in biosensing applications. Polyelectrolytes have dominated the biosensing arena. As will be revealed later in this review, however, they are prone to nonspecific interactions and complexities due to other charged ions.

Whitten and co-workers have applied their "QTL"- (the name, short for "quencher−tether−ligand", used to describe quenchers such as **57a**) based approach to developing analogous sensory systems for the detection of cholera toxin and hepatitis C (Figure 16).[92] Their cholera toxin sensor involved the use of a viologen-based quencher that was tethered to an oligosaccharide. The oligosaccharide employed was known to bind to the B subunit of cholera toxin. Addition of the oligosaccharide-functionalized quencher to a solution of polymer **56** resulted in fluorescence quenching. Fluorescence was recovered upon adding the recognition portion of cholera toxin.

The assay for hepatitis C relied on antibody−antigen binding.[92] An oligohistidine-tagged antibody to hepatitis C was generated. The assay was carried out by quenching polyelectrolyte **56** emission with Cu^{2+}. Addition of the oligohistidine-tagged antibody resulted in additional fluorescence quenching. The authors proposed that the histidine-tagged antibody bound Cu^{2+} and that the antibody−Cu^{2+} complex was a more potent quencher than Cu^{2+} alone. Addition of hepatitis C to a quenched solution containing polymer **56**, Cu^{2+}, and the histidine-tagged antibody resulted in fluorescence recovery.

Whitten et al. also evaluated **56**-coated beads as biosensory materials.[93] In contrast to free polymer **56**, the polymer-coated beads were not quenched by dimethyl viologen. Anionic anthroquinone-2,6-disulfonate, however, did quench the beads. Polymer fluorescence was also quenched by a biotin-functionalized anthroquinone quencher ($K_{SV} \approx 10^5$); avidin (3.7 μM) almost completely reversed this quenching. Combining anionic conjugated polyelectrolyte **56** with a dye-functionalized, cationic poly L-lysine-based polymer resulted in energy transfer from **56** to a J-aggregated state of the polylysine-bound dye. The efficient energy transfer provided evidence that the oppositely charged polymers associated with each other in solution. Although the complex between **56** and the lysine-based polymer (or aggregates of these two macromolecules) was likely overall charge neutral, the polymer mixture displayed behavior that was consistent with the individual behavior of each polymer; both cationic and anionic quenchers attenuated the fluorescence of the polymer mixture.

Song and co-workers employed a cationic poly(acetylene) in a fluorescence-based assay for avidin.[94] Their sensory system, although similar to Whitten's avidin sensor, was unique in that it used a conjugated polymer as the fluorescence quencher as opposed to the fluorophore. Water-soluble cationic polyacetylene **58** was employed as a fluorescence

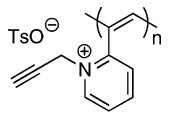

58

quencher for fluorescent biotin-functionalized Lucifer Yellow dyes. The sulfonate-functionalized dyes were anionic and, due to electrostatic attraction, associated strongly with the cationic conjugated polymer in water. Upon complexation with **58**, energy transfer from the dye to **58** efficiently quenched Lucifer Yellow fluorescence. Addition of avidin to a solution of biotin-functionalized dye and conjugated polyelectrolyte resulted in recovery of Lucifer Yellow fluorescence, thus providing an assay for avidin. Detection of avidin at a concentration of 1 nM was demonstrated.

4.2. Conjugated Polyelectrolytes and Viologen Quenchers

In the years since Whitten and co-workers published their often-cited 1999 paper,[3] the application of fluorescent conjugated polyelectrolytes to sensing in aqueous environments has intensified. In particular, the fluorescence response of anionic conjugated polyelectrolytes to viologen quenchers has been extensively studied. Heeger et al. investigated the fluorescence quenching of an anionic butoxy-substituted poly(*p*-phenylene vinylene) (**59**) by dimethyl viologen.[95] The

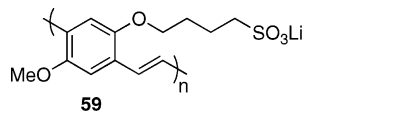

59

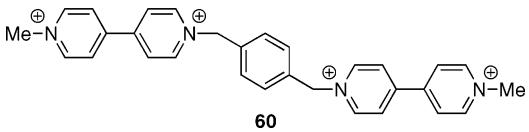

60

authors proposed that the anionic conjugated polymer and cationic quencher formed an electrostatic complex in low ionic strength solutions. Consistent with a static quenching mechanism, variable temperature quenching studies revealed that the quenching response decreased as temperature increased. Quenching was most effective in pure water, in which the estimated binding energy between dimethyl viologen and anionic polymer **59** was determined to be about 150 meV with a mean quencher−polymer distance of 10 Å. The presence of aqueous buffer significantly reduced the effectiveness of dimethyl viologen as a quencher, as buffer ions screened the electrostatic attraction between the conjugated polyelectrolyte and the complementarily charged quencher. Therefore, the polymer−quencher binding energy decreased with increasing ionic strength. The Stern−Volmer

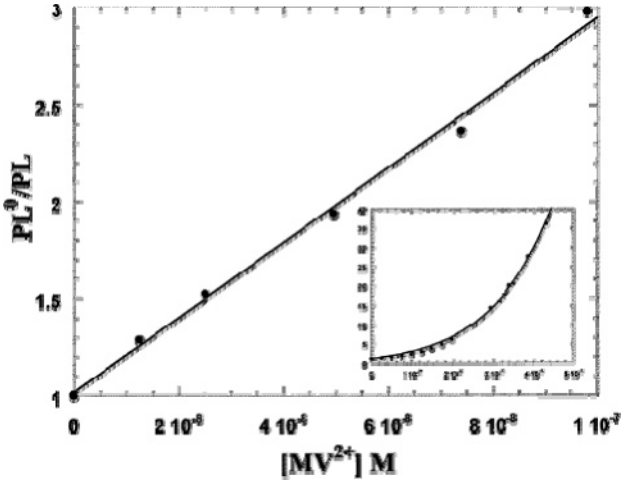

Figure 17. Stern−Volmer plot for the fluorescence quenching of conjugated polyelectrolyte **59** by dimethyl viologen in water. Inset: the same plot extended to higher quencher concentration (from 1×10^{-8} M to 4.3×10^{-7} M), where the plot exhibited upward curvature. (Reprinted with permission from ref 95a. Copyright 2000 American Chemical Society.)

plot for fluorescence quenching of polymer **59** by dimethyl viologen was linear at low quencher concentration, allowing for the determination of the Stern−Volmer quenching constant. However, as quencher concentration increased, the plot displayed upward curvature, or "superlinear behavior" (Figure 17). The authors attributed the superlinear response to a sphere-of-action quenching mechanism[28] that became significant at high quencher concentration. Although reasonable fits of the quenching data with conventional equations were obtained, a number of subsequent studies to be discussed later in this review show that the overwhelming reason for the upward curvature in polyelectrolyte quenching with multivalent cations is polymer aggregration.

Heeger and co-workers also examined the charge dependence of the fluorescence quenching response.[96] In general, as the degree of positive charge on the viologen quencher increased, so too did the observed quenching constant. Viologen **60** ($K_{SV} = 2.2 \times 10^7$ in water), which carried an overall charge of +4, was the most effective quencher they examined. This study also confirmed the negative effect of buffer ions upon quenching efficiency. At high ionic strength, the quenching efficiency of cationic viologens was greatly reduced. However, increased solution ionic strength did not affect fluorescence quenching by a neutral quencher, 4,4′-dipyridyl. These results support a quenching mechanism for cationic viologens that involves the formation of an electrostatic polymer−quencher complex. In addition to changes in total charge, the effect of adding hydrophobic groups to the viologen quencher has also been investigated by Heeger and co-workers.[97] Dimethyl-, diethyl-, di-*n*-hexyl-, and dibenzyl viologen were all evaluated. The quenching constants increased with increasing hydrophobicity of the viologen side chains. Dibenzyl viologen was the most effective, and most hydrophobic, quencher of those investigated.

Surfactants exert a strong influence on the fluorescence of polyelectrolyte **56** as well as on the fluorescence quenching response to dimethyl viologen. Whitten and co-workers found that polymer **56** fluorescence increased by about a factor of 20 in the presence of the detergent dodecyltrimethylammonium bromide.[98] The increased fluorescence efficiency was ascribed to the formation of an electrostatic complex between the anionic polymer and the cationic surfactant that served to inhibit polymer aggregation and to straighten the polymer backbone. Consistent with these proposed changes, polymer absorption was sharper and red-shifted in the presence of surfactant. In addition, whereas a pure aqueous solution of **56** exhibited excitation wavelength-dependent fluorescence, in the presence of the surfactant, this site-selective fluorescence was diminished. Surfactant also had a large effect on fluorescence quenching; the quenching constant for dimethyl viologen dropped more than 100-fold in a surfactant-containing solution compared to that of pure water. In contrast, the presence of surfactant increased the sensitivity of polyelectrolyte **56** to neutral quenchers such as 2,4,6-trinitrotoluene (TNT).[99] Small angle neutron scattering provided additional evidence that polyelectrolyte **56** formed aggregates in aqueous solution and that polymer aggregation was inhibited by the surfactant dodecyltrimethylammonium bromide.[100]

Bazan, Heeger, and co-workers investigated the water-soluble phenylene vinylene oligomer **61** as an oligomeric model of polyelectrolytes **56** and **59**.[101] Dimethyl viologen quenched the fluorescence of the sulfonated oligomer with a Stern−Volmer constant of 4.5×10^5 in water. The

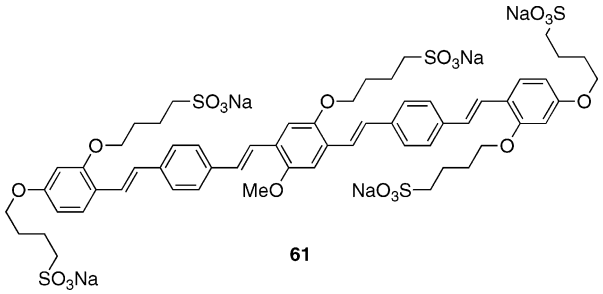

61

oligomer quenching response was approximately 38-fold less sensitive toward dimethyl viologen in comparison to those of conjugated polyelectrolytes **56** and **59**.[3,95] Light scattering experiments revealed that **61** aggregated in aqueous solution. Upon addition of dodecyltrimethylammonium bromide as a surfactant, emission from oligomer **61** increased by a factor of 6. This response was similar to, although not as large as, the increased fluorescence efficiency of polyelectrolyte **56** in the presence of surfactant.[98] However, in contrast to the case of polyelectrolyte **56**, the fluorescence quenching response of oligomer **61** to dimethyl viologen increased with increasing surfactant concentration; at $[\mathbf{61}] = 4 \times 10^{-6}$ M and [surfactant] $= 1.56 \times 10^{-6}$ M, $K_{SV} = 1.2 \times 10^6$. Oligomer **61** actually provided higher sensitivity than conjugated polyelectrolyte **56** in surfactant-rich solution. The enhanced sensitivity of the oligomer in the presence of surfactant was attributed to the formation of smaller aggregates with greater surface area. Bazan, Heeger, and co-workers also studied fluorescence quenching of cationic oligo- and polyfluorenes by anionic phenylene vinylene oligomer **61**.[102] Quenching of fluorene-based emission was due to energy transfer to **61**. Fluorescence quenching of a polycationic polyfluorene by **61** exhibited an unusual dependence upon surfactant (sodium dodecylsulfate) concentration. Upon addition of small amounts of surfactant, the quenching response was reduced. However, as the surfactant concentration increased, a turning point was reached at which the addition of more surfactant resulted in enhanced sensitivity. The increased sensitivity at high surfactant concentration was attributed to surfactant-induced aggregation-state changes.

Dalvi-Malhotra and Chen studied the impact of the surfactant 1,2-dioleoyl-3-trimethylammonium propane (DOTAP) on the fluorescence quantum yield and quenching sensitivity of polyelectrolyte **56**.[103] Similar to the cases of other surfactants, the fluorescence quantum yield increased and the quenching sensitivity decreased in surfactant-containing solutions. A viologen-based quencher functionalized with a long, hydrophobic alkyl chain proved to be a more effective quencher than dimethyl viologen in the presence of the DOTAP surfactant. The larger response to the aliphatically functionalized viologen in DOTAP solution was attributed to the formation of DOTAP-based bilayers along the conjugated polymer backbone that resulted in better interaction with the alkyl chain-functionalized quencher versus the dimethyl derivative. Surfactant effects upon an anionic polyfluorene in aqueous solution have also been examined.[104] In addition, Zhu and co-workers showed that anionic quantum dots can be used to break up aggregates of a cationic polyfluorene.[105]

Shen and co-workers recently published a study that illustrates how difficult it is to predict and anticipate fluorescence responses of conjugated polyelectrolytes to changes in aqueous solution composition.[106] The authors synthesized an anionic copolymer (**62**) from a sulfonated

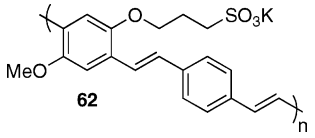

62

bisphosphonium-functionalized monomer and terephthalaldehyde. The fluorescence quantum yield of polymer **62** was approximately 10 times higher than that of polymer **56**. The authors attributed the higher quantum yield to the presence of the *p*-phenylene vinylene monomer units that decreased the overall flexibility of the polymer chain and increased conjugation in the polymer backbone. In marked contrast to the case of homopolymer **56**, addition of the surfactant dodecyltrimethylammonium bromide quenched copolymer **62** fluorescence, which the authors ascribed to surfactant-induced polymer aggregation. They proposed that polymer **62** formed micelle-like aggregates in aqueous solution in which the hydrophobic polymer backbone is buried inside and the sulfonate groups extend outward into solution, thereby preventing further aggregation. Addition of surfactant was suggested to facilitate aggregation of the polymer micelles, resulting in self-quenching.

Nagesh and Ramakrishnan synthesized a poly(acrylic acid)-functionalized derivative of poly[2-methoxy-5-(2′-ethylhexyloxy)-*p*-phenylene vinylene] (MEH-PPV).[107] The polymer was synthesized by radical polymerization of *tert*-butyl acrylate using a *N*,*N*-diethyl dithiocarbamate-functionalized precursor polymer as the radical initiator. After the *tert*-butyl acrylate groups had been grafted onto the MEH-PPV polymer backbone, treatment with acid deprotected the *tert*-butyl groups to afford the carboxylic acid-grafted polymer. The resulting polymer was not fully conjugated due to saturated sites at the points where the poly(acrylic acid) grafts were attached to the MEH-PPV scaffold. The fluorescence of the acrylic acid-grafted polymer was quenched by dimethyl viologen in methanol.

Kumar et al. studied the fluorescence quenching of carboxylate-functionalized **63** by dimethyl viologen in aqueous solution.[108] At low pH (pH < 7.5), polymer absorption and fluorescence did not significantly respond to the viologen cation. However, in basic solution (pH 11.5) the addition of

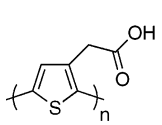

63

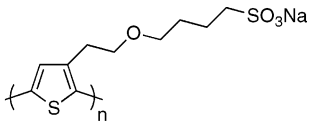

64

dimethyl viologen resulted in red-shifted polymer absorbance, which was attributed to the formation of a polymer−quencher complex. Polymer fluorescence was also quenched in basic aqueous solution ($K_{SV} = 3.5 \times 10^6$). Thin films of poly(thiophene) **63** were quenched with lower efficiency ($K_{SV} = 2.3 \times 10^4$).

Cabarcos and Carter studied fluorescence quenching of sulfonate-functionalized poly(thiophene) **64**.[109] Low molecular weight **64** ($M_W \approx 5000$) fluorescence was quenched by dimethyl viologen with a Stern−Volmer constant of 2.4×10^5. The authors observed downward curvature in the Stern−Volmer response and attributed it to the presence of multiple fluorophore populations, one of which was less accessible to fluorescence quenching. Addition of dimethyl viologen to an aqueous solution of **64** also resulted in red-shifted absorbance. High molecular weight **64** ($M_W \approx 1 \times 10^6$) was more sensitive to fluorescence quenching by dimethyl viologen ($K_{SV} = 8.4 \times 10^5$).[110] The better sensitivity of high molecular weight **64** was credited to greater exciton delocalization, better polymer solubility, and reduced polymer aggregation. Increased solution ionic strength resulted in reduced fluorescence intensity and lower sensitivity to quenching by dimethyl viologen. The effect was most significant in solutions containing divalent metal cations (Mg^{2+} and Ca^{2+}), which were suggested to facilitate polymer aggregation as well as screen the electrostatic attraction between the anionic conjugated polymer and the cationic viologen quencher.

In 2002, Tan, Pinto, and Schanze reported the synthesis and fluorescence quenching response of a sulfonated poly(*p*-phenylene ethynylene) **65**.[111] In methanol, the polymer was well solvated with absorption and fluorescence spectra

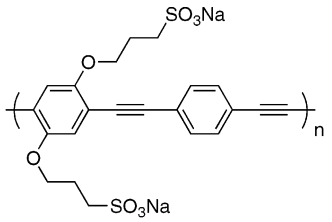

65

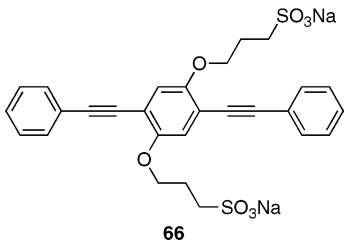

66

comparable to those of similar nonionic and nonaggregated organic-soluble poly(*p*-phenylene ethynylene)s. In water, however, polyelectrolyte **65** appeared to aggregate. The absorbance of **65** red-shifted and sharpened as the solvent was changed from methanol to water. The fluorescence spectrum of **65** red-shifted approximately 100 nm ($\lambda_{max} =$

548 nm in water, $\lambda_{max} = 447$ nm in methanol) in water and was very broad and weak in comparison to that of the polymer in methanol (in water, $\Phi = 0.10$; in methanol, $\Phi = 0.78$). These changes suggested increased conjugation due to straightening of polymer chains upon aggregation, and the broad red-shifted fluorescence in aqueous solution was attributed to excimer emission. Conjugated polyelectrolyte **65** was very sensitive to fluorescence quenching by dimethyl viologen in water ($K_{SV} = 2.7 \times 10^7$) and methanol ($K_{SV} = 1.4 \times 10^7$), and it was more than 1000-fold more sensitive than the small molecule model compound **66**.

Schanze and co-workers have also investigated fluorescence quenching of conjugated polyelectrolyte **65** by cationic cyanine dyes in methanol.[112] The cyanine dyes quenched polymer fluorescence via Förster-type energy transfer, as evidenced by a correlation between polymer fluorescence quenching and cyanine dye emission. The Stern−Volmer quenching response of polymer **65** to cyanine dyes displayed upward curvature as quencher concentration increased (Stern−Volmer constants were extracted from the data obtained at low quencher concentration, where the plots approached linearity). Somewhat surprisingly, the quenching response to the cyanine dyes was opposite to what was expected based on the calculated Förster radii of the dyes; the dye with the largest Förster radius (R_0) was the least effective quencher, and the dye with the smallest R_0 exhibited the highest Stern−Volmer constant (1.3×10^6). This trend was attributed to variations in polymer−dye binding constants. The dye with the smallest R_0, but largest K_{SV}, was the largest and most solvophobic dye and was proposed to associate with the conjugated polymer more strongly than the other dyes due to its poor solvation and superior ability to π-stack with the polymer backbone. A tricationic cyanine dye was proposed to induce polymer aggregation more efficiently than monocationic dyes, therefore leading to a Stern−Volmer response with a larger deviation from linearity at high dye concentration. The increased nonlinear Stern−Volmer response was attributed to the formation of polymer−dye aggregates, which facilitated interpolymer interactions and led to increased dimensionality for exciton transport. The authors carefully examined energy transfer from polymer **65** to 1,1′,3,3,3′,3′-hexamethylindotricarbocyanine iodide (HMIDC). Fluorescence lifetime experiments revealed that energy transfer to HMIDC took place with two distinct rates, a fast transfer ($k_1 > 0.25$ ps^{-1}) and a slower transfer ($k_2 > 0.001-0.05$ ps^{-1}). The fast quenching response was attributed to rapid quenching of polymer-based excitons produced within the Förster radius of a bound dye (Figure 18). The slower quenching process was proposed to be due to diffusion of excitons to distant quenching sites. In water, the conjugated polymer and HMIDC produced a tight complex in which the dye formed a J-aggregate, evidence for which included red-shifted dye absorbance, as well as dye fluorescence that was intense and red-shifted in the presence of the conjugated polyelectrolyte.

Schanze, Kleiman, and co-workers further studied the fluorescence quenching of polymer **65** by HMIDC using time-resolved spectroscopic experiments and mathematical modeling.[113] Their experimental results and modeling demonstrated that energy transfer from the polymer to a bound dye molecule was dominated by intramolecular energy migration (random walk/hopping mechanism) to the quenching site and that direct long-range energy transfer to a bound quencher made only a very small contribution to the total

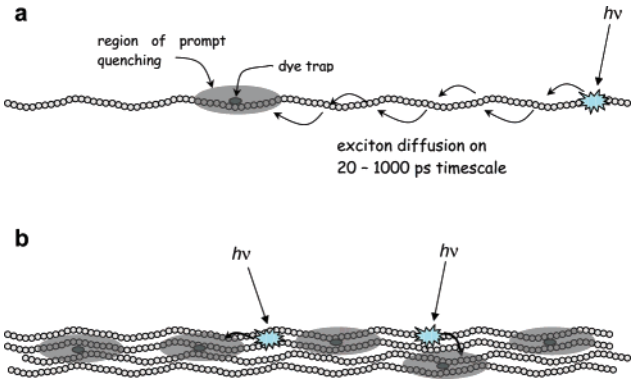

Figure 18. Illustration of exciton quenching by bound dye molecules. (a) Nonaggregated polymer chain at a high polymer/dye ratio. (b) Aggregated polymer at a low polymer/dye ratio. The gray ellipses represent fast quenching regions. (Reprinted with permission from ref 112. Copyright 2004 American Chemical Society.)

fluorescence quenching. The rate of exciton migration decreased with increasing time, presenting a significant limitation to the quenching amplification provided by the conjugated polymer. The hopping rate decreased because polymer-based low-energy trap sites, from site disorder in the conjugated polymer, were selectively populated, thereby inhibiting further migration. The authors concluded that quenching efficiency would increase 5-fold in the absence of energetic disorder within the conjugated polymer. The authors also proposed that the formation of loose aggregates (weak aggregates with large interpolymer distances and insignificant interpolymer energy transfer) also limited quenching efficiency because the available surface area of the polymer was reduced upon weak aggregation. Time-dependent emission anisotropy measurements on HMIDC, obtained by direct excitation of the dye at $\lambda = 640$ nm, showed that emission from unbound dye became isotropic fairly rapidly. However, anisotropic emission from polymer-bound dye molecules, obtained by excitation of polymer **65** at 425 nm and subsequent energy transfer to the polymer-bound dye, persisted for an extended time period. These emission anisotropy measurements support an energy-transfer mechanism that involves electrostatically associated polymer−dye complexes, and the meaurements are inconsistent with a significant contribution to polymer fluorescence quenching from dynamic energy transfer from polymer **65** to unbound quencher.

Schanze and co-workers have also synthesized an anionic, phosphonate-substituted poly(*p*-phenylene ethynylene) **67**.[114] The synthesis involved the preparation of a neutral, dibutyl phosphonate-functionalized polymer followed by deprotection of the phosphonate ester substituents using TMSBr to provide the water-soluble conjugated polyelectrolyte. Changes in solution pH (from pH 7.5 to 12.0) affected polymer photophysics in phosphate-buffered aqueous solution. As the pH decreased from 12.0 to 7.5, the absorption spectrum shifted 35 nm to the red. Polymer fluorescence changed more dramatically. At pH 11.0, polymer fluorescence was structured with a maximum at 447 nm, the quantum yield was 0.05, and the fluorescence lifetime was monoexponential ($\tau = 0.18$ ns at 450 nm). At pH 7.5, however, polymer fluorescence was very broad and red-shifted ($\lambda_{max} = 518$ nm), was less efficient ($\Phi = 0.03$), and was characterized by biexponential decay. The photophysical changes observed as solution pH decreased suggest increased polymer ag-

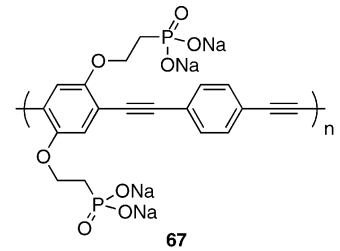

67

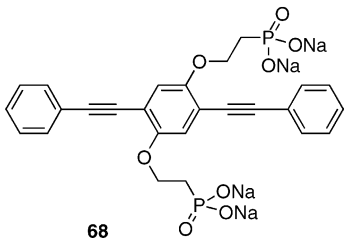

68

gregation at lower pH, and the broad red-shifted emission was attributed to excimer emission from π-associated polymer chains. Increased aggregation at pH 7.5 could result from partial protonation of the phosphonate side chains, which would reduce the overall negative charge surrounding the conjugated polymer backbone and thereby diminish negative electrostatic effects that hinder polymer−polymer association. In addition, partial phosphonate protonation was proposed to provide potential interpolymer hydrogen bonding interactions that would stabilize polymer aggregates. Fluorescence quenching experiments with polymer **67** were carried out in unbuffered aqueous solution with the cationic quenchers dimethyl viologen ($K_{SV} = 3.2 \times 10^7$), ethidium bromide ($K_{SV} = 1.1 \times 10^7$), and rhodamine 6G ($K_{SV} = 4.7 \times 10^7$). The conjugated polyelectrolyte quenching response was more than 100-fold more sensitive than that of the phosphonate-functionalized small molecule model **68**. The amplified quenching response of the conjugated polymer was attributed to efficient exciton delocalization.

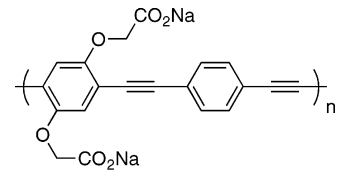

69

In 2006, Schanze and co-workers reported an investigation of Ca^{2+}-enhanced quenching of **69** by dimethyl viologen in methanol (Figure 19).[115] The study provides strong evidence that analyte-induced polymer aggregation is responsible for the superlinear Stern−Volmer quenching responses of conjugated polyelectrolytes toward multivalent analytes. Polymer **69** exhibited strong, structured fluorescence ($\lambda_{max} = 436$ nm, $\Phi = 0.24$) in dilute methanol solution, indicating the polymer was well solvated and not aggregated. However, polymer **69** aggregated in water; the fluorescence of **69** was red-shifted and weak ($\lambda_{max} = 524$ nm, $\Phi = 0.075$) in water. In water, **69** (aggregated) was strongly quenched by dimethyl viologen and the Stern−Volmer plot displayed upward curvature (superlinear response) through the entire range of quencher concentrations examined. In methanol, however, the quenching response was much weaker. The Stern−Volmer plot was linear at low quencher concentration, and the plot did not become superlinear until the quencher concentration was relatively high (>3 μM). Addition of Ca^{2+} to **69** in methanol resulted in red-shifted absorbance and

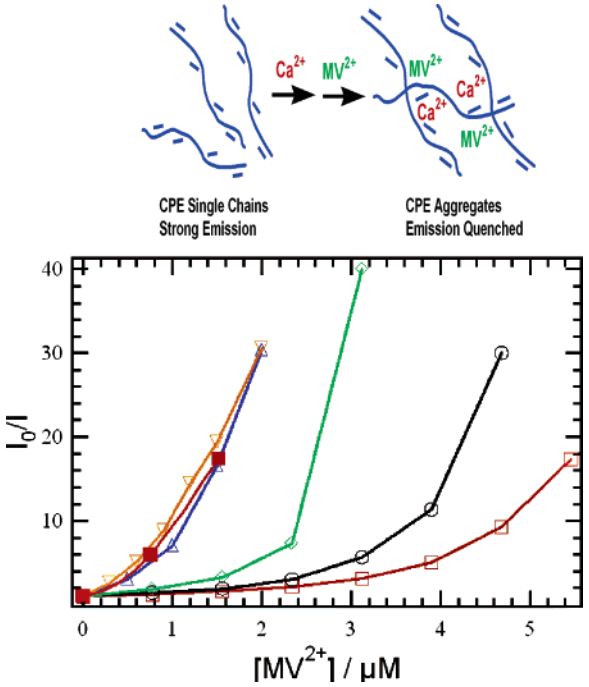

Figure 19. Top: Illustration of Ca^{2+}-induced aggregation of **69** and subsequent quenching by dimethyl viologen. Bottom: Quenching of **69** (10 μM) emission by dimethyl viologen in water (■) and in methanol with 0 μM (□), 2.5 μM (○), 5.0 μM (◇), 7.5 μM (△), and 10 μM (▽) $CaCl_2$. (Reprinted with permission from ref 115. Copyright 2006 American Chemical Society.)

relatively weak, broad, red-shifted emission. These photophysical changes were attributed to Ca^{2+}-induced aggregation of the carboxylate-functionalized polymer. Dimethyl viologen also appeared to promote polymer aggregation in methanol, as polymer absorbance red-shifted and narrowed in the presence of dimethyl viologen as well. In methanol, the Ca^{2+}-aggregated polymer was more sensitive than the unaggregated polymer to quenching by dimethyl viologen. As the concentration of Ca^{2+} was increased, the quenching response improved and the onset of superlinearity in the Stern−Volmer plot shifted to lower quencher concentration. In methanol solution containing >7.5 μM Ca^{2+}, the Stern−Volmer response was superlinear throughout and the quenching efficiency was similar to that observed in aqueous solution. The authors proposed that the sphere-of-action quenching mechanism[28,95a] does not account for the superlinear response of conjugated polyelectrolytes to polyvalent quenchers. Instead, their experimental results suggest that the superlinear quenching response in these systems can be attributed to quencher-induced conjugated polyelectrolyte aggregation leading to enhanced exciton delocalization.

In 2003, Heeger et al. reported that cationic conjugated polyelectrolyte **70** was quenched with exceptional efficiency by gold nanoparticles ($K_{SV} = 8.3 \times 10^{10}$) in water.[116] The gold nanoparticles were anionic due to citrate binding during the nanoparticle fabrication. The authors attributed the

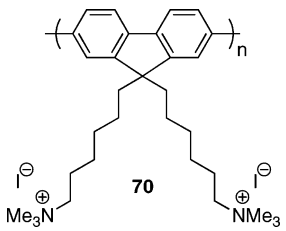

70

quenching response to electrostatic attraction between the cationic conjugated polymer and the anionic nanoparticles, and they postulated that numerous polymer chains may adhere to, and be quenched by, a single gold nanoparticle. The likely involvement of an electrostatic interaction was supported by the fact that the quenching response was significantly reduced in solutions of high ionic strength. In addition, the anionic nanoparticles did not quench the fluorescence of anionic polymer **59**. Nanoparticles with diameters of 5, 10, and 20 nm, which all absorbed strongly in the region of polymer emission, produced similar quenching responses. However, 2-nm gold nanoparticles were approximately 10^4 times less effective quenchers. The authors attributed the lower effectiveness of the 2-nm nanoparticles to poor spectral overlap between polymer emission and 2-nm nanoparticle absorption. The authors concluded that resonance energy transfer was the dominant quenching mechanism, potentially allowing the nanoparticles to engage in long-range polymer fluorescence quenching. A small molecule model of polymer **70** was approximately 10-fold less sensitive to fluorescence quenching, suggesting conjugated polymer-based amplification. The authors credited the high sensitivity of this system to a combination of long-distance energy-transfer quenching, conjugated polymer-based excitation energy transfer, and strong electrostatic nanoparticle−polymer complexation.

Anionic, benzimidazole-containing conjugated polymer **71** was synthesized by Yang et al., and its fluorescence quenching by dimethyl viologen was examined.[117] The polymer was prepared by postpolymerization functionalization with 1,3-propane sultone to install the sulfonate-containing side chains. In methanol, dimethyl viologen quenched polymer fluorescence with a Stern−Volmer constant of 3.7×10^5. Solvent studies revealed red-shifted absorption and reduced fluorescence efficiency in methanol/water mixtures, suggesting aggregation with increased water content.

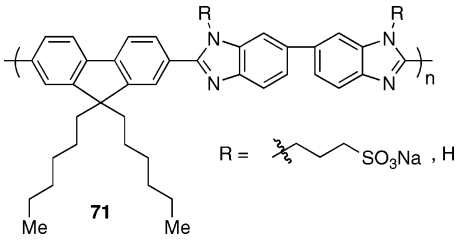

71

4.3. Detection of Small Biomolecules

Shinkai and co-workers reported a poly(thiophene)-based sensor for adenosine triphosphate (ATP) in 2005.[118] Exposure of cationic water-soluble poly(thiophene) (**72**) to increasing concentrations of ATP (up to 5×10^{-4} M) in water led to a pronounced 138 nm red shift in the absorbance spectra, changing the solution color from yellow to pink-red. The absorbance spectrum of **72** in the presence of an equimolar concentration of ATP was similar to that of a thin film of **72**, suggesting ATP-induced polymer aggregation. ^{1}H NMR studies also supported the formation of a polymer aggregate that incorporated ATP. The authors proposed that the changes in the absorbance of **72** upon exposure to ATP were due to formation of an electrostatic complex between the cationic polymer and anionic ATP, which led to increased planarity of the conjugated polymer backbone. As the ATP concentration was increased, the polymer chains became increasingly planar, thus facilitating the formation of π-stacked aggregates. The authors suggested that the nucleobase adenine played a key role in promoting polymer aggregation through hydrophobic effects, as smaller spectral changes were observed upon exposure of **72** to the phosphate anions triphosphate, pyrophosphate, and phosphate. The amount of negative charge on the analyte was also an important factor. The largest absorbance response was observed for ATP whereas smaller absorbance red shifts occurred upon exposure to adenosine diphosphate (ADP) or adenosine monophosphate (AMP). Polymer **72** was also selective for ATP over other anions such as Cl^-, HPO_4^{2-}, and HCO_3^{2-}. In addition to red-shifted absorbance, the addition of ATP to an aqueous solution of **72** also resulted in fluorescence quenching. The fluorescence response was most sensitive to ATP over ADP or AMP. The detection limit, based upon fluorescence quenching, for ATP was reported to be approximately 10^{-8} M.

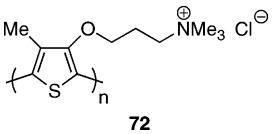

72

In 2002, Schanze, Lakowicz, and co-workers reported a conjugated polymer-based sensor for sugars.[119] Fluorescence from an aqueous solution of **65** was quenched very efficiently by boronic acid-functionalized viologen **73** ($K_{SV} = 3.5 \times 10^8$ in water). The Stern−Volmer constant was reduced by more than a factor of 10 in 6 mM phosphate-buffered solution at pH 7.4 ($K_{SV} = 2.8 \times 10^7$). Therefore, the large fluorescence quenching response was likely due to the formation of an electrostatic complex between the anionic conjugated polymer **65** and the cationic viologen quencher **73**. Similar to the cases of other polyelectrolyte systems discussed, the Stern−Volmer quenching plots displayed upward curvature as the quencher concentration was increased. The authors attributed this to a sphere-of-action mechanism at high quencher concentration. It is likely, however, that polymer aggregation plays a role. Sugars reacted with boronic acid-functionalized viologen **73** to generate the bisboronate derivatives, which were zwitterionic and overall charge neutral. In comparison to dicationic viologen **73**, the carbohydrate-bound charge-neutral viologen did not associate as strongly with anionic polymer **65**. As a

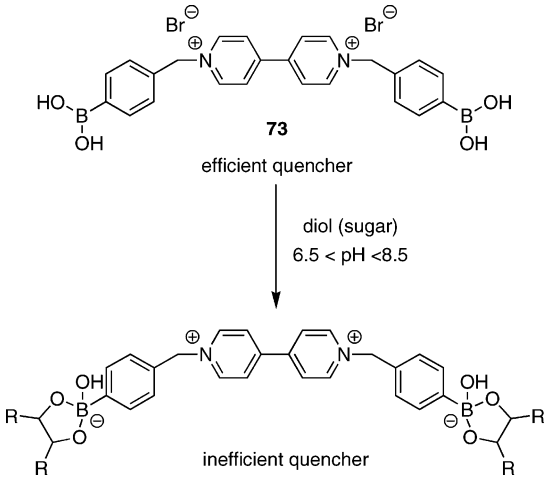

73

result, the addition of a sugar to an aqueous solution of polymer **65** and viologen **73** (quenched solution) produced an unquenching response (turn-on) as the boronic acid functional groups reacted with the sugar to produce the boronate-functionalized viologen, a much less efficient quencher. The addition of 40 mM δ-fructose to a solution of conjugated polymer **65** and viologen **73** increased polymer fluorescence by a factor of 50. On the basis of apparent dissociation constants for the 2:1 sugar−viologen complexes, the sensory system was selective toward δ-fructose (2×10^{-5} M^2) over δ-galactose (6×10^{-3} M^2) and δ-glucose (3×10^{-2} M^2).

Recently, Wang and co-workers developed a conjugated polymer-based method to detect hydrogen peroxide and were also able to couple this method to an enzymatic oxidase to indirectly detect glucose.[120] Conjugated polyelectrolyte **13**, which contained a polyfluorene backbone, was employed as the fluorescent reporter in conjunction with a boronate-functionalized fluoresceine derivative (**74**). In aqueous solution, the conjugated polymer did not strongly associate with the neutral boronate-functionalized dye **74** and fluorescence from **13** was strong. Addition of hydrogen peroxide (H_2O_2) resulted in liberation of the fluoresceine dye. At sufficiently high pH, the fluoresceine was dianionic and strongly associated with the polycationic conjugated polymer. Good spectral overlap between polymer fluorescence and fluoresceine absorption led to FRET from the polymer to fluoresceine, resulting in conjugated polymer quenching and dye emission. The highest sensitivity was obtained by monitoring polymer fluorescence quenching. Hydrogen peroxide could be detected down to 15 nM. The response was somewhat sensitive to pH; at pH 5.5 the response was approximately 20% lower than that at pH 9.0. The reduced response at lower pH was due to protonation of the dye to give the monoanionic derivative, which did not associate as strongly with the polycationic conjugated polymer as the dianionic derivative. However, changes in sensitivity as a function of pH were not large and likely do not limit the overall effectiveness of this methodology. The hydrogen peroxide sensor was adapted to serve as a sensor for β-D-(+)-glucose by incorporating glucose oxidase. Polymer **13** was combined with the boronate-functionalized dye and glucose oxidase in aqueous phosphate buffer. Addition of glucose to this mixture resulted in production of H_2O_2 and subsequent generation of fluoresceine, which quenched polymer fluorescence. The detection limit for glucose was 5 μM.

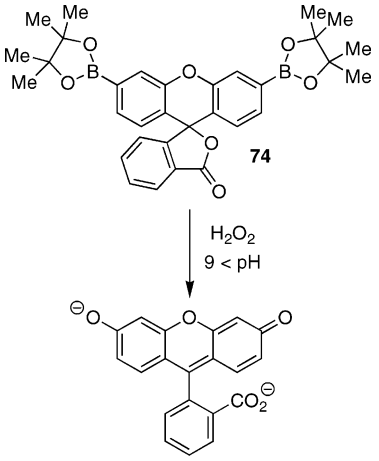

4.4. Detection of Proteins

Kinases and phosphatases control the phosphorylation/dephosphorylation of serine, threonine, and tyrosine residues, thereby affecting and regulating a wide range of cellular processes. In 2004, Whitten and co-workers reported a conjugated polymer-based fluorescence assay for kinase and phosphatase activity.[121] Quaternary ammonium-functionalized latex microspheres were coated with anionic conjugated polyelectrolyte **75**. The polymer-coated microspheres were then exposed to $GaCl_3$. The carboxylate groups of **75** complexed the Ga^{3+} ions, thereby providing Ga^{3+}-functionalized microspheres. The Ga^{3+} coat endowed the microspheres with an affinity for phosphorylated peptides. A turn-off fluorescence assay for kinase/phosphatase activity was developed using the Ga^{3+}-functionalized microspheres (Figure 20). The assay utilized a peptide substrate labeled with a rhodamine dye at its *N*-terminus. In the absence of kinase activity (peptide phosphorylation), the dye-labeled peptide did not bind to the fluorescent microspheres. Upon kinase-mediated phosphorylation, the peptide associated with the Ga^{3+}-coated microspheres via Ga^{3+}-phosphate binding. Polymer-coated microsphere fluorescence was quenched upon close association with the dye-labeled phosphorylated peptide. Both end-point and kinetic measurements were demonstrated using the fluorescence-quenching assay.

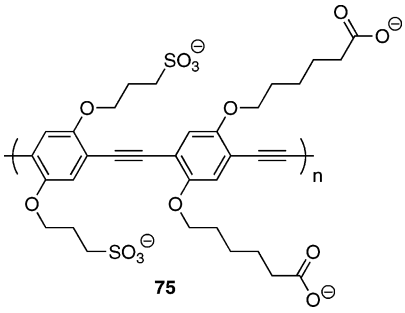

A fluorescence turn-on assay for protein phosphorylation was also described.[121] The turn-on assay did not require dye functionalization of the peptide/protein substrate. Instead, polymer fluorescence was quenched by a dye-labeled phosphorylated peptide (a peptide that was not a substrate for the kinase of interest). Phosphorylation of the substrate led to competition between the phosphorylated substrate and the phosphopeptide quencher for binding to the Ga^{3+}-functionalized microspheres. As more substrate was phosphorylated, more quencher-functionalized phosphopeptide was displaced from the fluorescent microspheres and fluorescence intensity increased. The competitive-binding-based fluorescence turn-on assay has been performed in a 384-well format, suggesting the potential application of this methodology to high-throughput assays.[122]

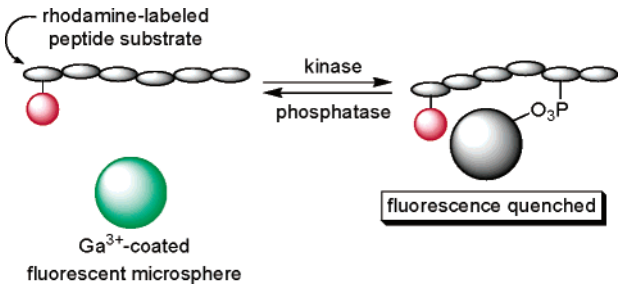

Figure 20. Polymer-coated microsphere assay for kinase/phosphatase activity.

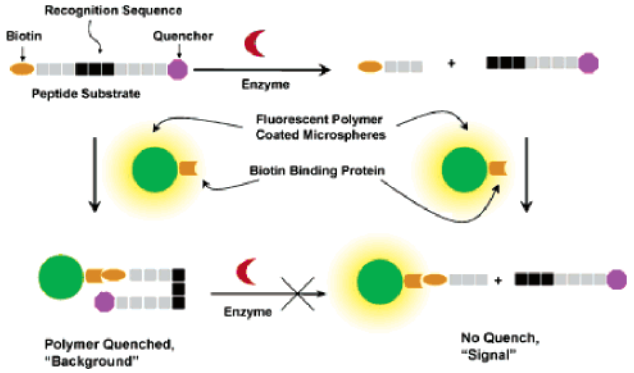

Figure 21. Whitten's microsphere-based protease sensor. (Reprinted with permission from ref 123. Copyright 2004 National Academy of Sciences, U.S.A.)

In 2004, Whitten and co-workers reported the use of conjugated polyelectrolyte-coated microspheres as sensors of protease activity (Figure 21).[123] Their approach relied on polypeptide substrates that were biotin-functionalized at one end and bound to a fluorescence quencher at the other end. The microsphere sensors were prepared by coating polystyrene-based microspheres with biotin-binding protein (either streptavidin or neutravidin) followed by functionalization with a poly(*p*-phenylene ethynylene). The fluorescent conjugated polymer was bound to the microspheres in one of two ways. The first approach was to expose streptavidin-coated microspheres to a dilute solution of biotin-functionalized polyanionic poly(*p*-phenylene ethynylene) **76**. The

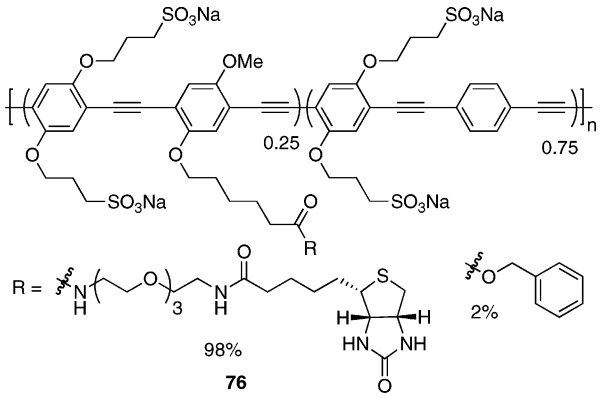

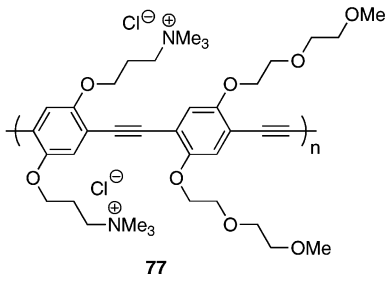

second approach involved coating neutravidin-functionalized microspheres with cationic poly(*p*-phenylene ethynylene) **77**. Microspheres coated with **77** could be used directly as sensors. However, a more sensitive sensory system was produced by additional functionalization with a biotin−R-phycoerythrin conjugate. When microspheres functionalized with **77** and biotin−R-phycoerythrin were excited at the conjugated polymer's absorption maximum (440 nm), efficient energy transfer occurred to the phycoerythrin chromophore, resulting in red-shifted emission from phycoerythrin at 576 nm. Protease assays had to be conducted in two steps. First, the biotin-quencher-functionalized polypeptide was incubated with a protease in aqueous solution. Polymer-coated microspheres were then combined with the enzymatic reaction mixture. The two-step procedure was necessary because protease activity was inhibited in the presence of polymer-coated microspheres. In the absence of protease-mediated oligopeptide cleavage, emission from the microspheres was strongly quenched by the intact quencher-functionalized oligopeptide. The oligopeptide was bound to the microspheres via the strong association between biotin and biotin-binding proteins, thereby colocalizing quenchers and fluorescent polymer-coated microspheres. Enzymatic oligopeptide hydrolysis cleaved the tether between biotin and the dye-based quencher. Therefore, in the presence of the appropriate protease, microsphere emission was more intense. The turn-on response required optimization of both microsphere and peptide concentration to achieve optimal sensitivity. Microspheres coated with **77** and phycoerythrin were used to assay the protease activity of β-secretase, enterokinase, and caspase-3/7. A 5 min reaction time allowed β-secretase detection down to 14 nM. Increasing the enzymatic reaction time to 1 h lowered the detection limit for β-secretase to 1.4 nM. The evaluation of a β-secretase inhibitor and the determination of K_M for a β-secretase substrate were also demonstrated. The protease assays were conducted in the wells of 96-well plates, suggesting potential application in high throughput screening.

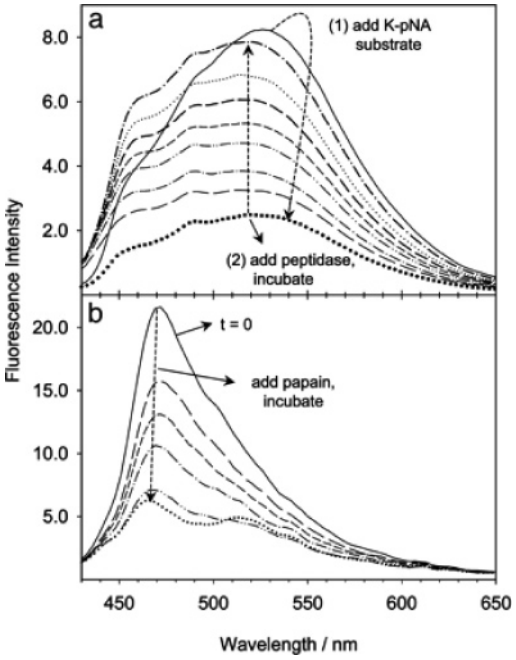

Figure 22. (a) Fluorescence changes during the turn-on protease assay. (—) initial fluorescence of **65**; (•••) fluorescence after addition of 167 nM substrate. Fluorescence intensity as a function of time after addition of porcine intestinal peptidase (c = 3.3 μg/mL): 5 (— — —), 20 (— • —), 50 (— •• —), 70 (- - -), 100 (— — —), 140 (•••), and 200 (—•—) min. (b) Fluorescence changes during the turn-off assay. (—) initial fluorescence, [**10**] = 1.0 μM, [**78**] = 500 nM. Fluorescence intensity as a function of time after addition of papain (3.5 nM): 1 (— — —), 3 (- - -), 6 (— • —), 18 (— •• —), and 28 (•••) min. (Reprinted with permission from ref 124. Copyright 2004 National Academy of Sciences, U.S.A.)

Schanze and Pinto have also reported the use of conjugated polyelectrolytes as protease sensors (Figure 22).[124] Their report appeared in 2004, simultaneously with Whitten's

publication on the same subject.[123] Schanze and Pinto used anionic poly(*p*-phenylene ethynylene)s functionalized with either sulfonate (**65**) or carboxylate (**10**) groups. They developed both fluorescence turn-on (protease-mediated unquenching) and turn-off (protease-mediated quenching) protease assays. The turn-on approach used **65** in conjunction with a cationic quencher. The quencher was a peptide substrate covalently bound to *p*-nitroaniline, the fluorescence quencher, via an amide bond. In this assay, the peptide substrate must contain a cationic amino acid residue such as lysine or arginine. Polyanion **65** and the cationic peptide substrate associated strongly due to electrostatic attraction. Enzymatic cleavage of the *p*-nitroaniline quencher from the peptide liberated the quencher and allowed it to dissociate from the conjugated polyelectrolyte. The pH of the aqueous buffer used in these experiments (pH > 7) ensured that free *p*-nitroaniline was a neutral molecule and, therefore, did not strongly associate with **65**. As a result, once cleaved from the cationic amino acid, *p*-nitroaniline was a much less effective quencher and the fluorescence of **65** increased in intensity. The turn-on assay was used to detect peptidase and thrombin. This assay could be conducted in one step and followed in real-time, allowing for the kinetic parameters of the enzymatic reaction to be determined.

The turn-off assay used polymer **10** in combination with the bis-arginine adduct of rhodamine **78**, which is colorless and nonemissive. Polymer **10** was used in this case because its emission was blue-shifted relative to that of **65** and thereby provided better spectral overlap with rhodamine-based absorption. Electrostatic attraction between **78** and polyelectrolyte **10** resulted in a high association constant. Bis-arginine-functionalized rhodamine **78** is colorless and nonemissive and therefore does not quench the fluorescence of **10**. Hydrolysis of one of the amide bonds between the dye and arginine, however, effectively liberated the rhodamine dye. Energy transfer from **10** to the electrostatically bound mono-arginine derivative was efficient, and a strong quenching response was observed; the mono-arginine adduct of **78** is colored, and its absorption spectrum overlapped well with the fluorescence spectrum of **10**. The turn-off sensor was used to detect papain down to a concentration of 3.5 nM. A signal enhancement of more than a factor of 10 was reported for the polymer **10**/**78** system over that of **78** alone.

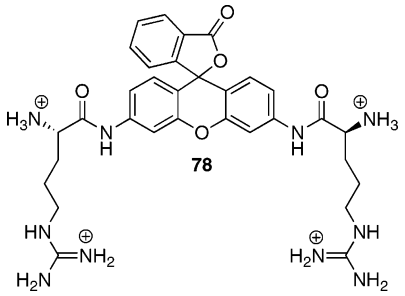

A molecular beacon-type protease assay was developed by Swager and co-workers (Figure 23).[125] They synthesized a water-soluble polypeptide-functionalized poly(*p*-phenylene ethynylene) (**79**) that served as both the enzyme substrate and the fluorescent reporter of protease activity. The peptide-functionalized conjugated polymer was synthesized from the corresponding carboxylic acid-substituted polymer. The oligopeptides served to tether the fluorescent polymer to 2,4-dinitroaniline quenchers. The material used to assay for protease activity contained from 0.25 to 1.7 peptides/polymer repeat. A polymer containing 1.7 peptides/polymer repeat was not visibly fluorescent. Fluorescence was increased approximately 10-fold upon exposure of **79** to the protease trypsin in buffered aqueous solution. Control experiments using a polymer in which the peptide linker had been replaced with an oligo(ethylene glycol) spacer confirmed that the fluorescence increase observed for polymer **79** was due to protease cleavage of the peptide tether. A small molecule model provided a smaller turn-on response (2.9-fold increase) than that for polymer **79**. The addition of the surfactant Triton X-100 to an aqueous solution of polymer **79** led to more intense polymer fluorescence both before and after exposure to enzyme. The surfactant effect was attributed to increased solubilization of the hydrophobic residues of the oligopeptide. More effective oligopeptide−quencher solubilization in the presence of surfactant decreased the interaction between quencher and fluorescent polymer prior to enzymatic peptide cleavage as well as after the quencher had been cleaved from the polymer backbone. The turn-on response to trypsin was smaller in the presence of surfactant, however, as the surfactant effect was more pronounced for intact polymer **79** than for the enzymatically cleaved material.

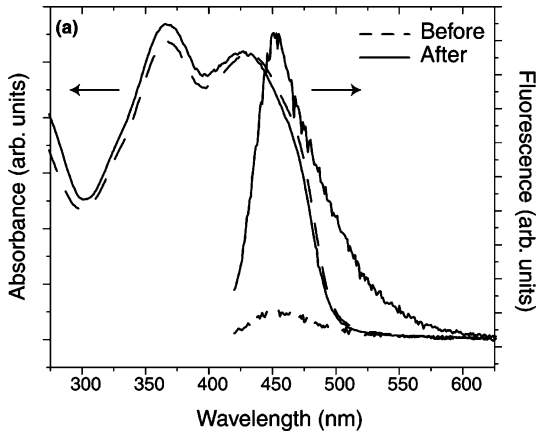

Figure 23. Absorbance (left) and fluorescence (right) spectra of substrate **79** (1.1 μM in repeat units) before and after treatment with trypsin (3 μg/mL). (Reprinted with permission from ref 125. Copyright 2005 American Chemical Society.)

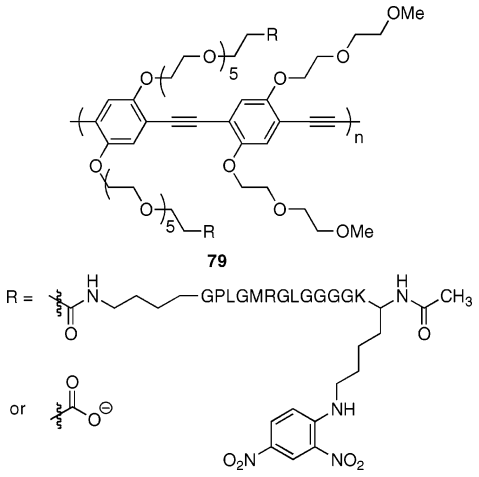

Kim and co-workers reported the synthesis of a water-soluble, anionic poly(*p*-phenylene ethynylene) that contained carboxylic acid-functionalized end caps (**80**).[126] The carboxylic acid-containing end caps provided a handle for carrying out peptide conjugation; the authors reported

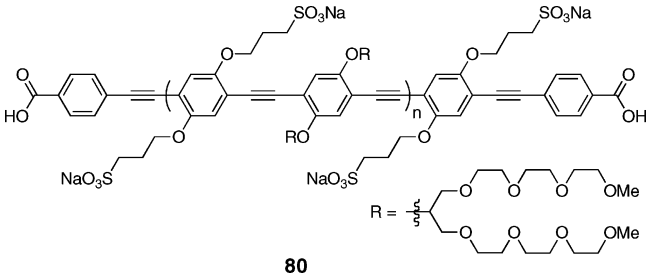

80

coupling a polystyrene-bound pentatyrosine unit to the ends of the conjugated polymer using standard peptide coupling conditions. The pentatyrosine-functionalized conjugated polymer was successfully released from the trityl-substituted resin by mild acid treatment. End-group analysis by ^{1}H NMR showed that both ends of the conjugated polymer were successfully functionalized. The authors speculated that their carboxylic acid-terminated polymer (**80**) may have utility in biosensing applications.

Poly(thiophene)s with ionic side chains have been used for the specific detection of DNA sequences (Section 5). This sensing relies upon conformational changes of the conjugated polymer backbone upon ssDNA hybridization with complementary ssDNA. These changes can be monitored optically by either absorbance or emission spectroscopy. In addition, Nilsson and co-workers have shown in a series of publications that this transduction mechanism is also effective for the detection of certain protein conformational changes. Similar to the DNA detection, one of the primary advantages of this scheme is that it relies upon noncovalent interactions and therefore does not require covalent labeling of biological macromolecules.

In an early report of their sensing strategy, which was published in 2003, Nilsson and co-workers described how the conformational changes of a synthetic peptide could alter the conformation of an electrostatically bound amino acid-substituted conjugated polyelectrolyte (**81**).[127] The negatively

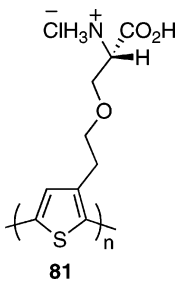

81

charged peptide (JR2E) bound to **81** via a combination of electrostatic attraction and hydrogen bonding. The polymer backbone became more planar upon binding to the peptide, as revealed by a red shifting of the optical spectra. Polymer aggregation was also observed and was attributed to interprotein hydrogen bonding which brought proteins and the associated conjugated polymers into close proximity. When a different, positively charged synthetic peptide (JR2K), designed to form a four-helix bundle with JR2E, was added, the conjugated polymer aggregates were disrupted, as seen by a blue shift of the emission peak and increased emission intensity. The authors attributed the deaggregation to interpeptide interactions that disrupted peptide−polymer binding, driving apart polymer aggregates.

Subsequent publications in this area have focused on the sensing of conformational changes of more biologically

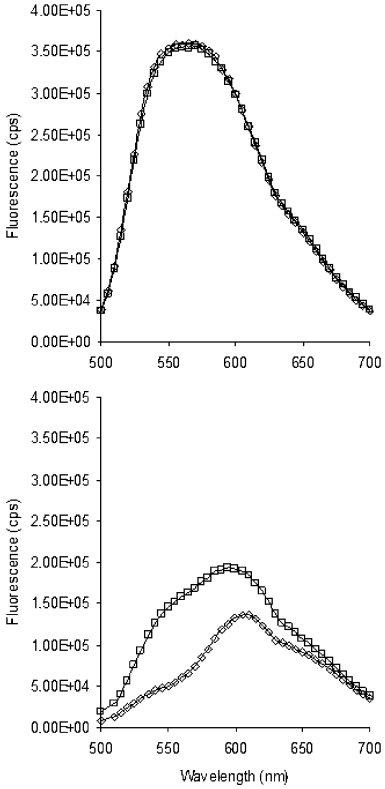

Figure 24. Emission spectra of **81** in 20 mM Tris-HCl pH 7.5 before (◇) and after (□) Ca^{2+} addition (10 mM). The bottom plot is with 1.2 mM CaM; the top plot is without the protein. (Reprinted with permission from ref 128. Copyright 2004 American Chemical Society.)

relevant proteins. In 2004, the same group published a paper concerning Ca^{2+}-induced conformation changes in the protein calmodulin (CaM).[128] In the presence of this protein, the backbone of **81** underwent planarization and/or aggregation, evidenced by a red shift of the absorbance (from 421 to 455 nm) and emission spectra (from 565 to 608 nm) and by a decrease in emission intensity. The authors again attributed these observations to the disruption of interchain interactions by charged groups on the peptide. Addition of Ca^{2+} (10 mM) caused blue shifts of the absorbance and emission spectra (Figure 24) of this protein−polymer complex, readily monitored by ratiometric detection. Ca^{2+} alone had no effect on the optical properties of the polymer, indicating the conformation changes in CaM upon Ca^{2+} binding were reflected in the optical properties of **81**. Further, the addition of Calcineurin, a CaM−Ca^{2+} binding protein, led to a change in the emission spectrum of the complex only when Ca^{2+} was present, whereas, in a control experiment, human serum albumin (HSA) gave no such change. More recently, the same research group reported that this scheme for the detection of conformational changes in CaM had been successfully carried out on a PDMS-based biochip.[129]

In 2005, Nilsson and co-workers reported a similar approach to the detection of amyloid fibril formation both with a zwitterionic conjugated oligomer **82**[130] and with anionic poly(thiophene) **63**.[131] In the presence of native bovine insulin (5 μM), **82** showed only a small increase in emission intensity. Upon addition of insulin that had been incubated at 65 °C for several hours to cause amyloid fibril formation, however, the authors observed a strong blue shift (from 600 to 560 nm) and an increase in fluorescence intensity. The authors attributed these changes to the twisting

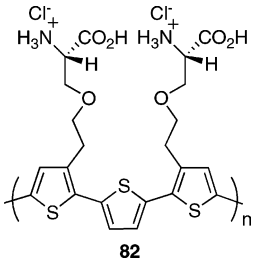

82

and deaggregation of **82** upon binding to the fibril. The experiments could also be carried out with **82** present during fibril formation. **82** showed similar spectral characteristics when the same experiment was performed with a different protein, chicken lysozyme. Interestingly, when similar experiments (with either insulin or chicken lysozyme) were carried out with **63**, the authors observed a red shift in both the absorbance (from 434 to 463 nm) and emission spectra (from 550 to 577 nm) along with a decrease in the emission intensity. The authors also monitored the kinetics of fibril formation using the optical properties of these materials and found that they agreed with the results obtained with transmission electron microscopy as well as circular dichroism. In addition, this group has also investigated the optical properties of enantiomerically pure ionic poly(thiophene)s[132] and investigated how these materials respond to chiral synthetic peptides.[133]

Leclerc has used the cationic **12** for sensing human thrombin without the need for covalently tagging any biological macromolecules.[20] When the ssDNA sequence GGTTGGTGTGGTTGG, a known nucleic acid ligand (aptamer) for thrombin, binds to this target, a compact unimolecular quadruplex structure is known to form. The authors found that the cationic **12** wrapped around this structure to form a 1:1:1 complex, which at least partially hindered aggregation, planarization, and duplex formation of the polymer in the presence of ssDNA (Figure 25). This ternary complex contained a more emissive polymer (6-fold) relative to when a nonspecific protein (bovine serum albumin) or ssDNA sequence that does not bind thrombin was used in the assay, because under these conditions the formation of a very weakly emissive polymer−ssDNA duplex occurred. The reported detection limit for human thrombin with this assay was 1×10^{-11} M.

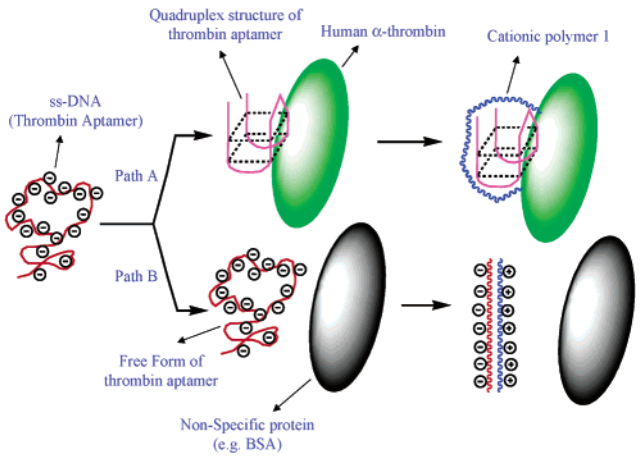

Figure 25. Schematic representation of the detection of thrombin by use of a ssDNA aptamer and the cationic conjugated polymer **12**. (Reprinted with permission from ref 20. Copyright 2004 American Chemical Society.)

4.5. Nonspecific Interactions of CPEs

Many conjugated polymer-based biosensors rely on indirect detection of the target analyte. This is especially true for the detection of biological macromolecules such as proteins. The sensory response usually requires a quencher or reporter small molecule that is not part of the biological macromolecule of interest. The availability/accessibility of the small molecule fluorescence modulator to the conjugated polymer can be affected by the macromolecular target, providing a mechanism to signal the presence of the biological target. However, the direct detection of proteins by conjugated polyelectrolytes has been demonstrated. Heeger and co-workers reported the direct detection of cytochrome *c* (cyt *c*), an iron-containing protein.[134] Cyt *c* quenched the fluorescence of conjugated polyelectrolyte **59** (Figure 26) in 10 mM potassium phosphate buffer (pH 7.4) with a Stern−Volmer constant of 3.2×10^8. Detection of cyt *c* at a concentration of 10^{-11} M was possible. The authors attributed the quenching response to electron transfer from the photoexcited polymer to cyt *c*, and they proposed that the large Stern−Volmer constant was due in part to the formation of an electrostatic complex between the polyanionic conjugated polymer and the polycationic protein. Polymer **59** was most sensitive to quenching by cyt *c* at low pH, conditions under which cyt *c* was positively charged. Nevertheless, cyt *c*, which carries an overall negative charge at pH 10, was still able to quench polymer emission at relatively high pH, albeit with reduced efficiency ($K_{SV} = 2.6 \times 10^6$ at pH 10). Myoglobin, an iron-containing protein with lower electron-transfer activity than cyt *c*, was a less effective fluorescence quencher. In comparison to cyt *c*, lysozyme quenched conjugated polyelectrolyte fluorescence with similar, though slightly lower, efficiency. However, lysozyme, a polycationic protein, was unable to quench conjugated polyelectrolyte fluorescence via electron transfer. Nonspecific quenching by lysozyme was attributed to fluorescence self-quenching due to aggregation of the polyanionic conjugated polymer in the presence of the polycationic protein. On first inspection, the fluorescence quenching response of **59** to cyt *c* appears to be highly desirable, as it provides the ability to *directly* detect this protein with high sensitivity using a simple, unfunctionalized conjugated polyelectrolyte. However, the quenching responses to cyt *c* and lysozyme suggest a significant

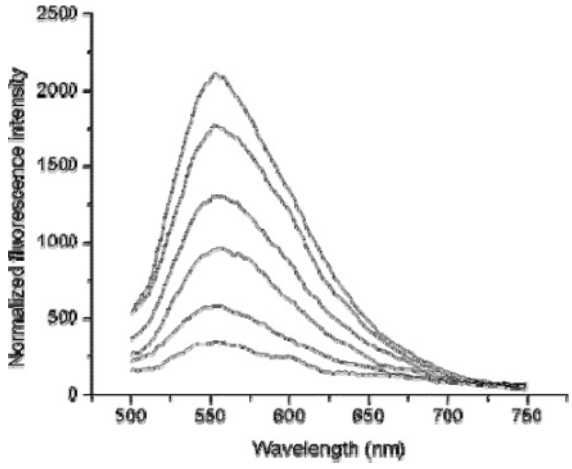

Figure 26. Fluorescence quenching response of **59** (1.0×10^{-6} M) to cyt *c*. Experiments were performed in 10 mM potassium phosphate buffer at pH 7.4. From top to bottom, [cyt *c*] = 0, 0.25, 1, 2.5, 5, and 9.4 nM. (Reprinted with permission from ref 134. Copyright 2002 American Chemical Society.)

problem associated with the use of conjugated polyelectrolytes as biosensors. Certainly, conjugated polyelectrolytes have demonstrated great potential as biosensory materials, especially in DNA-sensing applications, but nonspecific interactions with biological macromolecules pose a formidable challenge to the practical application of these promising polymers to biosensing. Sensor arrays may be able to overcome these problems.

The fluorescence of conjugated polyelectrolytes responds to a large assortment of biological (e.g., proteins and DNA) and nonbiological macromolecules due to wide-ranging nonspecific interactions between conjugated polyelectrolytes and other macromolecules. Waldeck et al. studied the fluorescence response of anionic poly(*p*-phenylene) **83** to cyt

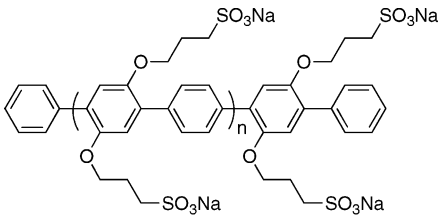

83

c as well as myoglobin and PAMAM (polyamidoamine) dendrimers.[135] Their investigation demonstrated that polymer fluorescence quenching correlated with both the size and the charge of the macromolecule. Furthermore, the study suggested that polymer fluorescence quenching by cyt *c*, myoglobin, and PAMAM dendrimers was not dominated by electron-transfer or energy-transfer processes. Instead, the authors proposed that macromolecule-conjugated polymer association (driven by electrostatic attraction between the polyanionic conjugated polymer and the cationic macromolecular analyte) produced conformational changes in the conjugated polyelectrolyte that resulted in increased self-quenching of polymer fluorescence. Polymer **83** was quenched by both the ferric ($K_{SV} = 5.2 \times 10^6$ M^{-1}) and ferrous ($K_{SV} = 3.6 \times 10^6$ M^{-1}) forms of cyt *c* with comparable efficiencies, suggesting that the fluorescence quenching was not due to electron transfer. In addition, PAMAM dendrimers, which cannot participate in electron-transfer- or energy-transfer-based quenching mechanisms with **83**, were more potent fluorescence quenchers than cyt *c*. The third-generation PAMAM dendrimer ($K_{SV} = 1.0 \times 10^7$ M^{-1}) was approximately twice as effective as the ferric form of cyt *c*. Fluorescence quenching by the third-generation PAMAM dendrimer was most efficient at low pH, conditions under which the dendrimer was completely protonated. At pH 12, no quenching by the PAMAM dendrimer was observed, illustrating the critical importance of quencher charge density to the quenching response. Myoglobin also quenched polymer fluorescence.

Valiyaveettil and co-workers have also investigated fluorescence quenching of sulfonate-functionalized poly(*p*-phenylene)s by cyt *c* and observed a maximum Stern−Volmer response of 3.0×10^6.[136] Shreve et al. have demonstrated that the fluorescence intensity of **56** increased and red-shifted in the presence of a generation 3.0 polypropylenimine hexadecaamine dendrimer.[137] The fluorescence changes were attributed to the formation of an electrostatically bound complex between polyanionic **56** and the polycationic dendrimer.

In 2006, Huang et al. investigated the fluorescence quenching of cationic poly(*p*-phenylene vinylene) **84** by

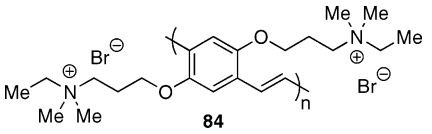

84

rubredoxin, an anionic iron-containing protein.[138] Polymer fluorescence was efficiently quenched by rubredoxin ($K_{SV} = 6.9 \times 10^7$) in aqueous Tris-HCl buffer. The authors attributed the fluorescence quenching to electron transfer from the excited conjugated polymer to the iron center in rubredoxin. Conjugated polymer−protein association was proposed to be driven by electrostatic attraction. Consistent with electrostatic attraction playing a critical role, the fluorescence response to cyt *c*, which was cationic under the conditions of the assay, was minimal in comparison to the response to rubredoxin. Insulin, which is anionic and does not contain an electroactive iron center, did not significantly quench **84** fluorescence, suggesting that the electroactive iron center in rubredoxin is necessary for the fluorescence quenching response.

Chen and co-workers found that the fluorescence quantum yield of polyelectrolyte **56** in aqueous solution increased upon exposure to poly(ethylene glycol) as well to the polyelectrolytes poly(diallyldimethylammonium chloride) and poly(acrylic acid).[139] The effect was largest for poly(acrylic acid); the fluorescence quantum yield of **56** increased from 0.02 in water to 0.25 in an aqueous solution that contained poly(acrylic acid). The authors proposed that, although both macromolecules were anionic, **56** and poly(acrylic acid) formed a complex in aqueous solution due to favorable hydrophobic effects.

Huang and co-workers synthesized water-soluble, ammonium-functionalized polysilanes by sonochemical-assisted Wurtz-type coupling of dichlorosilanes.[140] The quaternary ammonium groups were installed by a two-step postpolymerization synthetic sequence. The fluorescence of cationic polymer **85** was quenched by $Fe(CN)_6^{4-}$ ($K_{SV} = 1.88 \times 10^6$)

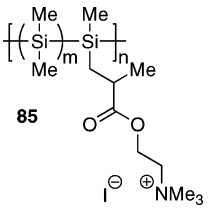

85

and sodium 3-(4-nitrophenyl)propane-1-sulfonate ($K_{SV} = 3.30 \times 10^5$). The authors proposed that polysilane **85** possessed greater conformational flexibility than conjugated polyelectrolytes with carbon-based backbones and suggested that this greater flexibility might allow **85** to better interact with biomolecules. The authors demonstrated biosensing capability by showing that pepsase quenched the emission of **85** ($K_{SV} = 7.8 \times 10^5$).

Heeger and co-workers investigated further the nonspecific interaction of anionic conjugated polyelectrolyte **59** with biological macromolecules and the subsequent fluorescence changes.[141] The authors found that polymer **59** (9.5×10^{-7} M) fluorescence increased approximately 30% in the presence of 150 nM mouse immunoglobulin (IgG). A viologen quencher-tethered antibody fragment (an antibody fragment that was specific for mouse IgG was used) quenched polymer fluorescence. The fluorescence could be recovered by the addition of mouse IgG. However, the fluorescence was also restored by antibodies that did not bind the quencher-

functionalized antibody fragment. Furthermore, the fluorescence could be restored to 150% of its original intensity. These experiments provide additional evidence of fluorescence-influencing nonspecific interactions between conjugated polyelectrolytes and proteins.

To combat these detrimental nonspecific interactions, the authors investigated a conjugated polyelectrolyte-containing charge-neutral complex (CNC) for biosensing. The fluorescent CNC was generated by combining anionic conjugated polyelectrolyte **59** with the cationic polymer poly(*N*,*N*-dimethylammonio-ethylene iodide) in a 1:1 ratio of repeat units. The conjugated polymer-containing CNC was less vulnerable to interference from nonspecific interactions with proteins. The authors proposed that the CNC was superior in this respect because it was neutral and therefore less prone to associate with charged proteins through electrostatic attraction. The authors also suggested that the CNC may have been more conformationally rigid and, therefore, less able to undergo fluorescence modifying conformational changes to accommodate, or in response to, association with a protein. In contrast to **59**, which is quenched by cationic quenchers, the CNC was quenched by both cationic and anionic quenchers. However, the CNC was generally less sensitive and higher quencher concentrations were required to effectively quench CNC fluorescence. The authors also applied the CNC to biosensing. CNC fluorescence was quenched by a 2,4-dinitrophenol-containing anionic quencher. Fluorescence was recovered by the addition of an anti-2,4-dinitrophenol antibody. The assay was sensitive down to approximately 300 nM antibody. The CNC was less sensitive than polymer **59**. However, the CNC did demonstrate lower susceptibility to nonspecific interaction with proteins, a significant advantage in biosensing applications.

In 2004, Bazan and co-workers published a significant study that examined the fluorescence quenching of conjugated polyelectrolyte **56** by viologen-based quenchers and proteins.[142] Bazan's study thoroughly reexamined Whitten's initial biosensing publication[3] and produced experimental results that were inconsistent with those originally reported by Whitten and co-workers. In water, conjugated polymer fluorescence was strongly quenched by the monocationic quenchers *N*-methyl-4,4′-pyridylpyridinium (**57c**) ($K_{SV} = 6.6 \times 10^6$), which lacked biotin functionalization, and biotin-functionalized quencher **57a** ($K_{SV} = 3.9 \times 10^6$). Consistent with Whitten's reported observations, addition of avidin to a solution (water) of polymer **56** and biotin-quencher conjugate **57a** produced an increase in polymer fluorescence (Figure 27). However, Bazan reported that avidin also brought about increased emission from an aqueous solution of polymer **56** and quencher **57c**, which lacked a biotin moiety (Figure 28). These two experiments suggest that the fluorescence recovery upon addition of avidin was not due to specific avidin−biotin interaction and steric shielding of the viologen quencher as originally proposed.[3] Furthermore, the authors reported that adding a sufficient amount of avidin to a **57a**- or **57c**-quenched solution of **56** resulted in more intense fluorescence than a solution of just the conjugated polymer alone; fluorescence ultimately recovered to approximately 150% of the original intensity of the unquenched polymer. The addition of avidin to a solution of only polymer **56** also produced an increase in fluorescence intensity. The authors suggested that the fluorescence increase in the presence of avidin was due to nonspecific interactions between the cationic protein and the anionic conjugated

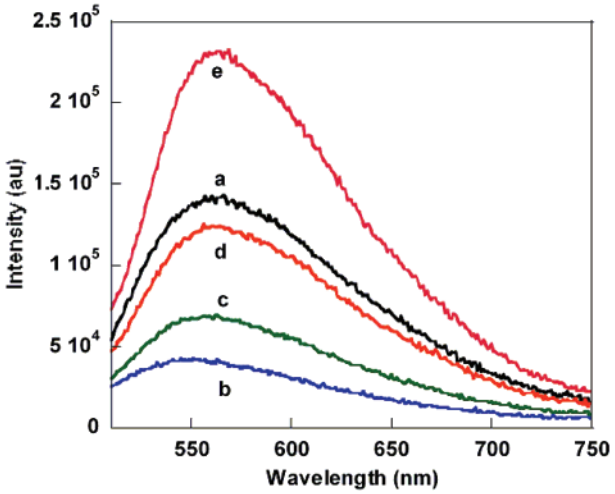

Figure 27. Fluorescence spectra ($\lambda_{ex} = 500$ nm) in water: (a) **56** ([RU] $= 1.0 \times 10^{-5}$ M) (black line); (b) **56** and [**57a**] $= 3.2 \times 10^{-7}$ M (blue line); (c) **56**, **57a**, and [avidin] $= 3.0 \times 10^{-8}$ M (green line); (d) **56**, **57a**, and [avidin] $= 8.0 \times 10^{-8}$ M (red line); (e) **56**, **57a**, and [avidin] $= 2.3 \times 10^{-7}$ M (pink line). (Reprinted with permission from ref 142. Copyright 2004 American Chemical Society.)

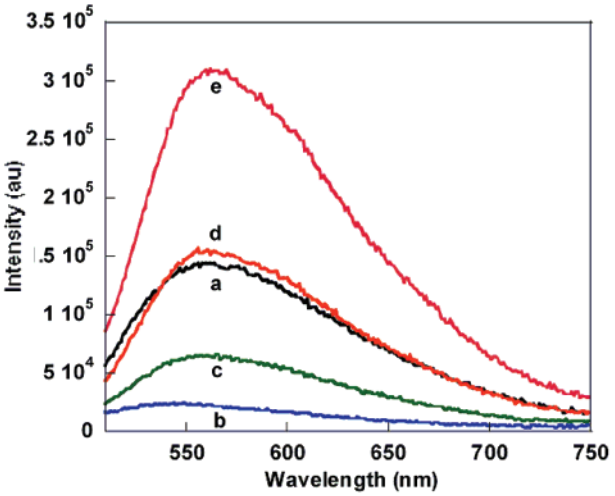

Figure 28. Fluorescence spectra ($\lambda_{ex} = 500$ nm) in water: (a) **56** ([RU] $= 1.0 \times 10^{-5}$ M) (black line); (b) **56** and [**57c**] $= 3.2 \times 10^{-7}$ M (blue line); (c) **56**, **57c**, and [avidin] $= 3.0 \times 10^{-8}$ M (green line); (d) **56**, **57c**, and [avidin] $= 8.0 \times 10^{-8}$ M (red line); (e) **56**, **57c**, and [avidin] $= 2.3 \times 10^{-7}$ M (pink line). (Reprinted with permission from ref 142. Copyright 2004 American Chemical Society.)

polymer. They also proposed that avidin-mediated fluorescence recovery of quenched polymer solutions was due to formation of an avidin−polymer complex that prevented close polymer−quencher association. Bovine serum albumin (BSA), pepsin A, and microtubule associated protein tau were also investigated. Under the experimental conditions, microtubule associated protein tau was positively charged, whereas BSA and pepsin A were negatively charged. All three of these proteins interacted with conjugated polyelectrolyte **56** in water and increased polymer fluorescence intensity. In addition, all three proteins were able to recover polymer fluorescence from solutions containing quenchers **57a** or **57c**, additional evidence that nonspecific protein−polymer interactions produced the fluorescence recovery.

In aqueous buffer (100 mM ammonium carbonate, pH 8.9) the quenching response of **56** decreased approximately 100-

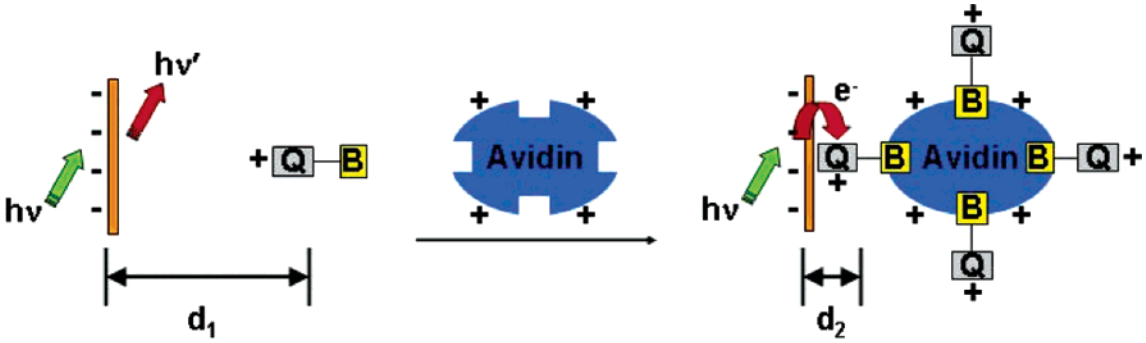

Figure 29. Bazan's proposed mechanism for enhancement of fluorescence quenching by addition of avidin under buffered conditions. (Reprinted with permission from ref 142. Copyright 2004 American Chemical Society.)

fold for both **57c** ($K_{SV} = 1.5 \times 10^4$) and **57a** ($K_{SV} = 6.3 \times 10^4$).[142] The large drop in sensitivity in buffered solution was attributed to screening of the electrostatic attraction between the anionic conjugated polymer and cationic quenchers. The authors proposed that the turnover in selectivity upon going from water to aqueous buffer (**57c** is the more effective quencher in water, whereas **57a** is superior in aqueous buffer) was due to the greater hydrophobicity of biotin-functionalized **57a** relative to **57c**. At higher ionic strength, hydrophobic interactions between **57a** and polymer **56** were relatively more important. In aqueous buffer, avidin addition did not result in increased fluorescence from a mixture of polymer **56** and **57c**. Avidin addition to a buffered solution of polymer **56** quenched by biotin-functionalized quencher **57a** resulted in additional quenching (opposite to the response in water). The authors proposed the additional quenching was due to formation of an avidin−quencher complex (with the potential to incorporate four quenchers onto a single avidin) in aqueous buffer. The avidin−quencher complex was positively charged, due to both the positive charge on avidin and the incorporation of positively charged quenchers, and was less affected by electrostatic screening due to buffer ions and was, therefore, better able to associate with the anionic conjugated polymer than the cationic quencher alone. Figure 29 is a graphical representation of this proposed mechanism.

In buffer, polymer **56** did not respond strongly to anionic proteins BSA and pepsin A. The cationic protein microtubule associated protein tau, however, increased polymer fluorescence even in buffered solution. In addition, this protein was able to produce a fluorescence recovery from solutions of polymer **56** and quenchers **57c** and **57a**. The fluorescence recovery was attributed to nonspecific polymer−protein interactions. Taken together, these careful and extensive experiments by Bazan and co-workers are inconsistent with the work of Whitten et al. and cast serious doubts on the conclusions drawn in Whitten's initial biosensing publication.[3] Moreover, Bazan's experiments highlight some of the significant problems, including nonspecific interactions with biological macromolecules and the influence of ionic strength on quenching processes, associated with the use of conjugated polyelectrolytes as biosensors.

In 2005, Wang and co-workers reported a biosensory system that took advantage of the nonspecific interaction between anionic conjugated polyelectrolytes and avidin,[143] an interaction elucidated by Bazan et al. in the previous year.[142] The authors used an anionic, sulfonate-substituted polyfluorene (**86**) as the fluorophore and an anionic, biotin-functionalized Lucifer dye as the quencher. Anionic polymer **86** was not effectively quenched by the anionic Lucifer dye in aqueous solution because the polymer and quencher were

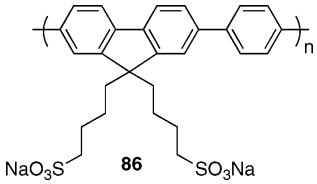

86

both negatively charged. Addition of avidin, which was cationic under the conditions of the assay, to a solution of **86** and the anionic quencher produced a fluorescence quenching response. Avidin-induced quenching ($K_{SV} = 3.2 \times 10^8$) was due to formation of an avidin−quencher complex, which was cationic overall and therefore electrostatically associated with the anionic conjugated polymer. Detection of avidin down to a concentration of 3.8×10^{-10} M was demonstrated. Avidin alone also quenched conjugated polymer fluorescence, a response that was attributed to avidin-induced polymer aggregation. Nevertheless, fluorescence quenching by avidin was 10-fold more effective in the presence of the biotin-functionalized dye.

Bunz and co-workers also investigated nonspecific interactions between conjugated polyelectrolytes and proteins.[144] The authors studied the fluorescence responses of anionic conjugated polymers **10** (originally reported by Schanze and used to detect protease activity)[124] and **87** to proteins in 10

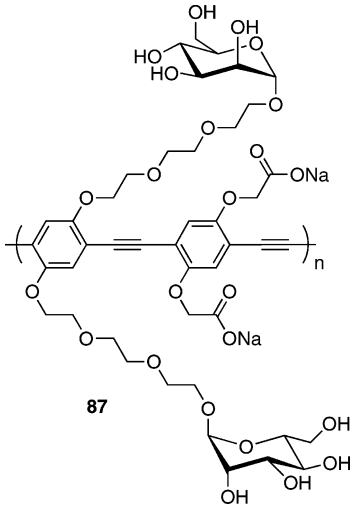

87

mM sodium phosphate aqueous buffer (pH 7.2). Cationic (cytochrome *c*, histone, and lysozyme), overall charge neutral (myoglobin and hemoglobin), and anionic (bovine serum albumin) proteins were evaluated. With the exception of bovine serum albumin, all the proteins quenched the fluorescence of **10** and **87**. The largest quenching response was

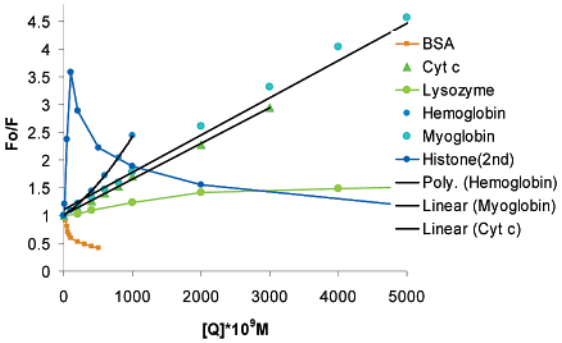

Figure 30. Fluorescence response of conjugated polyelectrolyte **10** to proteins in 10 mM phosphate buffer at pH 7.2. (Reprinted with permission from ref 144. Copyright 2005 American Chemical Society.)

between histone and polymer **10** ($K_{SV} = 2.8 \times 10^7$), and the weakest response was between hemoglobin and polymer **87** ($K_{SV} = 1.0 \times 10^5$). Bovine serum albumin, the only anionic protein included in the study, increased emission from both polymers. The fluorescence response of polymer **10** to the proteins is provided in Figure 30. The authors attributed fluorescence quenching by myoglobin and hemoglobin to an electron-transfer-based mechanism. Quenching by histone and lysozyme was attributed to self-quenching upon protein-induced polymer aggregation and/or to charge transfer. Consistent with lysozyme-mediated polymer aggregation, emission from **10** shifted 10 nm to the red in the presence of lysozyme. The authors ascribed the fluorescence increases upon addition of bovine serum albumin to the surfactant-like properties of this macromolecule.

As a result of their studies, the authors' experience led them to insightfully predict "that most conjugated polyelectrolyte's optical and fluorescent properties will be modulated by complex biological fluids". This statement appears to be accurate and suggests that practical applications of conjugated polyelectrolytes to real-world biosensing applications will be difficult to realize. In particular, the development of conjugated polyelectrolyte-based assays that are capable of being directly performed using biological fluids, which typically contain a complex mixture of biological macromolecules, will be challenging because of interference and poor specificity due to ubiquitous nonspecific interactions.

4.6. Nonionic AFPs for Biosensing

In order to circumvent the complications inherent to using ionic conjugated polymers for sensing charged biomolecules in aqueous environments, Kuroda and Swager developed a nonionic water-soluble poly(*p*-phenylene ethynylene) (**88**) as a potential platform for high specificity biosensory materials.[145] Instead of incorporating charged side chains, **88** had large numbers of hydrophilic hydroxy groups. The water-soluble polymer was synthesized by Sonogashira cross-coupling with a number-average molecular weight as determined by GPC in DMF of 32,000. Even at this significantly high molecular weight, **1** still dissolved in water instantaneously without heating. Kuroda and Swager also explored the potential for this polymer to be useful in a biosensing scheme based on thermal precipitation.[146] End-capping **88** with a di-*tert*-butyl nitroxide-based initiator and subsequently grafting poly(*N*-isopropylacrylamide) (polyNIPA) onto the termini of **88** gave a fluorescent material that was soluble in water at room temperature but precipitated at 50 °C. The authors realized precipitation-induced energy transfer, albeit

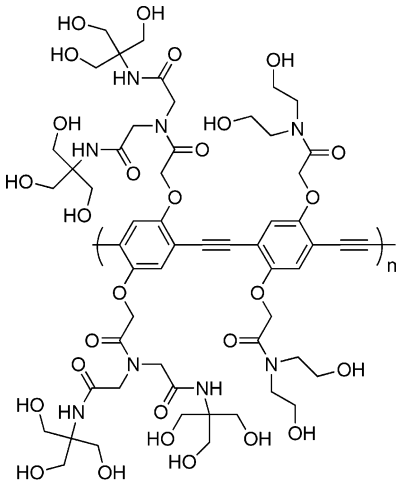

88

with only a 20% emission amplification over direct excitation of the dye, by either including a rhodamine B-containing methacrylate monomer in the end-capping graft or coprecipitating the polyNIPA-grafted PPE with a random copolymer of NIPA and the dye-containing monomer.

Bailey and Swager recently reported the synthesis and thiol conjugation of maleimide-functionalized poly(*p*-phenylene ethynylene)s.[147] The maleimide-containing polymers were synthesized by Pd-catalyzed cross-coupling of aryl diacetylene and aryl diiodide monomers. The maleimide functionality was not compatible with the cross-coupling-based polymerization conditions, likely due to undesired Heck chemistry involving the maleimide group. To circumvent this problem, a masked maleimide was taken through the polymerization reaction; the maleimide was protected as a Diels−Alder adduct with furan. The masked maleimide could be thermally deprotected, and the authors developed a convenient one-pot deprotection/thiol-functionalization procedure. A THF solution of the protected maleimide-containing polymer (**89**)

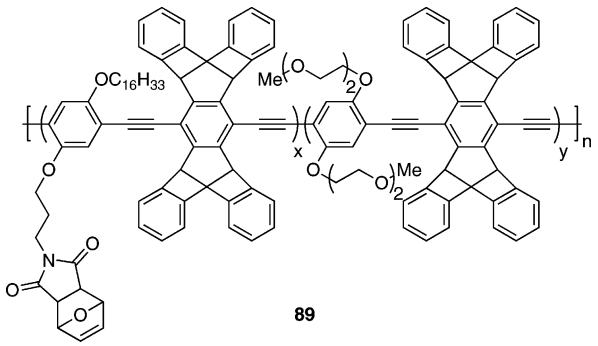

89

was heated to reflux. Then, a methanol/THF solution of a thiol-functionalized rhodamine dye was added to provide the rhodamine-tethered conjugated polymer. The authors confirmed thiol functionalization by GPC as well as by fluorescence experiments that demonstrated energy transfer from the conjugated polymer to the tethered rhodamine dye. As demonstrated, maleimide-functionalized poly(*p*-phenylene ethynylene)s have excellent potential to participate in conjugate addition and Diels−Alder chemistries, thereby rendering these fluorescent polymers potentially useful in the development of highly functionalized conjugated polymer-based sensors. In particular, biosensory applications of these polymers may be the most appealing due to the prevalence of well-established thiol-based biomolecule conjugation chemistry.

In 2004, Zheng and Swager reported unexpected results from FRET experiments between a biotin-substituted PPE (**90**) and dye-labeled streptavidin.[148] When the authors incubated **90** and fluorescein-labeled streptavidin at room

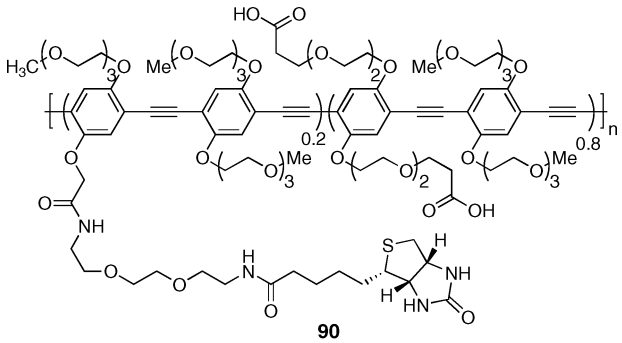

90

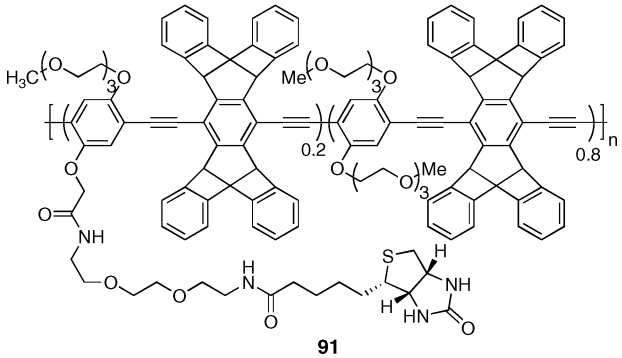

91

temperature, they observed only a very low degree of FRET-induced emission enhancement of the dye, even though the spectral overlap between the emission spectrum of the donor (**90**) and the absorbance of the acceptor (fluorescein) was excellent. Surprisingly, rhodamine-B-labeled streptavidin showed more efficient FRET-induced dye emission relative to the fluorescein analogue, even though the red-shifted rhodamine dye has a smaller spectral overlap integral with **90**. Furthermore, Texas Red-labeled streptavidin gave remarkable energy-transfer-induced dye emission (Figure 31). A structurally similar but non-biotinylated PPE gave no observable energy-transfer-induced emission, nor did the use of biotin-saturated, dye-labeled streptavidin. These results are further evidence that the factors controlling energy-transfer efficiency are indeed multifaceted and that reliance on spectral overlap to anticipate the effectiveness of an energy-transfer-based sensing scheme can lead to erroneous conclusions. The authors also reported similar aqueous-phase sensing experiments using thin films of water-insoluble, biotin-functionalized conjugated polymer **91**.

Swager and co-workers have further explored aqueous-phase sensing using thin films of water-insoluble poly(*p*-phenylene ethynylene)s. The sensitivity of hydrophobic crown ether-functionalized polymers to quenching by hydrophobically functionalized viologens was studied.[149] The Swager group had previously demonstrated amplified quenching of a crown ether-functionalized polymer (**92**) by viologens in organic solution.[150] In addition, the Swager group previously studied Langmuir−Blodgett (LB) films of this crown ether-functionalized polymer as well as the fluorescence-quenching response of the LB films to acridine orange[151] and dimethyl viologen[152] in organic solution.[153] Polymers such as **92** are strongly quenched by viologen cations in organic solvents because of the effective host−guest interac-

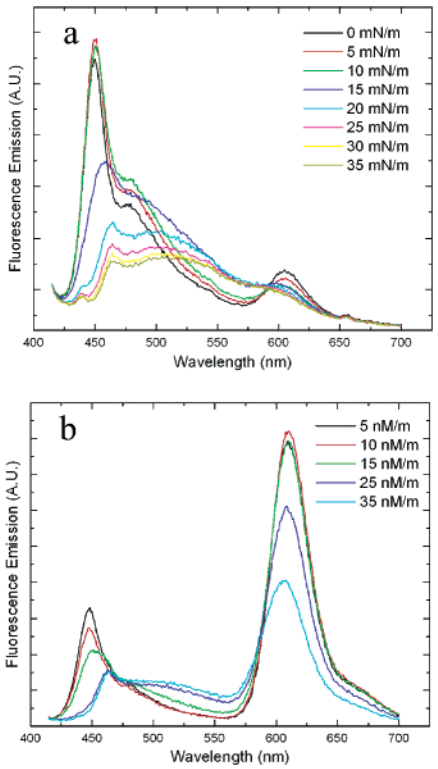

Figure 31. Addition of 0.017 nmol aliquots of (A) Rhodamine-B-labeled streptavidin or (B) Texas Red-labeled streptavidin to 1.51 nmol of **90**. (Reproduced from ref 148 by permission of The Royal Society of Chemistry. Copyright 2004.)

tion between the conjugated polymer-based host and the viologen guest. In aqueous solution, however, strong solvation of the cationic viologen quenchers obstructs the host−guest interaction and prevents efficient fluorescence quenching. To improve aqueous-phase sensitivity by increasing polymer film−quencher affinity, hydrophobically functionalized viologens were explored as quenchers of hydrophobic polymer thin films. A solution of polymer **92** in 9:1 aqueous Tris buffer/THF (the THF was required to dissolve the water-insoluble polymer) was weakly quenched by naphthyl-

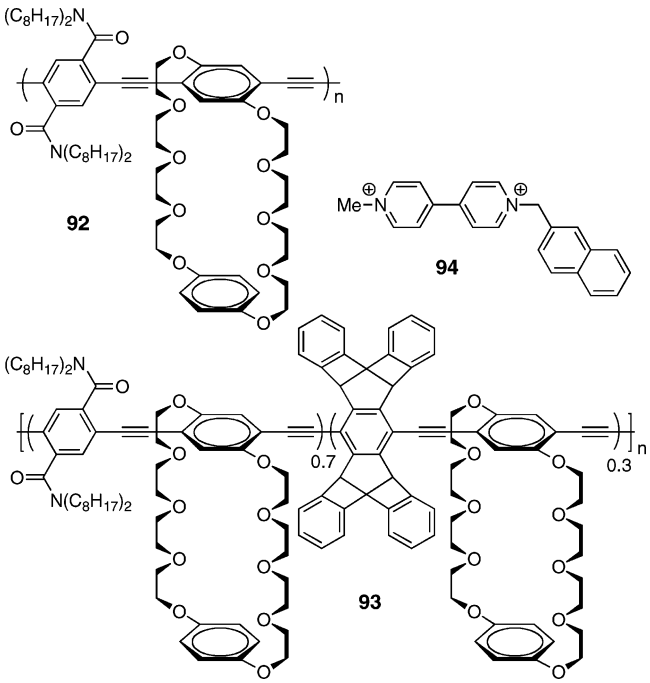

92

94

93

functionalized viologen **94** ($K_{SV} = 8.2 \times 10^2$). A LB monolayer film of **92**, however, was much more sensitive ($K_{SV} = 4.8 \times 10^5$). The higher sensitivity of the monolayer film was attributed to facilitated intra- and interpolymer exciton transport in the film. In addition, the film may provide a highly hydrophobic environment to favorably interact with the hydrophobically functionalized quenchers. LB monolayer quenching experiments revealed that quenching efficiency correlated with the hydrophobicity of the viologen quencher; the most hydrophobic quenchers provided the highest Stern−Volmer quenching constants. Remarkably, simple tuning of quencher hydrophobicity resulted in 370-fold better sensitivity. Sensitivity depended not only on hydrophobic interactions, as the host−guest association between the crown ether-functionalized polymer film and the viologen quencher was also essential. A polymer analogous to **92**, but which contained triethylene glycol substituents in place of the crown ether, was 30 times less sensitive. Polymer **93**, which incorporated a pentiptycene-based monomer, produced the most sensitive LB monolayers ($K_{SV} = 1.2 \times 10^6$ for viologen **94**). This aqueous-phase sensing system was less prone to interference from changes in solution ionic strength and the nature of the buffer ions than systems that rely on conjugated polyelectrolytes. The quenching response only varied by approximately 30% in solutions of pure water, 20 mM Tris buffer, and 100 mM phosphate buffer. Sensory systems that use thin films of hydrophobic, water-insoluble, conjugated polymer for sensing in aqueous solution have potential application in biosensing and may prove to be more resistant to detrimental nonspecific interactions than conjugated polyelectrolytes.

Almost all conjugated polymers used as fluorescent sensors have relatively low ionization potentials and are, therefore, quenched by electron-deficient aromatic analytes. In 2004, Swager, Kim, and Zhu reported the synthesis of poly(*p*-phenylene vinylene) polymers that contained electron-withdrawing [2.2.2] bicyclic ring systems.[154] The electron-withdrawing substituents (trifluoromethyl, ester, and carboxylic acid) influenced polymer properties via hyperconjugative and inductive interactions. Thin films of the electron-deficient

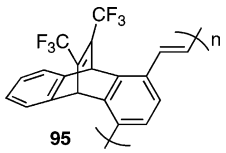

95

polymers were more sensitive to fluorescence quenching by an electron-rich analyte, *N*,*N*-dimethyl *p*-toluidine, than were films of an analogous electron-rich, alkoxy-substituted poly(*p*-phenylene vinylene). Sensitivity toward *N*,*N*-dimethyl-*p*-toluidine was highest for thin films of trifluoromethyl-substituted polymer **95**. The complementary sensory response of the electron-deficient poly(*p*-phenylene vinylene)s expanded the potential application of fluorescent conjugated polymer sensors to include electron-rich aromatic analytes.

Swager and co-workers continued to investigate electron-deficient conjugated polymer scaffolds and described the synthesis and photophysical characterization of high ionization potential poly(*p*-phenylene ethynylene)s in 2005.[155] These high ionization potential materials incorporated electron-withdrawing groups, such as perfluoroalkyl and ester substituents, which imparted the polymers with high excited-state electron affinities. Ultraviolet photoelectron spectroscopy

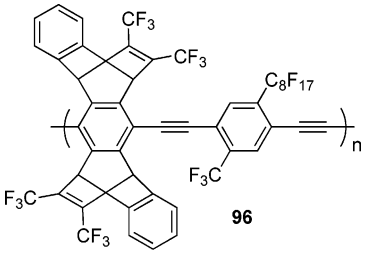

96

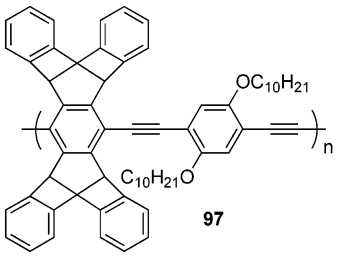

97

(UPS) was used to determine the ionization potential of spin-coated polymer thin films. Polymer **96**, which incorporated perfluoroalkyl substitution into the polymer main chain as well as a [2.2.2] bicyclic ring system containing a bis-trifluoromethyl-substituted alkene, had the highest ionization potential (6.75 eV) of the polymers investigated. In comparison, the ionization potential of electron-rich pentiptycene-containing polymer **97** was found to be 5.82 eV. Whereas the fluorescence of electron-rich polymers, such as **97**, was quenched by electron-poor aromatics (e.g., DNT, TNT), electron-poor polymers, such as **96**, responded to electron-rich aromatics. Fluorescence quenching by indole correlated with ionization potential; high ionization potential polymers were quenched more efficiently. Indole quenched the fluorescence of polymer **97** in THF solution with a Stern−Volmer constant of only 0.9 M^{-1}. However, fluorescence of electron-deficient polymer **96** was much more sensitive to quenching by indole ($K_{SV} = 25.6\ M^{-1}$). Thin films of **96** were quenched by indole vapor. The quenching response at the fluorescence maximum ($\lambda_{max} = 427$ nm) was accompanied by the appearance of a broad new emission at 496 nm. The complementary sensory responses of electron-rich polymer **97** and electron-poor analogue **96** are illustrated in Figure 32. Thin films of **97** were quenched by 2,4 DNT, but not by indole. In contrast, thin films of **96** were quenched by indole but not 2,4 DNT. Electron-deficient conjugated polymers such as **96** have further demonstrated utility in sensing biologically relevant analytes such as indole-containing proteins and phenol-containing compounds.[156]

Lippard et al. reported the first conjugated polymer fluorescence sensor for nitric oxide (NO), an important signaling molecule in biology, in 2005.[157] The authors

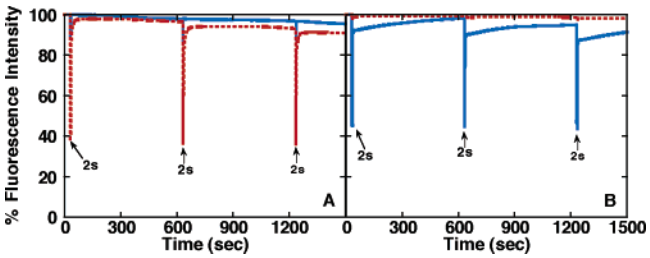

Figure 32. Changes in fluorescence intensity of (A) **97** and (B) **96** films exposed to indole (blue solid line) and 2,4-DNT (red dotted line) vapors for the time indicated. (Reprinted with permission from ref 155. Copyright 2005 American Chemical Society.)

utilized a poly(*p*-phenylene vinylene) that incorporated a 2,2′-bipyridine unit into the conjugated polymer backbone (**98**).

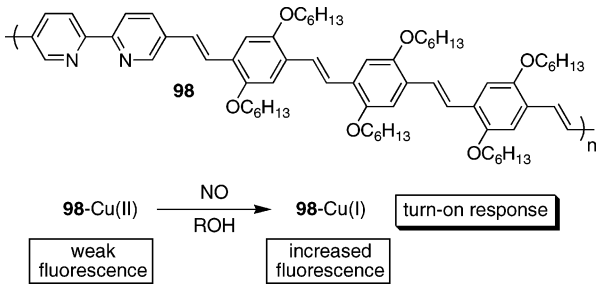

Polymer **98** was brightly fluorescent in solution (4:1 CH_2Cl_2/EtOH). Exposure of **98** to Cu(I) ($[Cu(NCMe)_4][BF_4]$) reduced the fluorescence intensity of **98** to approximately 70% of its original value, whereas the addition of Cu(II) ($Cu(OTf)_2$) to **98** resulted in a larger, 4-fold quenching response. The difference in fluorescence between the Cu(II)- ("off") and the Cu(I)-bound polymer ("on") was used to detect NO, as NO can reduce Cu(II) to Cu(I). Addition of NO to the **98**−Cu(II) complex produced a rapid fluorescence recovery; fluorescence increased by a factor of 2.8 in less than 1 min upon addition of 300 equiv of NO. Detection of NO down to 6.3 nM was possible using the **98**−Cu(II) complex. No change in polymer fluorescence occurred upon the addition of NO to **98** in the absence of Cu(II). The addition of acetic acid to **98** resulted in fluorescence quenching, thereby ruling out acid, generated upon addition of NO, as the source of the turn-on response. The fluorescence recovery was attributed to reduction of the quenched paramagnetic d^9 Cu(II) complex to a fluorescent diamagnetic d^{10} Cu(I) complex, although potential structural changes in the **98**−Cu complex upon going from Cu(II) to Cu(I) were not ruled out as the source of the fluorescence change. The conjugated polymer sensor was selective for NO over nitroxyl (HNO) and nitrosonium (NO^+). Exposure of **98**−Cu(II) to a nitrosothiol (*S*-nitroso-*N*-acetylpenicillamine) led to a slow increase in emission; fluorescence increased by a factor of 2.1 over the course of 24 h. The slow response was ascribed to generation of NO via copper-catalyzed decomposition of the nitrosothiol. In addition, O_2 was not a source of significant interference.

Conjugated polymers functionalized with sugar residues have found use in sensing applications related to the detection of lectins (sugar-binding proteins) and cells. Following the first synthesis of a carbohydrate-functionalized poly(*p*-phenylene ethynylene) by Bunz et al.,[158,159] Swager, Seeberger, and co-workers reported in 2004 the first use of a conjugated polymer for the detection of cells.[160] Poly(*p*-phenylene ethynylene) **99** was synthesized by a post-polymerization functionalization with 2′-aminoethyl mannoside. The functionalization was carried out on the carboxylate-substituted polymer and resulted in approximately 25% incorporation of mannose. Unfunctionalized residues were capped with ethanolamine. A galactose-substituted polymer was also synthesized for comparison. A solution containing mannose-functionalized polymer **99** was titrated with Alexa Fluor 594-labeled concanavalin A (Con A), a lectin that binds mannose. As the dye-labeled lectin was added, polymer **99** fluorescence decreased due to efficient FRET from the conjugated polymer to the lectin-functionalized dye, demonstrating that the mannose-functionalized polymer bound to Con A. An identical experiment was performed with an analogous galactose-substituted polymer;

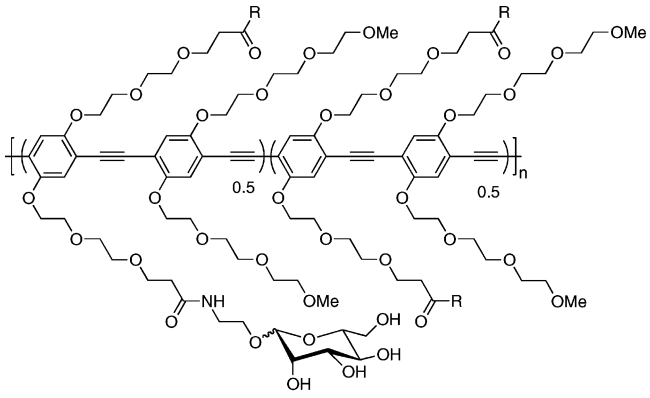

however, no fluorescence quenching occurred, as Con A does not bind galactose. Mannose-functionalized polymer **99** was also used to detect *Escherichia coli* (*E. coli*), a bacterial food contaminant. Experiments demonstrated that **99** fluorescently labeled mannose-binding *E. coli* but did not bind and stain mutant, non-mannose-binding *E. coli*. Furthermore, the galactose-functionalized polymer did not stain either the mannose-binding *E. coli* or the mutant bacteria. Cell staining using the mannose-functionalized polymer and *E. coli* produced fluorescent clusters of bacterial cells, presumably facilitated by multivalent interactions with the conjugated polymer. Cell-bound polymer fluorescence was red-shifted relative to the case of solution, suggesting bacterial cell-mediated conjugated polymer aggregation. Detection of as few as 10^4 bacterial cells was possible using mannose-functionalized polymer **99** (Figure 33). The multivalent nature of the interaction between mannose-functionalized polymer **99** and *E. coli* cells was crucial for low-level detection, as 2′-fluorescein aminoethyl mannoside, which cannot take advantage of multivalent interactions with the bacterial cells, was less sensitive. The advantage due to the multivalent interaction between the mannose-functionalized polymer and *E. coli* increased binding by a factor of 3.5×10^4.

Bunz and co-workers synthesized mannose-functionalized poly(*p*-phenylene ethynylene) **100a** via polymerization of an acetyl-protected mannose-substituted monomer.[161] The acetyl protecting groups were cleaved during the polymerization to provide the deprotected polymer directly. Conjugated polymer **100a** fluorescence was quenched by Con A in

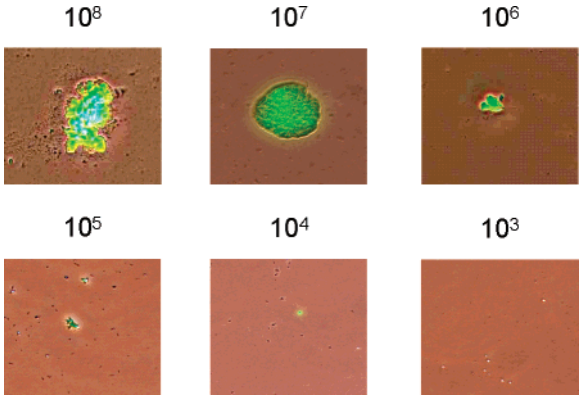

Figure 33. Detection of mannose-binding *E. coli* by **99**. The number of bacteria incubated with the polymer-containing solution is indicated above each image. (Reprinted with permission from ref 160. Copyright 2004 American Chemical Society.)

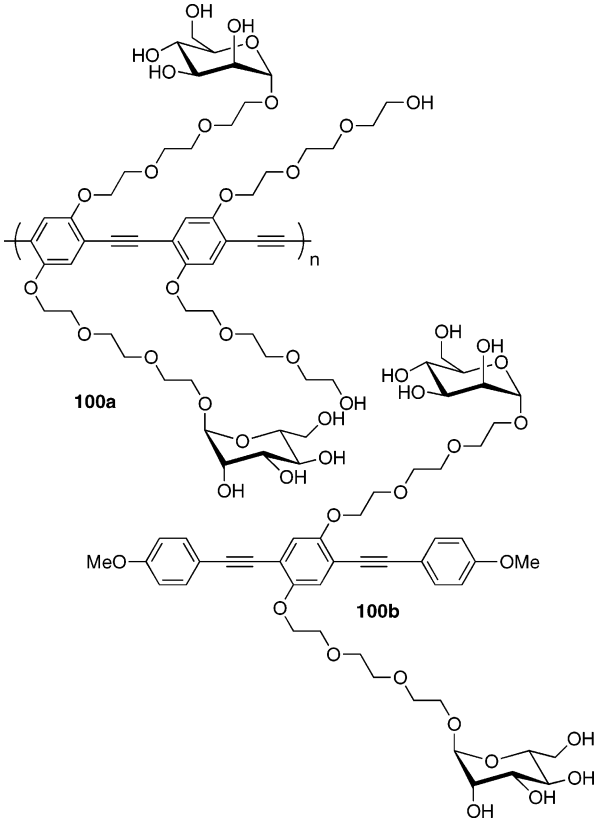

aqueous solution ($K_{SV} = 5.6 \times 10^6$). At high concentrations of Con A, the Con A−**100a** complex precipitated as 300−500 nm sized aggregates. Biotin-functionalized Con A also quenched **100a** fluorescence. The quenching response was made more sensitive through precipitation of a "super-aggregate" of the biotinylated Con A−**100a** complex with streptavidin-coated microspheres. The fluorescence of a small molecule model compound (**100b**), which was not able to participate in a multivalent interaction with the sugar-binding protein, was not altered in the presence of Con A. Polymer fluorescence was unchanged in the presence of bovine serum albumin, which does not bind mannose residues. In addition, polymer **100a** did not respond to jacalin, a galactose-binding protein. These control experiments are consistent with the mannose-binding properties of Con A being critical to fluorescence quenching of the mannosylated polymer and suggest that the response was not due to nonspecific interactions between the conjugated polymer and the biological macromolecule. Bunz et al. also studied the effects of surfactants on carbohydrate-functionalized conjugated polymer emission.[162] In addition, the absorbance of a carbohydrate-functionalized poly(*p*-phenylene vinylene) blue-shifted in the presence of Con A.[163] In a related study by Baek and co-workers, carbohydrate-functionalized poly(thiophene)s responded to lectins, Influenza virus, and *E. coli* by absorbance red shifts.[164]

4.7. AFPs for Biosensing on Unique Substrates

Bunz and Wilson have used an agglutination process to model the interactions of suitably functionalized conjugated polymers with bacteria.[165] The authors used streptavidin-coated polystyrene beads and biotin-substituted PPE **101a** in this model study. When polymer **101b** was mixed with the protein-coated microspheres, the polymer solution did not change, whereas polymer **101a** produced a precipitate.

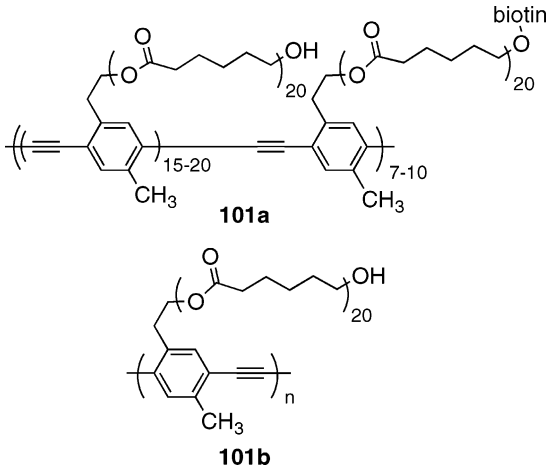

This precipitate, upon analysis with fluorescence microscopy, showed red-shifted fluorescence relative to solid-state **101a**. Scanning electron microscopy of the precipitate showed that the conjugated polymer evenly covered the beads, indicative of the interaction between the polymer and the particles. The authors observed no apparent interactions in the SEM of the microsphere/**101b** mixture.

Samuelson and co-workers coated electrospun fibers of cellulose acetate with an anionic poly(thiophene) and used the conjugated polymer-coated fibers to detect dimethyl viologen and cyt *c*.[166] The electrospun cellulose acetate fibers formed a water-insoluble web, or membrane-like structure, with a very high surface-to-volume ratio. The fibers were anionic due to partial acetate hydrolysis. Through electrostatic layer-by-layer (LBL) assembly, the fibers were alternately coated with layers of poly(allylamine hydrochloride) and anionic conjugated polyelectrolyte **102**. The fluorescence of

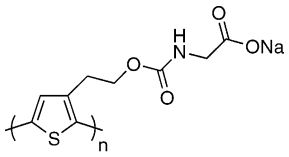

the membrane-supported conjugated polyelectrolyte was quenched by dimethyl viologen ($K_{SV} = 3.5 \times 10^6$) and cyt *c* ($K_{SV} = 6.9 \times 10^6$). The high sensitivity was attributed to a combination of amplified sensing, strong quencher−polymer interactions, and the very high surface-to-volume ratio (10−100 times higher than that of continuous thin films) of the membrane-supported polymer, which facilitated quencher−polymer association.

Swager and co-workers used the layer-by-layer deposition technique to produce thin films composed of cationic conjugated polyelectrolyte **103** and an anionic, fluorescein-amine-functionalized polyacrylate (**104**).[167] The fluorescein-

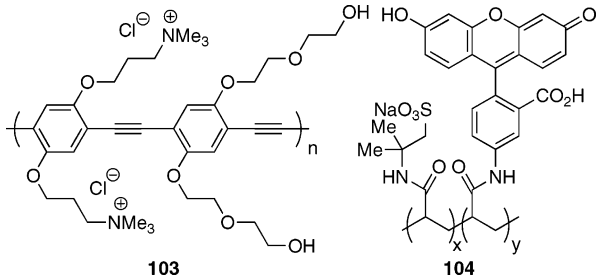

amine dye was pH sensitive. At high pH, the dye was deprotonated and existed as the strongly absorbing and fluorescent phenolate. The dye was protonated at low pH, resulting in weak absorption and emission. Conjugated polymer (**103**) fluorescence (λ_{max} = 471 nm) and dye absorption (λ_{max} = 490 nm) were well matched, therefore encouraging FRET from the conjugated polymer to the dye. The authors produced bilayer films by depositing **103** onto a base-washed glass slide followed by dipping the cationic polymer-coated slide into a solution of **104**. Fluorescence of the bilayer films was responsive to pH. Experiments were conducted by exciting the conjugated polymer at 420 nm. More than 90% of the conjugated polymer fluorescence was quenched at pH 11 due to efficient FRET to the fluoresceinamine dye, which resulted in an intense red-shifted emission from the dye. At pH 6, however, the conjugated polymer fluorescence was strong and no fluoresceinamine emission was observed. The conjugated polymer acted as an efficient light harvester in the thin films; the authors observed about 10-times stronger dye emission upon excitation of the conjugated polymer (420 nm) versus direct excitation of the dye (500 nm).

Wosnick, Liao, and Swager have reported the use of LBL films on silica microspheres for sensory amplification.[168] Microspheres can be readily functionalized by solid-phase synthetic techniques, are easily manipulated, and offer an increased surface area for interaction with analytes. The authors used PDAC (**105**) as the polycation and synthesized

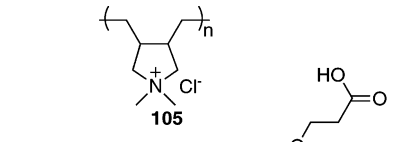

105

106

106, a nonaggregating PPE with carboxylate-terminated side chains, via Sonogashira polymerization (M_n = 19,000 Da) for use as the polyanion in the LBL thin film deposition process. By alternately treating base-treated, commercially available monodisperse microspheres with aqueous solutions of **105** and **106**, the authors could isolate brightly fluorescent microspheres that remained smoothly spherical and had an emission spectral shape similar to that of **106** in DMF solution. Solution quenching experiments revealed that the LBL films on silica microspheres gave higher quenching constants in aqueous environments than an electronically similar polymer in solution, whereas in organic solvent they showed similar performance, suggesting that hydrophobic effects were important in this system. In addition, spheres coated with two layer pairs showed more efficient quenching than spheres coated with one layer pair.

Whitten, Lopez, and co-workers coated borosilicate microspheres with cationic conjugated polyelectrolyte **107** and used flow cytometry to examine the fluorescence quenching of the polymer-coated microspheres.[169] Small-molecule quencher 9,10-anthraquinone-2,6-disulfonic acid quenched the microsphere fluorescence with a Stern−Volmer constant of 8 × 10^5. The authors also studied the effect of lipid bilayers on the fluorescence of polymer-coated microspheres. The addition of zwitterionic lipids to the microspheres increased the fluorescence intensity while still allowing the microsphere-supported conjugated polymer to be quenched by the anionic quencher. An anionic lipid (1,2-dimyristoyl-*sn*-glycero-3-[phosphor-*rac*-(1-glycerol)] sodium salt), however, slightly attenuated polymer fluorescence and protected the microspheres from complete quenching by the anionic anthraquinone. The authors proposed that the anionic lipid formed a lipid bilayer over the surface of the polymer-coated microspheres, thereby preventing close association of the anionic quencher and the cationic conjugated polymer. Fluorescence quenching of the bilayer-coated microspheres could be restored by the addition of a surfactant (Triton X-100) that disrupted the lipid bilayer. The authors proposed that lipid bilayer-protected fluorescent microspheres could be useful in biosensing applications, particularly in detecting analytes that are capable of disrupting lipid bilayers or creating pores or channels through the bilayer that would allow quenchers to access the conjugated polymer coating.

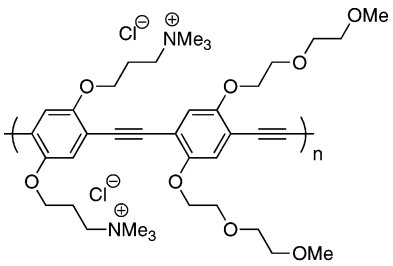

107

In 2003, Hancock and co-workers reported the preparation and oligonucleotide sensing properties of PPE particles.[170] By precipitating the polymer from a homogeneous DMSO solution into SSPE buffer, the authors could isolate nearly spherical polymer particles with diameters between 500 and 800 nm, as observed by TEM. Cy-5 labeled oligonucleotides nonselectively quenched dispersions of these particles in SSPE buffer down to 1 × 10^{-10} M (K_{sv} = 8.8 × 10^{-7} M^{-1}), a 2 order of magnitude improved detection threshold relative to direct excitation of the Cy-5 fluorophore.

5. Detection of DNA

5.1. Regioregular Cationic Poly(thiophene)s for DNA Detection[171]

The group of Leclerc at Laval pioneered DNA detection with conjugated polymers, using a scheme that is based on the electrostatic attraction between a cationic conjugated polymer and DNA. This scheme utilizes cationic poly(3-alkoxy-4-methylthiophene)s, which can be synthesized via oxidative polymerization by either electrochemical or chemical (ferric chloride) means. Some of the initial sensing studies

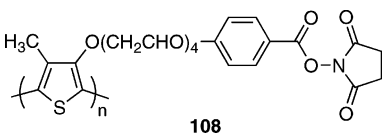

108

on this class of polymers focused on postpolymerization modification of an *N*-hydrosuccinimide (NHS) ester-derivatized polymer (**108**). Specific binding moieties were intro-

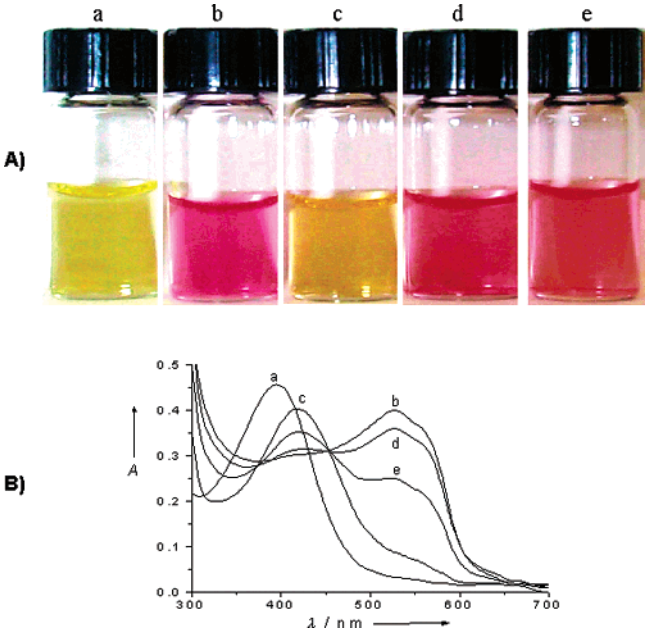

Figure 34. (A) Photographs of solutions of (a) **12**, (b) the **12**−ssDNA duplex, (c) the **12**−dsDNA triplex, (d) the **12**−ssDNA duplex plus a complementary target with a two-base mismatch, and (e) **12**−ssDNA plus a complementary target with a one-base mismatch after mixing at 55 °C for 5 min. (B) UV/vis spectra corresponding to photograph A. (Reprinted with permission from ref 173. Copyright 2002 Wiley-VCH publishers.)

duced to induce an affinitychromic optical transition in this material.[172] The binding moieties included a crown ether for the sensing of alkali metal ions, and biotin for the detection of avidin.

In addition, Leclerc and co-workers found that the water-soluble imidazolium-substituted poly(thiophene) **12**, which was oxidatively synthesized using $FeCl_3$, was highly sensitive to the presence of oligonucleotides, as pictured in Figure 34.[173] Upon addition of 1.0 equiv (per monomer unit of polymer) of a 20-base segment of ssDNA to **12** in 0.1 M aqueous NaCl, the color of the solution changed from yellow (λ_{max} = 397 nm) to red (λ_{max} = 527 nm) within 5 min. This was attributed to the formation of a "duplex" between **12** and the ssDNA driven by electrostatic attraction. The authors observed precipitation from the red mixture after several hours. If, however, 1.0 equiv of the complementary ssDNA was added to the red mixture at elevated temperature (>45 °C), the solution became yellow (λ_{max} = 421 nm), which the authors attributed to the formation of a "triplex", formed by the complexation of **12** with the hybridized dsDNA. Further addition of ssDNA did not change the optical properties of the mixture. The existence of a clean isosbestic point upon addition of complementary ssDNA indicated the existence of only two structures (duplex and triplex).

The authors could also follow this sequence of events by fluorescence spectroscopy. The fluorescence of the initial yellow form of **12**, with a quantum yield of 0.03 and λ_{max} of 530 nm, was slightly red-shifted and strongly quenched upon formation of the red duplex. Triplex formation, induced by addition of complementary ssDNA, gave a 5-fold increase in emission intensity. Using this fluorescence recovery as the sensing signal, the authors could measure as few as 3×10^6 molecules of complementary ssDNA in a liquid volume of 200 μL (2×10^{-14} M), which was a 7 order of magnitude improvement over using the colorimetric change as a sensing signal.

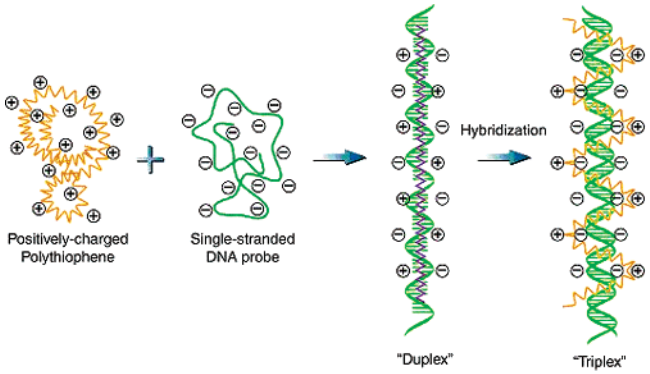

Figure 35. Schematic illustration of the formation of a planar **12**−ssDNA duplex and a helical **12**−dsDNA triplex. (Reprinted with permission from ref 171. Copyright 2005 Wiley-VCH publishers.)

In addition to the high sensitivity, the authors also observed high selectivity. It was possible to distinguish the true complementary ssDNA from strands that contained two or even one mismatch by stopping the hybridization reaction (by cooling from 55 °C to room temperature) after 5 min, because the rate of complexation for the mismatched sequences was significantly slower.

On the basis of previous work related to color changes of regioregular poly(3-alkoxy-4-methylthiophene)s,[174] the original hypothesis the authors adopted to explain the color changes observed upon duplex and triplex formation was that the red color (duplex) was due to a highly conjugated and planar conformation of the polymer, whereas the yellow color (triplex) represented a less conjugated, nonplanar, and helical conformation. This process is schematically illustrated in Figure 35. Color changes were also observed in solvatochromism, affinitychromism, and thermochromism experiments. Leclerc, Louarn, and co-workers also carried out detailed spectroscopic studies of the initial yellow (random-coil) and red forms, changes between which were induced thermally, of a structurally related, nonionic poly(3-alkoxy-4-methylthiophene).[175] The combination of evidence from absorbance, infrared, and Raman spectroscopies confirmed that the observed color changes were due, at least in part, to main-chain twisting transitions. The authors hypothesized that interchain interactions could also contribute to the observed optical changes.

In 2003, Nilsson and Inganäs reported a zwitterionic poly(3-alkylthiophene) (**81**) that showed qualitatively similar optical transitions, in comparison to Leclerc's work with **12**, upon the addition of oligonucleotides.[176] However, the authors successfully performed this procedure at room temperature using **81**. Upon addition of 1.0 equiv of a 20-base segment of ssDNA, the absorbance of the solution red-shifted and the fluorescence decreased. The authors attributed these changes to interchain interactions caused by aggregation induced by electrostatic and hydrogen-bonding interactions between **81** and the oligonucleotide, as well as to polymer backbone planarization caused by disruptions of internal interactions between the amino and carboxyl groups on the polymer side chain. Addition of the complementary ssDNA strand gave a blue shift of absorbance and an increase in emission intensity, attributed to polymer chains interacting with dsDNA, which resulted in a less elongated conformation. The authors used ratiometric sensing (540/670 nm) to successfully detect 10^{-11} mol of DNA in a 1.5 mL liquid volume as well as to discriminate single-base mismatches within 5 min. Further studies on this system subsequently

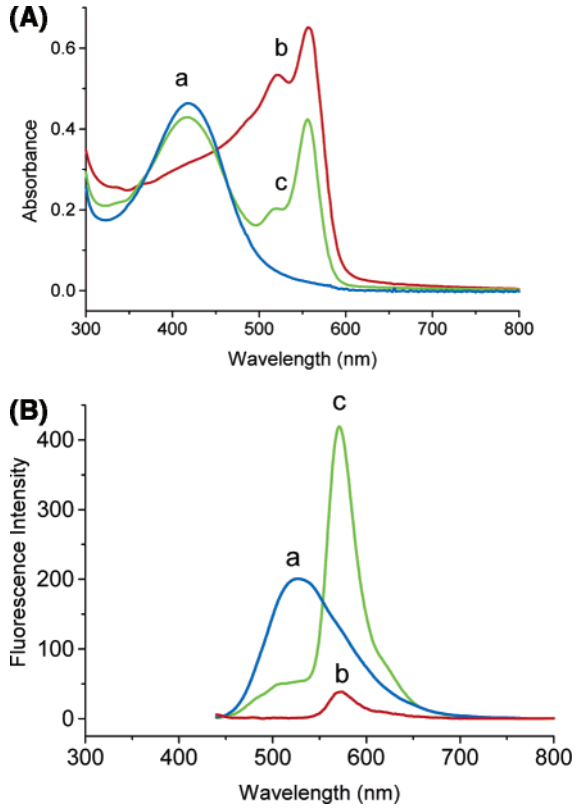

Figure 36. UV/vis (A) and emission (B) spectra of (a) a **12**−unlabeled dsDNA triplex, (b) a **12**−labeled ssDNA duplex, and (c) a **12**−labeled dsDNA triplex in water at 55 °C. (Reprinted with permission from ref 181. Copyright 2005 American Chemical Society.)

revealed that substitution of the ssDNA "probe" strand can occur in the presence of other DNA strands in solution, potentially limiting sensitivity and selectivity.[177]

More recently, Leclerc and co-workers have published papers concerning various improvements they have made to their homogeneous DNA-sensing assay based on **12**. In 2004, they reported that the addition of 20% formamide as a denaturant precluded the need for elevated temperatures and allowed for DNA detection at ambient temperature. This advance may allow Leclerc's sensing methodology to be incorporated into microfluidic systems, a potentially important development in terms of practical utility.[178] Leclerc and co-workers also reported the development of a PNA microarray-based DNA sensor on a solid support.[179]

In 2004, Leclerc and co-workers reported a substantial improvement in the sensitivity of their DNA assay.[180] The primary manner by which they accomplished this improvement was the development of a tailored detection platform specifically designed for this application. The platform they reported combined a powerful and stable blue LED source with a narrow (16 nm) bandwidth for polymer excitation, a nondispersive optical design using interference filters, and a photomultiplier tube detector. The authors reported that this improved design gave detection limits that were about 2 orders of magnitude better than those with a conventional spectrofluorometer. In addition, the use of 0.3 mM of a nonionic surfactant (Triton X-100) improved the detection limit by another order of magnitude, which the authors attributed to an increase in polymer extinction coefficient and fluorescence quantum yield because of the release of interfacial water molecules. With these combined improvements to the assay and the detection hardware, a lower detection limit of 220 50-base ssDNA molecules in 150 μL (2.4×10^{-18} M) was achieved. Selectivity over single-base mismatches was retained. To further illustrate the applicability of this method, the authors reported the detection of 750 genome copies of a 1028-nucleoside single-stranded RNA segment generated by the Influenza virus, all without tagging any of the oligonucleotide strands.

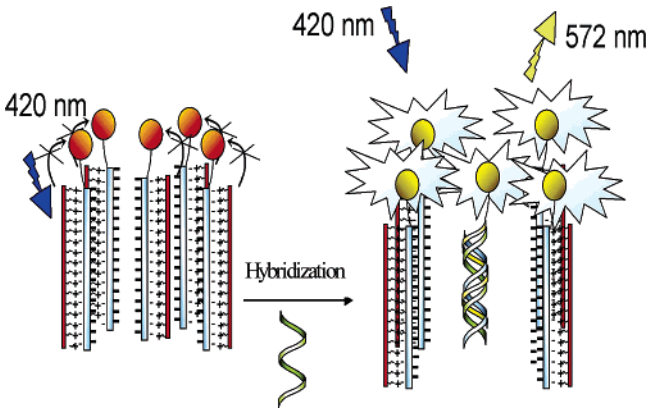

Figure 37. Schematic illustration of the proposed signal amplification mechanism based on conformational change of **12** upon dsDNA formation within an aggregate and the "superlighting" resulting from energy transfer from one emissive "triplex" to multiple nearby acceptors. (Reprinted with permission from ref 181. Copyright 2005 American Chemical Society.)

In 2005, the Leclerc group reported that, by tagging their capture ssDNA strand with a fluorophore (Alexa Fluor 546), they achieved even more sensitive DNA detection while still retaining specificity.[181] Similar to previous reports, the addition of the labeled ssDNA capture strand (20-mer) gave a very weakly emissive, red-colored duplex. When the duplex hybridized with the complementary ssDNA, however, very efficient FRET from the emissive helical **12** to the acceptor dye gave strong emission at 572 nm (Figure 36). This system demonstrated outstanding sensitivity; the authors reported that five copies of target DNA in a 3 mL volume (3 zM) could be detected by this method. In addition, by conducting the experiment at 65 °C in pure water, the authors were able to selectively enhance the recognition reaction between the polymer-bound capture probe and the target. This enhancement was presumably because under these conditions the cationic polymer promoted the reaction, possibly by reducing electrostatic repulsion between DNA chains.

A more detailed investigation of this "turn-on" detection scheme, published in 2006, showed that the sensitivity was 4000 times greater when the acceptor chromophore tag was included.[182] The authors have attributed this extraordinary sensitivity in part to aggregate formation, which reduced quenching of the fluorophores by insulating them from quenchers, provided orientation for the polymers, and improved photostability. Light-scattering measurements demonstrated the presence of duplex aggregates of ~80 nm in diameter that were retained upon DNA hybridization. In addition, the authors also found it likely that the very fast rate of energy transfer from the helical polymer to the acceptor dye within these aggregates allowed for the excitation of a large number of acceptor dyes from only one triplex donor within an aggregate. This is schematically illustrated in Figure 37. The authors demonstrated the utility of this detection system by successfully distinguishing a SNP associated with hereditary tyrosinemia type I from non-

amplified clinical samples within 5 min and with no attenuation of sensitivity.

5.2. DNA Detection Based on Fluorescence Resonance Energy Transfer from Cationic Poly(fluorene-*co*-phenylene)s

Fluorescence resonance energy transfer (FRET, also known as Förster energy transfer) is a commonly used signal transduction pathway in biochemical research. This long-range, dipole−dipole interaction allows the excitation of a donor chromophore to result in emission from the lower energy excited state of another chromophore. FRET has often been used as a "molecular yardstick" in the study of protein conformations.

The strong distance dependence makes FRET useful for sensing and other applications because events that affect changes in the distance between chromophores can be monitored by acceptor emission intensity. Sensing schemes based on FRET could rely on either the enhancement or the diminution of acceptor fluorescence. Stem−loop DNA structures labeled at their termini with donor and acceptor chromophores (Molecular Beacons) are examples of a robust DNA detection technology that relies on FRET.

Conjugated polymers have the potential to be excellent energy donors in FRET-based sensing schemes. They have high extinction coefficients stemming from their delocalized backbone, and many emit light efficiently. In addition, excitons generated by photoexcitation throughout the entire polymer can migrate to a position on the chain from which FRET is efficient, allowing for amplified fluorescence from the energy acceptor and increased sensitivity due to the resultant enhancement in signal-to-noise. The groups of Bazan and Heeger at UC Santa Barbara have used water-soluble cationic conjugated polymers to detect specific DNA sequences via FRET to dye-labeled probe molecules.[183] In their systems, electrostatic attraction between the positively charged conjugated polymer and the polyanionic DNA results in short distances between the conjugated polymer donor and the acceptor-labeled probe strand.[184]

Gaylord, Bazan, and Heeger reported an example of this technology in 2002.[185] Figure 38 is a schematic representation of how the system works. This sensing system consists of three parts: the cationic conjugated poly(fluorene-*co*-phenylene) **13**, a probe peptide nucleic acid (PNA) strand labeled at the 5′ end with an appropriate energy-accepting chromophore (fluorescein) having strong spectral overlap with **13**, and the target DNA strand. PNA forms stable Watson−Crick base pairs with single-stranded DNA (ssDNA) but is neutral because the phosphate linkages have been replaced with neutral amide linkages.[186] Therefore, there could be no electrostatic interaction between PNA and the conjugated polymer, and the average distance between chromophores was too great for efficient FRET. When ssDNA that had a complementary sequence to the PNA was included, however, the resulting DNA−PNA complex had a strong net negative charge, binding it electrostatically to the conjugated polymer. The greatly reduced average distance between chromophores allowed for efficient FRET to take place, signaling the presence of the target ssDNA strand with a "turn-on" fluorescence signal at lower energy. Noncomplementary ssDNA gave little observable FRET.

At optimized concentrations (1:1 polymer chain to DNA ratio at 2.5×10^{-8} M), the authors observed greater than

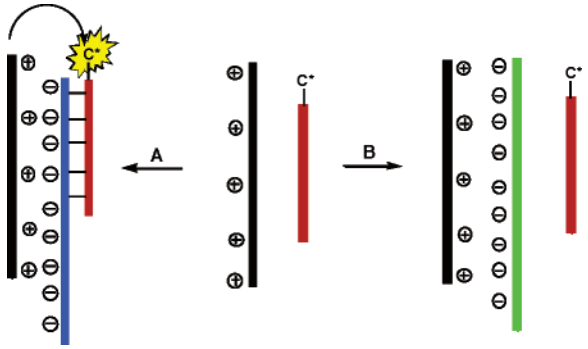

Figure 38. Schematic representation of the PNA−ssDNA assay using a water-soluble CP with a specific labeled PNA probe strand. Electrostatic attraction between the complementary PNA−ssDNA complex brings the energy donor (polymer) and acceptor (dye) close enough for efficient FRET (A). Noncomplementary ssDNA results in no attraction between donor and acceptor and no energy transfer (B). (Reprinted with permission from ref 184. Copyright 2004 American Chemical Society.)

25-times amplification of fluorescein emission upon polymer excitation versus direct dye excitation at 480 nm. A structurally similar *p*-difluorenylbenzene model compound gave significantly lower amplification. The detection limit in this study was 10 pM. The authors also determined that hydrophobic interactions were important in the binding of the probe strand to the conjugated polymer; they observed a small amount of FRET to the PNA-bound acceptor even without any ssDNA present. Detrimental background FRET was nearly eliminated by using a 10% ethanol solution, which decreased the effects of nonspecific hydrophobic interactions.

Heeger, Bazan, and co-workers used time-resolved fluorescence techniques to perform a more detailed investigation of the hydrophobic and electrostatic interactions in this system.[187] They took advantage of pump−dump emission spectroscopy (PDES), a technique useful for enhancing the signal-to-noise for dilute solutions relative to pump−probe experiments. The authors found that in moderately concentrated aqueous solutions the energy-transfer dynamics between the conjugated polymer and PNA-tagged fluorescein were biexponential, with time constants of 11.5 and 85 ps. Under these conditions, noncomplementary DNA also showed FRET, highlighting the importance of hydrophobic interactions. Using 10% *N*-methylpyrrolidone (NMP) in the aqueous solution reduced this nonspecific FRET, and the FRET observed using complementary DNA became monoexponential with an 88 ps time constant. On the basis of this data, the authors proposed an equilibrating two-conformation binding model. In water, the complex was bound by both conformations [controlled by hydrophobic interactions (τ = 11.5 ps) and electrostatics (τ = 85 ps)], whereas in the water/organic solvent mixture only electrostatic attraction (τ = 88 ps) played a role.

Bazan and co-workers also developed a complementary method that relied upon more traditional double-stranded DNA (dsDNA) helix formation for the sensing recognition chemistry (Figure 39), instead of using the more expensive PNA.[188] In this case, however, the tagged probe ssDNA strand does have some electrostatic attraction to **13**. Nevertheless, when a target 20-base ssDNA strand complementary to the 20-base-tagged probe was included in the solution, the authors observed a 3-fold increase in fluorescence intensity from fluorescein relative to when a noncomple-

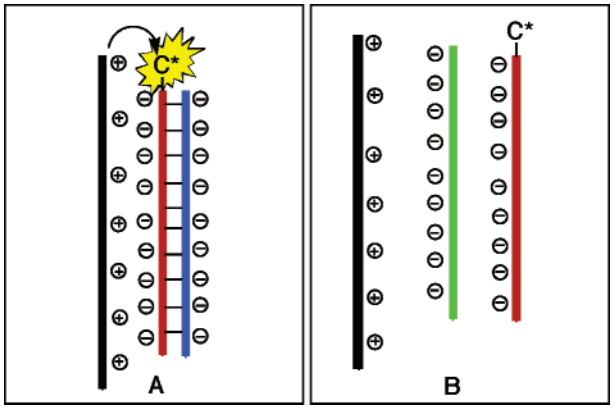

Figure 39. Schematic illustration of a dsDNA assay using **13** and a dye-labeled ssDNA probe strand. Noncomplementary ssDNA partially screens the energy acceptor from **13**, reducing FRET (B). This screening is removed when complementary ssDNA is used, enhancing FRET efficiency (A). (Reprinted with permission from ref 188. Copyright 2003 American Chemical Society.)

mentary strand was added. In addition, a 4-fold amplification of intensity upon polymer irradiation versus direct excitation of the dye demonstrated amplification in this sensing scheme. The authors also demonstrated the 20-base probe strand could also selectively lead to the detection of an appropriate 40-base target. A decrease in FRET efficiency as a function of NaCl concentration, according to Debye−Hückel theory, demonstrated the importance of electrostatic interactions. Solvent-dependence studies revealed that solvent mixtures of THF and water of intermediate polarity allowed for the highest FRET efficiency from **13** to dye-labeled ssDNA because the amphiphilic nature of the polymer led to the formation of distinct aggregates that adversely affected sensitivity in low-polarity and high-polarity solvents.[189]

A more detailed investigation highlighted the important interplay between hydrophobic interactions and electrostatics.[190] The authors studied the FRET characteristics of oligomers (**109a**−**d**) with different alkyl chain lengths

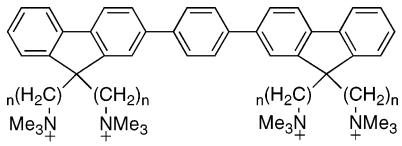

109a: n = 3
109b: n = 4
109c: n = 6
109d: n = 8

between the conjugated framework and the charged tetraalkylammonium bromide groups. In aqueous solutions with an artificial conjugated anion, ssDNA, or dsDNA, **109d** always gave the highest FRET efficiency, followed by **109c**. Compounds **109a** and **109b** were the least efficient, showing no observable FRET with DNA in water. The trend of chain-length-dependent FRET efficiency to the artificial conjugated anion, however, was reversed in methanol, in which the donors with the shortest tether gave the most efficient energy transfer. The authors attributed this phenomenon to a decreased importance of hydrophobic interactions between the longer tethers and the target strands in methanol. Another important conclusion of this work was that the reason for the observed selectivity for energy transfer to dsDNA over ssDNA in this sensing scheme was not stronger dsDNA−conjugated polymer interactions. Rather, unlabeled, non-complementary ssDNA screened the electrostatic interactions between the probe strand and the conjugated polymer.

Further oligomer studies revealed some size specificity, in that longer oligomers (6 fluorene units) showed more fluorescence quenching and FRET with dsDNA, while shorter oligomers (2 or 4 fluorene units) were more sensitive to ssDNA.[191] These experiments emphasized that a typical polydisperse sample of conjugated polymer can show a distribution of selectivities, only the average of which is observable.

Nonspecific electrostatic interactions between the dye-labeled ssDNA probe strand and the conjugated polymer limit the specificity and sensitivity of the scheme depicted in Figure 39. Therefore, Bazan and co-workers sought to use a

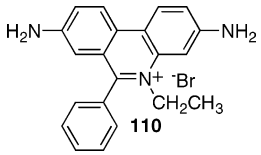

110

well-known DNA intercalating dye, ethidium bromide (EB, **110**), as an energy acceptor to improve the performance of this ssDNA-based assay.[192] EB is known to have an increased fluorescence quantum yield upon intercalating between the stacked bases of dsDNA. Theoretically, energy transfer from the conjugated polymer to EB, as illustrated in Figure 40, would only take place if complementary ssDNA strands (target and probe) were present, since the electrostatic attraction between the resulting dsDNA, with EB intercalated, would bring **13** and EB into close contact. If only non-complementary strands were present, EB would not associate with the anionic DNA and no FRET could occur. The authors found, however, that efficient FRET to EB did not occur when they carried out this experiment, even though the distance between the chromophores (r) and spectral overlap (J) were appropriate for a high rate of FRET. Suspecting that inefficient energy transfer was due to a nearly orthogonal arrangement of donor and acceptor transition dipole moments, the authors instead employed a two-step FRET scheme with a ssDNA probe bearing a fluorescein molecule at the 5′ terminus, as illustrated in Figure 41.

Including fluorescein as an intermediate "FRET gate" provided much more efficient energy transfer to EB, with an 8-fold amplification relative to direct excitation of the intercalator. Furthermore, the selectivity was greatly improved, in that only the use of ssDNA complementary to

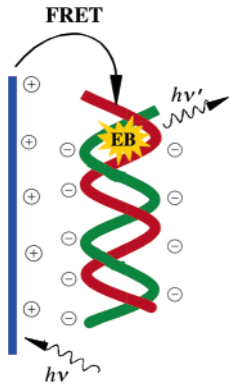

Figure 40. Inefficient one-step energy transfer from a cationic conjugated polymer to intercalated ethidium bromide. (Reprinted with permission from ref 192. Copyright 2004 American Chemical Society.)

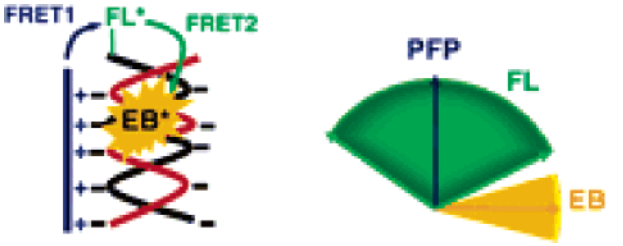

Figure 41. Left: Two-step energy transfer with fluorescein acting as a "gate" between the conjugated polymer donor and the EB receptor. Right: Relative orientations of the three optical components. (Reprinted with permission from ref 193. Copyright 2005 National Academy of Sciences, U.S.A.)

the probe strand resulted in observable EB emission. Time-resolved fluorescence that was monitored upon excitation of **13** confirmed the two-step nature of energy transfer; the fluorescein lifetime decreased from 0.93 to 0.32 ns upon inclusion of EB in the assay. A more detailed investigation of this system using time-dependent anisotropy measurements confirmed that the inefficient one-step FRET from **13** to intercalated EB was indeed due to a nearly orthogonal orientation of their transition dipole moments.[193] This study also revealed that the transition dipole moment of the ssDNA-bound fluorescein was distributed over a wide range of angles (Figure 41), allowing it to act as the intermediary in the two-step FRET. Recently, this DNA intercalator-based two-step FRET sensing scheme has been applied to the direct observation of the G-quadruplex-to-duplex transition in guanine-rich DNA strands.[194] The assay, which employed **13** as the cationic conjugated polymer, functioned because EB only intercalated into the duplex and not into the ssDNA quadruplex. The authors demonstrated good selectivity over even single-base mismatches, which inhibit the G-quadruplex-to-duplex transition.

In addition to modifications to how the assay is executed, Bazan and co-workers have also explored ways by which rational design of the conjugated polymer itself can improve the sensitivity and selectivity of the DNA assay. In 2004, they reported a three-color DNA-sensing assay that employed the random copolymer **111**, which was synthesized by a

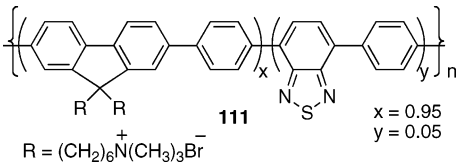

Suzuki cross-coupling polymerization with a number-average molecular weight of 11 kDa and included, on average, one 2,1,3-benzothiadizole (BT) unit per polymer chain.[195] In deionized water, **111** showed photophysical properties characteristic of **13** (blue emission and a fluorescence quantum yield of 22%). Upon increasing the concentration of **111** above 1×10^{-6} M, however, the green emission characteristic of BT sites emerged and increased at the expense of the blue emission. The authors attributed this phenomenon to aggregate formation and efficient interchain energy transfer to the lower energy BT sites. Upon addition of ssDNA to dilute **111**, a similar growing in of green emission was observed as a function of DNA concentration with a well-anchored isosbestic point, attributed to DNA-induced contraction and aggregation of the polymer chains allowing for more efficient energy transfer to BT.

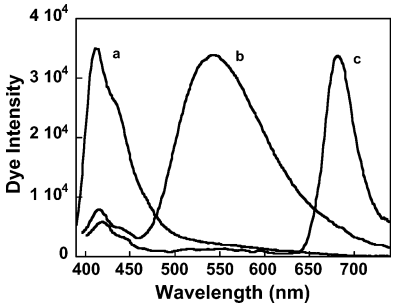

Figure 42. Normalized fluorescence in water of (a) **111** and Cy5-labeled PNA, (b) **111**, Cy5-labeled PNA, and noncomplementary ssDNA, and (c) **111**, Cy5-labeled PNA, and complementary ssDNA. (Reprinted with permission from ref 195. Copyright 2004 American Chemical Society.)

As illustrated in Figure 42, this effect was used in a multicolor DNA-sensing assay. The probe strand was Cy5-tagged PNA, which had no electrostatic attraction to the cationic conjugated polymer, resulting in blue emission from **111**. Addition of noncomplementary ssDNA/Cy5-PNA resulted in no hybridization, and the nonspecific electrostatic attraction of the ssDNA to **111** resulted in green BT-based emission. Under similar conditions, addition of complementary ssDNA/Cy5-PNA resulted in electrostatic attraction of the PNA/DNA complex to **111** and efficient FRET to the red-emitting Cy5.

In addition to this RGB DNA hybridization assay, polymers analogous to **111** (only containing different percentages of BT groups) have been reported in an assay for the quantitative determination of total DNA concentration in aqueous solution by monitoring the relative intensities of blue and green emission from the polymer.[196] The reported sensitivity of this assay (6×10^{-10} M bp of dsDNA), however, was lower than those of the commercially available PicoGreen or OliGreen probes. Moreover, the purely electrostatic nature of the assay limits its versatility because of charge screening and preaggregation in solutions with high salt concentrations.

Bazan's group has explored other improvements to the structure of their cationic conjugated polymers. In 2003 they reported the use of *meta*-conjugation (**112**) to increase conformational freedom for tighter binding to the secondary structure of dsDNA.[197] They observed that increasing *meta* content along the polymer backbone gave improved FRET efficiency. They also published studies of poly(fluorene-*co*-

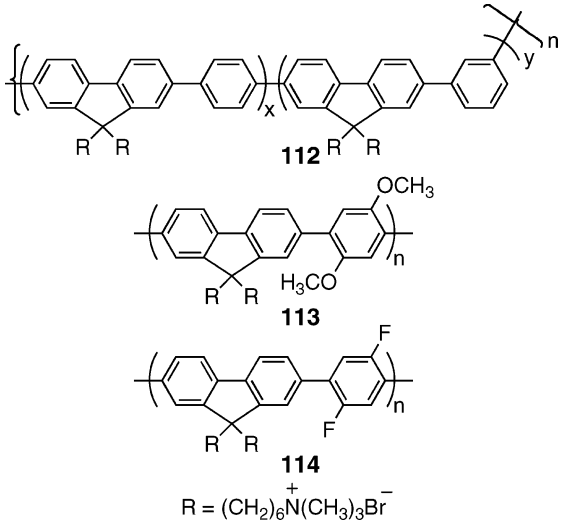

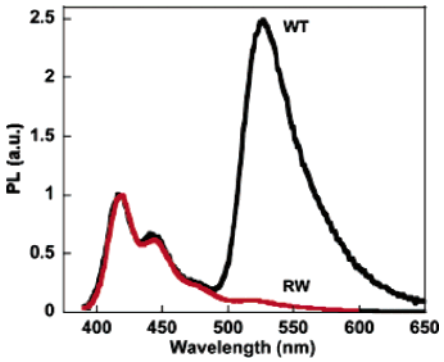

Figure 43. Normalized fluorescence of S1-treated hybridization products with 249-base ssDNA after addition of **13** in 30 mM potassium phosphate buffer. WT = wild-type ssDNA + dye-labeled PNA. RW = SNP ssDNA + dye-labeled PNA. (Reprinted with permission from ref 200. Copyright 2005 National Academy of Sciences, U.S.A.)

phenylene)s containing substituents designed to perturb the electronics of the polymer backbone (**113** and **114**).[198] By doing so, they found that the relative efficiencies of FRET and photoinduced electron-transfer quenching could be improved by optimizing the frontier molecular orbital energies of both the conjugated polymer donor and the energy-accepting dye.

The aforementioned studies using FRET from a cationic conjugated polymer as a detection signal for DNA sensing have all sensed short strands of oligonucleotides in pure aqueous or buffered solutions. New ways to carry out these amplified fluorescence assays, however, must be developed in order to make this technology practically useful and commercially viable.[199] Several groups have demonstrated the specific and sensitive detection of DNA under more realistic conditions. For example, Bazan and co-workers have used their PNA/ssDNA assay in conjunction with S1 nuclease enzyme in order to reliably detect single nucleotide polymorphisms (SNPs), the most common form of sequence variation in human DNA.[200] The SNP they targeted is responsible for an arginine to tryptophan substitution at amino acid position 406 in the microtubule-associated protein tau. The mutant has been linked to frontotemporal dementia. The probe strand was a 14-base, fluorescein-labeled PNA probe that targeted the R406W mutation.

Using this scheme, complementary (wild-type) ssDNA (249 bp) was successfully detected over the SNP, with an emission intensity amplification of 1 order of magnitude over direct acceptor excitation. Shorter 28-base-pair target ssDNA, however, showed much better selectivity as opposed to the more realistic 249-bp target. The reason for this was that the conjugated polymer could electrostatically bind anywhere on the long DNA chain, not just near where the tagged PNA was bound to the 14-base target sequence. This resulted in a random distribution of polymer along the longer DNA target, a mixture of different donor−acceptor distances, and an overall diminution of signal-to-noise. In order to increase the observed selectivity, the authors introduced an S1 nuclease digestion step after PNA/ssDNA annealing. PNA molecules and complexes with ssDNA were stable to the nuclease, while S1 (as confirmed by gel analysis) digested all nonannealed ssDNA, segments of ssDNA not complexed, and unbound mismatches. As illustrated in Figure 43, this resulted in strong selectivity for the targeted wild-type 249-base DNA target while using the same 14-base PNA probe.

In another step toward commercial viability, Fan and co-workers used magnetic force to assist in selectivity enhancement of an assay using a cationic poly(fluorene-*co*-phenylene) similar to **13**.[201] Their assay, schematically

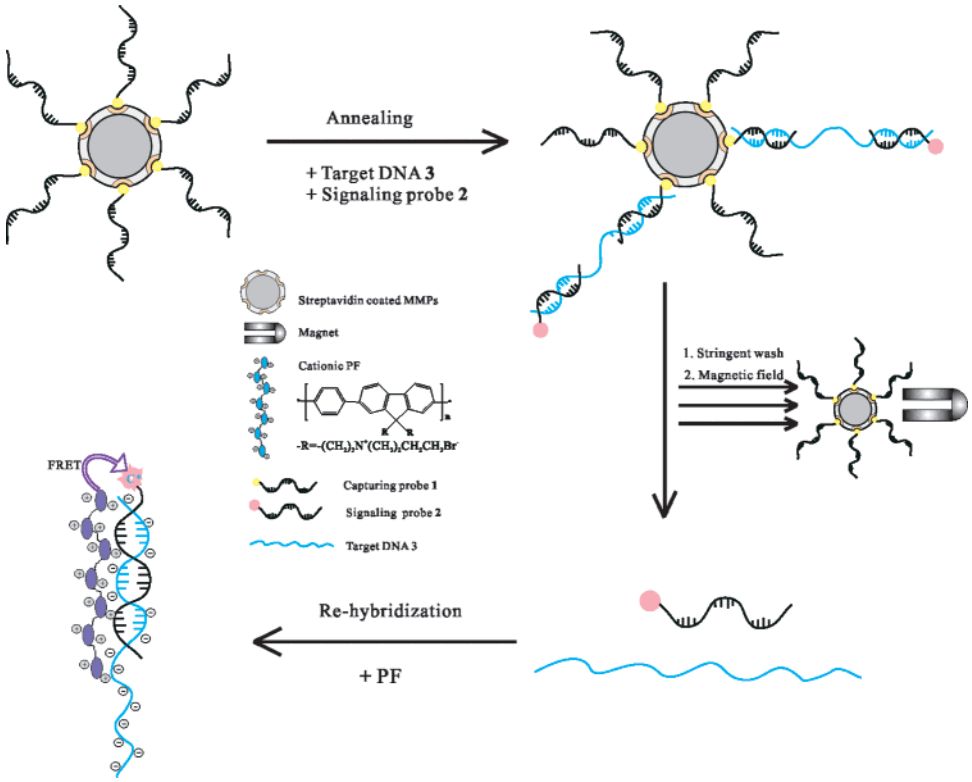

Figure 44. In the presence of the target DNA, an MMP-anchored sandwich complex between the target, the MMP-bound capture probe, and the dye-labeled signal probe was formed. Addition of the conjugated polymer to the washed and magnetically purified sample gave amplified emission from fluorescein. (Reprinted with permission from reference 201. Copyright 2005 Oxford Publishing.)

illustrated in Figure 44, used streptavidin-coated magnetic microparticles (MMPs) that were appended with biotin-terminated capture DNA strands (15-base sequence). Annealing with target ssDNA (40 bases) and a fluorescein-substituted signaling probe that was complementary to another section of the target formed sandwich complexes on the MMPs. These MMPs were selectively collected with magnetic force and washed with buffer of low ionic strength to remove single-nucleotide mismatches. The target and signaling DNA was then removed from the MMP with sodium hydroxide. Addition of conjugated polymer to rehybridized DNA gave observable amplified fluorescence down to 100 pM of the target. Moreover, the observed fluorescence intensity was a linear function of target DNA concentration up to 10 nM, allowing for quantification in this range. Even more importantly, the authors observed the same sensitivity and selectivity whether the target ssDNA was in pure buffer, an artificial matrix of random DNA sequences and proteins at high concentrations, or diluted human serum. Therefore, this magnetically assisted assay was less sensitive to nonspecific interactions.

6. Concluding Remarks

In writing this review, we have endeavored to be most comprehensive for literature published before June 2006 and not included in a previous *Chemical Reviews* paper published by this group.[1] It was our intention to not simply give a cataloging of results, but also to guide new researchers in the field. In any new emerging area there will be an evolution of critical thinking and the underlying mechanisms. As a result, some of the interpretations published earlier need to be reconsidered in light of recent results, and we have pointed out these issues where necessary. Clearly, the field of amplifying fluorescent polymers is far from mature, and the future promises exciting new discoveries and commercial technologies that impact national security, environmental sensing, and healthcare.

The amplification displayed by these materials is the result of exciton transport. Conjugated polymers can also transport charge when oxidized or reduced. This feature can similarly provide signal gain in the form of resistivity changes, and there continue to be advances in chemoresisitive conjugated polymers. A persistent issue in chemoresistive materials is the fact that the carriers have charge (generally positive) and are subject to interferences from ions and other polar molecules. In contrast, the excitions in most amplifying fluorescent polymers are relatively immune to electrostatic and dielectric variations. There are also many well-established sensory methods including those that make use of PCR amplification and catalysis by enzymes. It is important to note that these methods can be used in conjunction with signal transduction by amplifying fluorescent polymers to give superior performance. There is also great interest in new chemical sensing methods based on nanoparticles; the best-known examples are based upon gold nanoparticles.[202] It is often the case in sensory systems that different applications are best served by different methods, and given the ever expanding role of chemical sensors in science, healthcare, consumer products, and environmental monitoring, opportunities for a diversity of sensory systems will continue to grow. It is our hope that the readers find our perspective useful in guiding their own research, and we hope that this review assists new researchers to help to further advance the applications and science of amplifying fluorescent polymers, in particular, and the field of chemical sensors, in general.

7. Note Added after ASAP Publication

This paper was published ASAP on March 27, 2007, with an error in eq 2. The corrected paper was posted on April 5, 2007.

8. References

(1) McQuade, D. T.; Pullen, A. E.; Swager, T. M. *Chem. Rev.* **2000**, *100*, 2537.
(2) Zhou, Q.; Swager, T. M. *J. Am. Chem. Soc.* **1995**, *117*, 7017.
(3) Chen, L.; McBranch, D. W.; Wang, H.-L.; Helgeson, R.; Wudl, F.; Whitten, D. G. *Proc. Natl. Acad. Sci. U.S.A.* **1999**, *96*, 12287.
(4) Heeger, P. S.; Heeger, A. J. *Proc. Natl. Acad. Sci. U.S.A.* **1999**, *96*, 12219.
(5) Cotts, P. M.; Swager, T. M.; Zhou, Q. *Macromolecules* **1996**, *29*, 7323.
(6) Yang, J.-S.; Swager, T. M. *J. Am. Chem. Soc.* **1998**, *120*, 11864.
(7) Nesterov, E. E.; Zhu, Z.; Swager, T. M. *J. Am. Chem. Soc.* **2005**, *127*, 10083.
(8) McQuade, D. T.; Kim, J.; Swager, T. M. *J. Am. Chem. Soc.* **2000**, *122*, 5885.
(9) Yang, J.-S.; Swager, T. M. *J. Am. Chem. Soc.* **1998**, *120*, 5321.
(10) Kim, J.; McQuade, D. T.; McHugh, S. K.; Swager, T. M. *Angew. Chem., Int. Ed.* **2000**, *39*, 3868.
(11) Béra-Abérem, M.; Ho, H.-A.; Leclerc, M. *Tetrahedron* **2004**, *60*, 11169.
(12) Liu, H.; Wang, S.; Luo, Y.; Tang, W.; Yu, G.; Li, L.; Chen, C.; Liu, Y.; Xi, F. *J. Mater. Chem.* **2001**, *11*, 3063.
(13) Chen, Z.; Xue, C.; Shi, W.; Luo, F.-T.; Green, S.; Chen, J.; Liu, H. *Anal. Chem.* **2004**, *76*, 6513.
(14) Ramachandran, G.; Simon, G.; Cheng, Y.; Smith, T. A.; Dai, L. *J. Fluoresc.* **2003**, *13*, 427.
(15) Baskar, C.; Lai, Y.-H.; Valiyaveettil, S. *Macromolecules* **2001**, *34*, 6255.
(16) Tang, Y.; He, F.; Yu, M.; Feng, F.; An, L.; Sun, H.; Wang, S.; Li, Y.; Zhu, D. *Macromol. Rapid Commun.* **2006**, *27*, 389.
(17) Kim, I.-B.; Erdogan, B.; Wilson, J. N.; Bunz, U. H. F. *Chem.—Eur. J.* **2004**, *10*, 6247.
(18) Kim, I.-B.; Dunkhorst, A.; Gilbert, J.; Bunz, U. H. F. *Macromolecules* **2005**, *38*, 4560.
(19) Kim, I.-B.; Bunz, U. H. F. *J. Am. Chem. Soc.* **2006**, *128*, 2818.
(20) Ho, H.-A.; Leclerc, M. *J. Am. Chem. Soc.* **2004**, *126*, 1384.
(21) For a review of conjugated polyelectrolytes, see: Pinto, M. R.; Schanze, K. S. *Synthesis* **2002**, 1293.
(22) He, F.; Tang, Y.; Wang, S.; Li, Y.; Zhu, D. *J. Am. Chem. Soc.* **2005**, *127*, 12343.
(23) Kwan, P. H.; MacLachlan, M. J.; Swager, T. M. *J. Am. Chem. Soc.* **2004**, *126*, 8638.
(24) Balanda, P. B.; Ramey, M. B.; Reynolds, J. R. *Macromolecules* **1999**, *32*, 3970.
(25) Harrison, B. S.; Ramey, M. B.; Reynolds, J. R.; Schanze, K. S. *J. Am. Chem. Soc.* **2000**, *122*, 8561.
(26) Ramey, M. B.; Hiller, J. A.; Rubner, M. F.; Tan, C.; Schanze, K. S.; Reynolds, J. R. *Macromolecules* **2005**, *38*, 234.
(27) Fan, Q.-L.; Zhou, Y.; Lu, X.-M.; Hou, X.-Y.; Huang, W. *Macromolecules* **2005**, *38*, 2927.
(28) For a discussion of sphere-of-action quenching, see: Lakowicz, J. R. *Principles of Fluorescence Spectroscopy*; Plenum Press: New York, 1986; p 244.
(29) For an early discussion related to the use of the sphere-of-action concept to explain the "superlinear" or "superquenching" response of conjugated polyelectrolytes, see (a) ref 95. For the use of the term "superquenching" to describe the fluorescence quenching behavior of conjugated polyelectrolytes, see (b) ref 93. The use of conjugated polyelectrolytes as sensors for cationic viologens and as biosensors will be covered in greater detail in section 4.
(30) Fan, Q.-L.; Zhang, G.-W.; Lu, X.-M.; Chen, Y.; Huang, Y.-Q.; Zhou, Y.; Chan, H. S. O.; Lai, Y.-H.; Xu, G.-Q.; Huang, W. *Polymer* **2005**, *46*, 11165.
(31) Ramachandran, G.; Smith, T. A.; Gómez, D.; Ghiggino, K. P. *Synth. Met.* **2005**, *152*, 17.
(32) Tan, C.; Pinto, M. R.; Kose, M. E.; Ghiviriga, I.; Schanze, K. S. *Adv. Mater.* **2004**, *16*, 1208.
(33) For a review on the topic of luminescent sensors for transition metal ions, see: Prodi, L.; Bolletta, F.; Montalti, M.; Zaccheroni, N. *Coord. Chem. Rev.* **2000**, *205*, 59.
(34) Wang, B.; Wasielewski, M. R. *J. Am. Chem. Soc.* **1997**, *119*, 12.

(35) Liu, B.; Yu, W.-L.; Pei, J.; Liu, S.-Y.; Lai, Y.-H.; Huang, W. *Macromolecules* **2001**, *34*, 7932.
(36) Ding, A.-L.; Pei, J.; Yu, W.-L.; Lai, Y.-H.; Huang, W. *Thin Solid Films* **2002**, *417*, 198.
(37) Pei, J.; Ding, A.-L.; Yu, W.-L.; Lai, Y.-H. *Macromol. Rapid Commun.* **2002**, *23*, 21.
(38) Zhang, M.; Lu, P.; Ma, Y.; Shen, J. *J. Phys. Chem. B* **2003**, *107*, 6535.
(39) Yasuda, T.; Yamamoto, T. *Macromolecules* **2003**, *36*, 7513.
(40) Wang, W.-L.; Xu, J.-W.; Lai, Y.-H. *J. Polym. Sci., Part A: Polym. Chem.* **2006**, *44*, 4154.
(41) Na, J.; Kim, Y.-S.; Park, W. H.; Lee, T. S. *J. Polym. Sci., Part A: Polym. Chem.* **2004**, *42*, 2444.
(42) Na, J.; Park, W. H.; Lee, T. S. *React. Funct. Polym.* **2004**, *59*, 225.
(43) Vetrichelvan, M.; Valiyaveettil, S. *Chem.—Eur. J.* **2005**, *11*, 5889.
(44) Huang, H.; Wang, K.; Tan, W.; An, D.; Yang, X.; Huang, S.; Zhai, Q.; Zhou, L.; Jin, Y. *Angew. Chem., Int. Ed.* **2004**, *43*, 5635.
(45) Tong, H.; Wang, L.; Jing, X.; Wang, F. *Macromolecules* **2002**, *35*, 7169.
(46) Tong, H.; Wang, L.; Jing, X.; Wang, F. *Macromol. Rapid Commun.* **2002**, *23*, 877.
(47) Bangcuyo, C. G.; Rampey-Vaughn, M. E.; Quan, L. T.; Angel, S. M.; Smith, M. D.; Bunz, U. H. F. *Macromolecules* **2002**, *35*, 1563.
(48) Bangcuyo, C. G.; Ellsworth, J. M.; Evans, U.; Myrick, M. L.; Bunz, U. H. F. *Macromolecules* **2003**, *36*, 546.
(49) Wu, T.-Y.; Chen, Y. *J. Polym. Sci., Part A: Polym. Chem.* **2004**, *42*, 1272.
(50) Lee, J. K.; Lee, T. S. *J. Polym. Sci., Part A: Polym. Chem.* **2005**, *43*, 1397.
(51) (a) Yang, N. C.; Jeong, J. K.; Suh, D. H. *Chem. Lett.* **2003**, *32*, 40. (b) Mikroyannidis, J. A.; Spiliopoulos, I. K.; Kasimis, T. S.; Kulkarni, A. P.; Jenekhe, S. A. *J. Polym. Sci., Part A: Polym. Chem.* **2004**, *42*, 2112. (c) Wu, T.-Y.; Sheu, R. B.; Chen, Y. *Macromolecules* **2004**, *37*, 725. (d) Yang, N. C.; Chang, S.; Suh, D. H. *Polymer* **2003**, *44*, 2143.
(52) Zhang, Y.; Murphy, C. B.; Jones, W. E., Jr. *Macromolecules* **2002**, *35*, 630.
(53) Murphy, C. B.; Zhang, Y.; Troxler, T.; Ferry, V.; Martin, J. J.; Jones, W. E., Jr. *J. Phys. Chem. B* **2004**, *108*, 1537.
(54) Fan, L.-J.; Zhang, Y.; Jones, W. E., Jr. *Macromolecules* **2005**, *38*, 2844.
(55) Fan, L.-J.; Jones, W. E., Jr. *J. Phys. Chem. B* **2006**, *110*, 7777.
(56) Fan, L.-J.; Jones, W. E., Jr. *J. Am. Chem. Soc.* **2006**, *128*, 6784.
(57) Zhou, X.-H.; Yan, J.-C.; Pei, J. *Macromolecules* **2004**, *37*, 7078.
(58) Zhou, G.; Qian, G.; Ma, L.; Cheng, Y.; Xie, Z.; Wang, L.; Jing, X.; Wang, F. *Macromolecules* **2005**, *38*, 5416.
(59) Miyata, M.; Chujo, Y. *Polym. J.* **2002**, *34*, 967.
(60) Saxena, A.; Fujiki, M.; Rai, R.; Kim, S.-Y.; Kwak, G. *Macromol. Rapid Commun.* **2004**, *25*, 1771.
(61) Tong, H.; Wang, L.; Jing, X.; Wang, F. *Macromolecules* **2003**, *36*, 2584.
(62) Zhou, G.; Cheng, Y.; Wang, L.; Jing, X.; Wang, F. *Macromolecules* **2005**, *38*, 2148.
(63) Wu, C.-Y.; Chen, M.-S.; Lin, C.-A.; Lin, S.-C.; Sun, S.-S. *Chem.—Eur. J.* **2006**, *12*, 2263.
(64) Kim, T.-H.; Swager, T. M. *Angew. Chem., Int. Ed.* **2003**, *42*, 4803.
(65) Kim, Y.; Lee, J. K.; Park, W. H.; Lee, T. S. *Thin Solid Films* **2005**, *477*, 100.
(66) Ho, H. A.; Leclerc, M. *J. Am. Chem. Soc.* **2003**, *125*, 4412.
(67) Yinon, J. *Anal. Chem.* **2003**, *75*, 99A.
(68) Moore, D. S. *Rev. Sci. Instrum.* **2004**, *75*, 2499.
(69) Levitsky, I. A.; Kim, J.; Swager, T. M. *J. Am. Chem. Soc.* **1999**, *121*, 1466.
(70) Cumming, C. J.; Aker, C.; Fisher, M.; Fox, M.; la Grone, M. J.; Reust, D.; Rockley, M. G.; Swager, T. M.; Towers, E.; Williams, V. *IEEE Trans. Geosci. Remote Sensing* **2001**, *39*, 1119.
(71) Rose, A.; Lugmair, C. G.; Swager, T. M. *J. Am. Chem. Soc.* **2001**, *123*, 11298.
(72) Yamaguchi, S.; Swager, T. M. *J. Am. Chem. Soc.* **2001**, *123*, 12087.
(73) Zahn, S.; Swager, T. M. *Angew. Chem., Int. Ed.* **2002**, *41*, 4225.
(74) Other research groups have observed chiral assemblies of conjugated polymers. See for example: (a) Wilson, J. N.; Steffen, W.; McKenzie, T. G.; Lieser, G.; Oda, M.; Neher, D.; Bunz, U. H. F. *J. Am. Chem. Soc.* **2002**, *124*, 6830. (b) Oda, M.; Nothofer, H.-G.; Scherf, U.; Sunjic, V.; Richter, D.; Regenstein, W.; Neher, D. *Macromolecules* **2002**, *35*, 6792.
(75) Rose, A.; Zhu, Z.; Madigan, C. F.; Swager, T. M.; Bulovic, V. *Nature* **2005**, *434*, 876.
(76) Zhou, D.; Swager, T. M. *Macromolecules* **2005**, *38*, 9377.
(77) For a description by this group on the detection of nitroaromatics by quenching of porous silicon luminescence, see: Content, S.; Trogler, W. C.; Sailor, M. J. *Chem.—Eur. J.* **2000**, *6*, 2205.
(78) Sohn, H.; Calhoun, R. M.; Sailor, M. J.; Trogler, W. C. *Angew. Chem., Int. Ed.* **2001**, *40*, 2104.
(79) Sohn, H.; Sailor, M. J.; Magde, D.; Trogler, W. C. *J. Am. Chem. Soc.* **2003**, *125*, 3821.
(80) Walt and co-workers have developed a fluorescence-based sensor array aimed at the detection of explosive vapors. See: (a) Albert, K. J.; Walt, D. R. *Anal. Chem.* **2000**, *72*, 1947. (b) Albert, K. J.; Myrick, M. L.; Brown, S. B.; James, D. L.; Milanovich, F. P.; Walt, D. R. *Environ. Sci. Technol.* **2001**, *35*, 3193.
(81) Toal, S. J.; Magde, D.; Trogler, W. C. *Chem. Commun.* **2005**, 5465.
(82) Toal, S. J.; Jones, K. A.; Magde, D.; Trogler, W. C. *J. Am. Chem. Soc.* **2005**, *127*, 11661.
(83) Liu, Y.; Mills, R. C.; Boncella, J. M.; Schanze, K. S. *Langmuir* **2001**, *17*, 7452.
(84) Chang, C.-P.; Chao, C.-Y.; Huang, J. H.; Li, A.-K.; Hsu, C.-S.; Lin, M.-S.; Hsieh, B. R.; Su, A.-C. *Synth. Met.* **2004**, *144*, 297.
(85) Huang, H.-M.; Wang, K.-M.; Xiao, D.; Yang, R.-H.; Yang, X.-H. *Anal. Chim. Acta* **2001**, *439*, 55.
(86) Kim, T. H.; Kim, H. J.; Kwak, C. G.; Park, W. H.; Lee, T. S. *J. Polym. Sci., Part A: Polym. Chem.* **2006**, *44*, 2059.
(87) Thomas, S. W., III; Amara, J. P.; Bjork, R. E.; Swager, T. M. *Chem. Commun.* **2005**, 4572.
(88) Amara, J. P.; Swager, T. M. *Macromolecules* **2005**, *38*, 9091.
(89) Thomas, S. W., III; Swager, T. M. *Adv. Mater.* **2006**, *18*, 1047.
(90) For a review of the synthesis and applications of conjugated polyelectrolytes, see (a) ref 21. For a review of biosensing applications of conjugated polyelectrolytes, see: (b) Achyuthan, K. E.; Bergstedt, T. S.; Chen, L.; Jones, R. M.; Kumaraswamy, S.; Kushon, S. A.; Ley, K. D.; Lu, L.; McBranch, D.; Mukundan, H.; Rininsland, F.; Shi, X.; Xia, W.; Whitten, D. G. *J. Mater. Chem.* **2005**, *15*, 2648.
(91) Shi, S.; Wudl, F. *Macromolecules* **1990**, *23*, 2119.
(92) Whitten, D.; Jones, R.; Bergstedt, T.; McBranch, D.; Chen, L.; Heeger, P. In *Optical Sensors and Switches*; Ramamurthy, V., Schanze, K. S., Eds.; Marcel Dekker: New York, 2001; p 189 ff.
(93) Jones, R. M.; Bergstedt, T. S.; McBranch, D. W.; Whitten, D. G. *J. Am. Chem. Soc.* **2001**, *123*, 6726.
(94) Song, X.; Wang, H.-l.; Shi, J.; Park, J.-W.; Swanson, B. I. *Chem. Mater.* **2002**, *14*, 2342.
(95) (a) Wang, J.; Wang, D.; Miller, E. K.; Moses, D.; Bazan, G. C.; Heeger, A. J. *Macromolecules* **2000**, *33*, 5153. (b) Wang, J.; Wang, D.; Miller, E. K.; Moses, D.; Heeger, A. J. *Synth. Met.* **2001**, *119*, 591.
(96) (a) Wang, D.; Wang, J.; Moses, D.; Bazan, G. C.; Heeger, A. J. *Langmuir* **2001**, *17*, 1262. (b) Wang, D.; Wang, J.; Moses, D.; Bazan, G. C.; Heeger, A. J.; Park, J.-H.; Park, Y.-W. *Synth. Met.* **2001**, *119*, 587.
(97) Fan, C.; Hirasa, T.; Plaxco, K. W.; Heeger, A. J. *Langmuir* **2003**, *19*, 3554.
(98) Chen, L.; Xu, S.; McBranch, D.; Whitten, D. *J. Am. Chem. Soc.* **2000**, *122*, 9302.
(99) Chen, L.; McBranch, D.; Wang, R.; Whitten, D. *Chem. Phys. Lett.* **2000**, *330*, 27.
(100) (a) Wang, D.; Moses, D.; Bazan, G. C.; Heeger, A. J.; Lal, J. *J. Macromol. Sci., Part A: Pure Appl. Chem.* **2001**, *38*, 1175. (b) Wang, D.; Lal, J.; Moses, D.; Bazan, G. C.; Heeger, A. J. *Chem. Phys. Lett.* **2001**, *348*, 411.
(101) Gaylord, B. S.; Wang, S.; Heeger, A. J.; Bazan, G. C. *J. Am. Chem. Soc.* **2001**, *123*, 6417.
(102) Stork, M.; Gaylord, B. S.; Heeger, A. J.; Bazan, G. C. *Adv. Mater.* **2002**, *14*, 361.
(103) Dalvi-Malhotra, J.; Chen, L. *J. Phys. Chem. B* **2005**, *109*, 3873.
(104) Burrows, H. D.; Lobo, V. M. M.; Pina, J.; Ramos, M. L.; de Melo, J. S.; Valente, A. J. M.; Tapia, M. J.; Pradhan, S.; Scherf, U.; Hintschich, S. I.; Rothe, C.; Monkman, A. P. *Colloids Surf., A* **2005**, *270−271*, 61.
(105) Nguyen, B. T.; Gautrot, J. E.; Ji, C.; Brunner, P.-L.; Nguyen, M. T.; Zhu, X. X. *Langmuir* **2006**, *22*, 4799.
(106) Gu, Z.; Bao, Y.-J.; Zhang, Y.; Wang, M.; Shen, Q.-D. *Macromolecules* **2006**, *39*, 3125.
(107) Nagesh, K.; Ramakrishnan, S. *Synth. Met.* **2005**, *155*, 320.
(108) Kim, Y.-G.; Samuelson, L. A.; Kumar, J.; Tripathy, S. K. *J. Macromol. Sci., Part A: Pure Appl. Chem.* **2002**, *39*, 1127.
(109) Cabarcos, E. L.; Carter, S. A. *Macromolecules* **2005**, *38*, 4409.
(110) Cabarcos, E. L.; Carter, S. A. *Macromolecules* **2005**, *38*, 10537.
(111) Tan, C.; Pinto, M. R.; Schanze, K. S. *Chem. Commun.* **2002**, 446.
(112) Tan, C.; Atas, E.; Müller, J. G.; Pinto, M. R.; Kleiman, V. D.; Schanze, K. S. *J. Am. Chem. Soc.* **2004**, *126*, 13685.
(113) Müller, J. G.; Atas, E.; Tan, C.; Schanze, K. S.; Kleiman, V. D. *J. Am. Chem. Soc.* **2006**, *128*, 4007.
(114) Pinto, M. R.; Kristal, B. M.; Schanze, K. S. *Langmuir* **2003**, *19*, 6523.
(115) Jiang, H.; Zhao, X.; Schanze, K. S. *Langmuir* **2006**, *22*, 5541.

(116) Fan, C.; Wang, S.; Hong, J. W.; Bazan, G. C.; Plaxco, K. W.; Heeger, A. J. *Proc. Natl. Acad. Sci. U.S.A.* **2003**, *100*, 6297.
(117) Choi, H. W.; Kim, Y. S.; Yang, N. C.; Suh, D. H. *J. Appl. Polym. Sci.* **2004**, *91*, 900.
(118) Li, C.; Numata, M.; Takeuchi, M.; Shinkai, S. *Angew. Chem., Int. Ed.* **2005**, *44*, 6371.
(119) DiCesare, N.; Pinto, M. R.; Schanze, K. S.; Lakowicz, J. R. *Langmuir* **2002**, *18*, 7785.
(120) He, F.; Tang, Y.; Yu, M.; Wang, S.; Li, Y.; Zhu, D. *Adv. Funct. Mater.* **2006**, *16*, 91.
(121) Rininsland, F.; Xia, W.; Wittenburg, S.; Shi, X.; Stankewicz, C.; Achyuthan, K.; McBranch, D.; Whitten, D. *Proc. Natl. Acad. Sci. U.S.A.* **2004**, *101*, 15295.
(122) Rininsland, F.; Stankewicz, C.; Weatherford, W.; McBranch, D. *BMC Biotechnol.* **2005**, *5*, 16.
(123) Kumaraswamy, S.; Bergstedt, T.; Shi, X.; Rininsland, F.; Kushon, S.; Xia, W.; Ley, K.; Achyuthan, K.; McBranch, D.; Whitten, D. *Proc. Natl. Acad. Sci. U.S.A.* **2004**, *101*, 7511.
(124) Pinto, M. R.; Schanze, K. S. *Proc. Natl. Acad. Sci. U.S.A.* **2004**, *101*, 7505.
(125) Wosnick, J. H.; Mello, C. M.; Swager, T. M. *J. Am. Chem. Soc.* **2005**, *127*, 3400.
(126) Lee, K.; Cho, J. C.; DeHeck, J.; Kim, J. *Chem. Commun.* **2006**, 1983.
(127) Nilsson, K. P. R.; Rydberg, J.; Baltzer, L.; Inganäs, O. *Proc. Natl. Acad. Sci. U.S.A.* **2003**, *100*, 10170.
(128) Nilsson, K. P. R.; Inganäs, O. *Macromolecules* **2004**, *37*, 9109.
(129) Åsberg, P.; Nilsson, K. P. R.; Inganäs, O. *Langmuir* **2006**, *22*, 2205.
(130) Herland, A.; Nilsson, K. P. R.; Olsson, J. D. M.; Hammarström, P.; Konradsson, P.; Inganäs, O. *J. Am. Chem. Soc.* **2005**, *127*, 2317.
(131) Nilsson, K. P. R.; Herland, A.; Hammarström, P.; Inganäs, O. *Biochemistry* **2005**, *44*, 3718.
(132) Nilsson, K. P. R.; Olsson, J. D. M.; Konradsson, P.; Inganäs, O. *Macromolecules* **2004**, *37*, 6316.
(133) Nilsson, K. P. R.; Olsson, J. D. M.; Stabo-Eeg, F.; Lindgren, M.; Konradsson, P.; Inganäs, O. *Macromolecules* **2005**, *38*, 6813.
(134) Fan, C.; Plaxco, K. W.; Heeger, A. J. *J. Am. Chem. Soc.* **2002**, *124*, 5642.
(135) Liu, M.; Kaur, P.; Waldeck, D. H.; Xue, C.; Liu, H. *Langmuir* **2005**, *21*, 1687.
(136) Vetrichelvan, M.; Hairong, L.; Ravindranath, R.; Valiyaveettil, S. *J. Polym. Sci., Part A: Polym. Chem.* **2006**, *44*, 3763.
(137) Montaño, G. A.; Dattelbaum, A. M.; Wang, H.-L.; Shreve, A. P. *Chem. Commun.* **2004**, 2490.
(138) Cheng, F.; Zhang, G.-W.; Lu, X.-M.; Huang, Y.-Q.; Chen, Y.; Zhou, Y.; Fan, Q.-L.; Huang, W. *Macromol. Rapid Commun.* **2006**, *27*, 799.
(139) Abe, S.; Chen, L. *J. Polym. Sci., Part B: Polym. Phys.* **2003**, *41*, 1676.
(140) Wang, W.-Z.; Fan, Q.-L.; Cheng, F.; Zhao, P.; Huang, W. *J. Polym. Sci., Part A: Polym. Chem.* **2006**, *44*, 3513.
(141) Wang, D.; Gong, X.; Heeger, P. S.; Rininsland, F.; Bazan, G. C.; Heeger, A. J. *Proc. Natl. Acad. Sci. U.S.A.* **2002**, *99*, 49.
(142) Dwight, S. J.; Gaylord, B. S.; Hong, J. W.; Bazan, G. C. *J. Am. Chem. Soc.* **2004**, *126*, 16850.
(143) Huang, F.; Wang, X.; Wang, D.; Yang, W.; Cao, Y. *Polymer* **2005**, *46*, 12010.
(144) Kim, I.-B.; Dunkhorst, A.; Bunz, U. H. F. *Langmuir* **2005**, *21*, 7985.
(145) (a) Kuroda, K.; Swager, T. M. *Chem. Commun.* **2003**, 26. (b) Kuroda, K.; Swager, T. M. *Macromol. Symp.* **2003**, *201*, 127.
(146) Kuroda, K.; Swager, T. M. *Macromolecules* **2004**, *37*, 716.
(147) Bailey, G. C.; Swager, T. M. *Macromolecules* **2006**, *39*, 2815.
(148) Zheng, J.; Swager, T. M. *Chem. Commun.* **2004**, 2798.
(149) Joly, G. D.; Geiger, L.; Kooi, S. E.; Swager, T. M. *Macromolecules* **2006**, *39*, 7175.
(150) See ref 2 and: Zhou, Q.; Swager, T. M. *J. Am. Chem. Soc.* **1995**, *117*, 12593.
(151) Levitsky, I. A.; Kim, J.; Swager, T. M. *J. Am. Chem. Soc.* **1999**, *121*, 1466.
(152) Levitsky, I. A.; Kim, J.; Swager, T. M. *Macromolecules* **2001**, *34*, 2315.
(153) For additional previous studies involving Langmuir−Blodgett films of poly(*p*-phenylene ethynylene)s, see: (a) Kim, J.; Swager, T. M. *Nature* **2001**, *411*, 1030. (b) Kim, J.; Levitsky, I. A.; McQuade, D. T.; Swager, T. M. *J. Am. Chem. Soc.* **2002**, *124*, 7710. (c) Kim, J.; McQuade, D. T.; Rose, A.; Zhu, Z.; Swager, T. M. *J. Am. Chem. Soc.* **2001**, *123*, 11488. (d) Kim, J.; McHugh, S. K.; Swager, T. M. *Macromolecules* **1999**, *32*, 1500.
(154) Kim, Y.; Zhu, Z.; Swager, T. M. *J. Am. Chem. Soc.* **2004**, *126*, 452.
(155) Kim, Y.; Whitten, J. E.; Swager, T. M. *J. Am. Chem. Soc.* **2005**, *127*, 12122.
(156) Kim, Y.-M.; Swager, T. M. *Macromolecules* **2006**, *39*, 5177.
(157) Smith, R. C.; Tennyson, A. G.; Lim, M. H.; Lippard, S. J. *Org. Lett.* **2005**, *7*, 3573.
(158) Erdogan, B.; Wilson, J. N.; Bunz, U. H. F. *Macromolecules* **2002**, *35*, 7863.
(159) For an additional, subsequent report describing the synthesis of carbohydrate-functionalized poly(*p*-phenylene ethynylene)s, see: Babudri, F.; Colangiuli, D.; Di Lorenzo, P. A.; Farinola, G. M.; Omar, O. H.; Naso, F. *Chem. Commun.* **2003**, 130.
(160) Disney, M. D.; Zheng, J.; Swager, T. M.; Seeberger, P. H. *J. Am. Chem. Soc.* **2004**, *126*, 13343.
(161) Kim, I.-B.; Wilson, J. N.; Bunz, U. H. F. *Chem. Commun.* **2005**, 1273.
(162) Lavigne, J. J.; Broughton, D. L.; Wilson, J. N.; Erdogan, B.; Bunz, U. H. F. *Macromolecules* **2003**, *36*, 7409.
(163) Takasu, A.; Iso, K.; Dohmae, T.; Hirabayashi, T. *Biomacromolecules* **2006**, *7*, 411.
(164) Baek, M-G.; Stevens, R. C.; Charych, D. H. *Bioconjugate Chem.* **2000**, *11*, 777.
(165) Wilson, J. N.; Wang, Y.; Lavigne, J. J.; Bunz, U. H. F. *Chem. Commun.* **2003**, 1626.
(166) Wang, X.; Kim, Y.-G.; Drew, C.; Ku, B.-C.; Kumar, J.; Samuelson, L. A. *Nano Lett.* **2004**, *4*, 331.
(167) McQuade, D. T.; Hegedus, A. H.; Swager, T. M. *J. Am. Chem. Soc.* **2000**, *122*, 12389.
(168) Wosnick, J. H.; Liao, J. H.; Swager, T. M. *Macromolecules* **2005**, *38*, 9287.
(169) Zeineldin, R.; Piyasena, M. E.; Bergstedt, T. S.; Sklar, L. A.; Whitten, D.; Lopez, G. P. *Cytometry A* **2006**, *69A*, 335.
(170) Moon, J. H.; Deans, R.; Krueger, E.; Hancock, L. F. *Chem. Commun.* **2003**, 104.
(171) A portion of this work has been previously reviewed in a "Concepts" article: Ho, H.-A.; Béra-Abérem, M.; Leclerc, M. *Chem.—Eur. J.* **2005**, *11*, 1718.
(172) Bernier, S.; Garreau, S.; Béra-Abérem, M.; Gravel, C.; Leclerc, M. *J. Am. Chem. Soc.* **2002**, *124*, 12463.
(173) Ho, H.-A.; Boissinot, M.; Bergeron, M. G.; Corbeil, G.; Doré, K.; Boudreau, D.; Leclerc, M. *Angew. Chem., Int. Ed.* **2002**, *41*, 1548.
(174) Leclerc, M. *Adv. Mater.* **1999**, *11*, 1491.
(175) Garreau, S.; Leclerc, M.; Errien, N.; Louarn, G. *Macromolecules* **2003**, *36*, 692.
(176) Nilsson, K. P. R.; Inganäs, O. *Nat. Mater.* **2003**, *2*, 419.
(177) Karlsson, K. F.; Åsberg, P.; Nilsson, K. P. R.; Inganäs, O. *Chem. Mater.* **2005**, *17*, 4204.
(178) Béra-Abérem, M.; Ho, H.-A.; Leclerc, M. *Tetrahedron* **2004**, *60*, 11169.
(179) Raymond, F. R.; Ho, H.-A.; Peytavi, R.; Bissonnette, L.; Boissinot, M.; Picard, F. J.; Leclerc, M.; Bergeron, M. G. *BMC Biotechnol.* **2005**, *5*, Art. No. 10.
(180) Doré, K.; Dubus, S.; Ho, H.-A.; Lévesque, I.; Brunette, M.; Corbeil, G.; Boissinot, M.; Boivin, G.; Bergeron, M. G.; Boudreau, D.; Leclerc, M. *J. Am. Chem. Soc.* **2004**, *126*, 4240.
(181) Ho, H.-A.; Doré, K.; Boissinot, M.; Bergeron, M. G.; Tanguay, R. M.; Boudreau, D.; Leclerc, M. *J. Am. Chem. Soc.* **2005**, *127*, 12673.
(182) Doré, K.; Leclerc, M.; Boudreau, D. *J. Fluoresc.* **2006**, *16*, 259.
(183) Bazan and his co-workers have developed similar amplified conjugated polymer-based detection schemes to probe RNA−RNA assemblies and RNA−protein interactions. See: (a) Wang, S.; Bazan, G. C. *Adv. Mater.* **2003**, *15*, 1425. (b) Liu, B.; Baudrey, S.; Jaeger, L.; Bazan, G. C. *J. Am. Chem. Soc.* **2004**, *126*, 4076.
(184) A review of homogenous fluorescence-based DNA detection with ionic conjugated polymers was published in 2004. See: Liu, B.; Bazan, G. C. *Chem. Mater.* **2004**, *16*, 4467.
(185) Gaylord, B. S.; Heeger, A. J.; Bazan, G. C. *Proc. Natl. Acad. Sci. U.S.A.* **2002**, *99*, 10954.
(186) For a detailed discussion of PNA−DNA complexes that is specifically related to sensory systems employing polymer **A13**, see: Baker, E. S.; Hong, J. W.; Gaylord, B. S.; Bazan, G. C.; Bowers, M. T. *J. Am. Chem. Soc.* **2006**, *128*, 8484.
(187) Xu, Q.-H.; Gaylord, B. S.; Wang, S.; Bazan, G. C.; Moses, D.; Heeger, A. J. *Proc. Natl. Acad. Sci. U.S.A.* **2004**, *101*, 11634.
(188) Gaylord, B. S.; Heeger, A. J.; Bazan, G. C. *J. Am. Chem. Soc.* **2003**, *125*, 896.
(189) Wang, S.; Bazan, G. C. *Chem. Commun.* **2004**, 2508.
(190) Liu, B.; Gaylord, B. S.; Wang, S.; Bazan, G. C. *J. Am. Chem. Soc.* **2003**, *125*, 6705.
(191) Wang, S.; Liu, B.; Gaylord, B. S.; Bazan, G. C. *Adv. Funct. Mater.* **2003**, *13*, 463.
(192) Wang, S.; Gaylord, B. S.; Bazan, G. C. *J. Am. Chem. Soc.* **2004**, *126*, 5446.
(193) Xu, Q.-H.; Wang, S.; Korystov, D.; Mikhailovsky, A.; Bazan, G. C.; Moses, D.; Heeger, A. J. *Proc. Natl. Acad. Sci. U.S.A.* **2005**, *102*, 530.
(194) He, F.; Tang, Y.; Yu, M.; Feng, F.; An, L.; Sun, H.; Wang, S.; Li, Y.; Zhu, D.; Bazan, G. C. *J. Am. Chem. Soc.* **2006**, *128*, 6764.
(195) Liu, B.; Bazan, G. C. *J. Am. Chem. Soc.* **2004**, *126*, 1942.

(196) Hong, J. W.; Hemme, W. L.; Keller, G. E.; Rinke, M. T.; Bazan, G. C. *Adv. Mater.* **2006**, *18*, 878.
(197) Liu, B.; Wang, S.; Bazan, G. C.; Mikhailovsky, A. *J. Am. Chem. Soc.* **2003**, *125*, 13306.
(198) Liu, B.; Bazan, G. C. *J. Am. Chem. Soc.* **2006**, *128*, 1188.
(199) In addition to this MMP-based assay, DNA-sensing chips have also been developed using a red-shifted cationic poly(fluorene-*co*-benzothiadiazole) and surface-bound PNA. Liu, B.; Bazan, G. C. *Proc. Natl. Acad. Sci. U.S.A.* **2005**, *102*, 589.
(200) Gaylord, B. S.; Massie, M. R.; Feinstein, S. C.; Bazan, G. C. *Proc. Natl. Acad. Sci. U.S.A.* **2005**, *102*, 34.
(201) Xu, H.; Wu, H.; Huang, F.; Song, S.; Li, W.; Cao, Y.; Fan, C. *Nucleic Acids Res.* **2005**, *33*, e83.
(202) Elghanian, R.; Storhoff, J. J.; Mucic, R. C.; Letsinger, R. L.; Mirkin, C. A. *Science* **1997**, *277*, 1078−1081.

CR0501339